LIFETIMES OF EXCITED LEVELS OF NEUTRAL AND IONIZED STRONTIUM BY THE HANLE EFFECT

Koh Thong-Khng

Department of Physics

University of Manitoba

Winnipeg, Canada.

May 1974

A thesis submitted to the Faculty of Graduate Studies of the University of Manitoba in partial fulfillment of the requirements for the Degree of Doctor of Philosophy.

LIFETIMES OF EXCITED LEVELS OF NEUTRAL AND IONIZED STRONTIUM BY THE HANLE EFFECT

by

Koh Thong-Khng

A dissertation submitted to the Faculty of Graduate Studies of the University of Manitoba in partial fulfillment of the requirements of the degree of

DOCTOR OF PHILOSOPHY

TABLE OF CONTENTS

Abstract		(i)
Acknowledgments		(ii)
List of Figures		(iii)
List of Tables		(iv)
CHAPTER I	INTRODUCTION	1
CHAPTER II	THEORY	
	Hanle effect in the ideal case	14
	Departures from the ideal case	27
	Note on oscillator strengths	43
CHAPTER III	EXPERIMENTAL DETAILS	
	Introduction	48
	The hollow cathode lamp	50
	Scattering chamber and atomic beam	55
	The magnetic fields	59
	Data taking and analysis	63
CHAPTER IV	RESULTS AND DISCUSSION	
	The neutral strontium atom	72
	The strontium ion	108
CHAPTER V	CONCLUSIONS	128
References		132

ABSTRACT

The lifetimes of the 5s5p, 5s6p, 5s7p and 5s8p $^1P_1$ levels of neutral strontium, and 5p $^2P_{3/2}$ and 5p $^2P_{1/2}$ levels of the strontium ion have been determined using the Hanle effect. The related oscillator strengths of transitions from these levels have been calculated from the measured lifetimes. The depolarization cross section between the collisions of normal strontium atoms with atoms in the excited 5s5p $^1P_1$ level, and between the excited 5p $^2P_{3/2}$ strontium ions with atoms in the excited 5s5p $^1P_1$ level and with atoms in the ground level have also been determined. The results are

$$\tau(5s5p\ ^1P_1) = 4.68 \pm 0.10 \quad \text{ns}$$
$$\tau(5s6p\ ^1P_1) = 3.64 \pm 0.14 \quad \text{ns}$$
$$\tau(5s7p\ ^1P_1) = 4.93 \pm 0.35 \quad \text{ns}$$
$$\tau(5s8p\ ^1P_1) = 5.46 \pm 0.17 \quad \text{ns}$$
$$\tau(5p\ ^2P_{3/2}) = 5.63 \pm 0.17 \quad \text{ns}$$
$$\tau(5p\ ^2P_{1/2}) = 6.74 \pm 0.20 \quad \text{ns}$$

$$f(4607) = 1.94 \pm 0.06$$
$$f(7169) = 1.22 \pm 0.05$$
$$f(2932) = (6.60 \pm 0.22)10^{-3}$$
$$f(5331) = 0.485 \pm 0.04$$
$$f(2570) = (1.38 \pm 0.04)10^{-2}$$
$$f(4755) = 0.34 \pm 0.02$$
$$f(2428) = (4.10 \pm 0.13)10^{-2}$$
$$f(4077) = 0.83 \pm 0.03$$
$$f(4215) = 0.37 \pm 0.02$$

$$\sigma_{\bar{v}}(^1S_o \text{—} 5s5p\ ^1P_1) = [(5.2)10^{-7}/\bar{v}] \ \text{cm}^2$$

$$\sigma\ (5p\ ^2P_{3/2} \text{—} ^1S_o;\ 5s5p\ ^1P_1) = 8400\ \text{Å}^2$$

ACKNOWLEDGMENTS

It is a pleasure to express my gratitude to my advisor, Dr. F. M. Kelly, for suggesting the project and for his guidance in all the phases of the work. I should also like to thank Dr. M. S. Mathur and Dr. L. O. Dickie and Mr. F. C. Suk for helping during the data taking and data analysis time and also for useful discussions.

LIST OF FIGURES

1	Energy level diagram for the singlet levels of neutral strontium.	12
2	Partial energy level diagram for the strontium ion.	13
3	Geometry of the Hanle experiment.	15
4	Coordinate and polarization system used in the calculation of the Hanle effect.	21
5	Schematic diagram of the experimental apparatus.	49
6	Hollow cathode lamp used in this work.	52
7	Gas handling system for the hollow cathode lamp.	54
8	Scattering chamber and furnace.	58
9	Block diagram of the electronic system.	64
10	Spectrum of the hollow cathode lamp.	67
11	Hanle resonance curve for the 4607 Å transition.	75
12	The variation of the Hanle width of 4607 Å transition with atomic density.	78
13	Zeeman structure of upper and lower levels for $^1P_1 - - - ^1D_2$ transitions.	93
14	Hanle resonance curve for the 7169 Å transition.	99
15	Composite Hanle curve for 5331 Å transition.	101
16	Composite Hanle curve for 4755 Å transition.	106
17	The variation of the Hanle width of 4077 Å line with atomic density.	114
18	Hanle curve for 4215 Å transition.	125

LIST OF TABLES

1	Calibration of Helmholtz coils.	60
2	Calibration of multichannel analyzer	69
3	Data: Hanle effect of $5s5p\ ^1P_1$ level of SrI.	73
4	Data: Hanle effect of $5s5p\ ^1P_1$ level of SrI.	77
5	Lifetime of the $5s5p\ ^1P_1$ level of SrI and the related oscillator strengths.	89
6	Lifetime of the $5s6p\ ^1P_1$ level of SrI and the related oscillator strengths.	98
7	Lifetime of the $5s7p\ ^1P_1$ level of SrI and the related oscillator strengths.	104
8	Lifetime of the $5s8p\ ^1P_1$ level of SrI and the related oscillator strengths.	107
9	Data: Hanle effect of $5p\ ^2P_{3/2}$ level of SrII.	113
10	Depolarization cross section of collisions between strontium ions , strontium atoms and rubidium atoms with the foreign gases.	118
11	Data: Hanle effect of $5p\ ^2P_{1/2}$ level of SrII.	124
12	Lifetimes of the $5p\ ^2P$ levels of the strontium ions and the related oscillator strengths.	127

CHAPTER I INTRODUCTION

Since the pioneering work of Balmer (1885) on the spectrum of hydrogen, and the demonstration of the existence of series of lines in many spectra by Rydberg (1889), there has been a considerable development in our knowledge of atomic spectra and the associated theory. Measurements of the wavelengths of the spectral lines of many atoms and ions have led to the compilation of energy level tables by Moore (1952). Bohr (1911) using quantum theory provided the first acceptable description of the hydrogen atom. Difficulties with the Bohr theory, particularly with atoms with more than one electron, have led to the rapid development of quantum mechanics. Among the many books on quantum mechanics the one by Condon and Shortley (1936) is still outstanding.

The first observation of the effect of a magnetic field on the radiation emitted by an atom was reported by Zeeman (1897). In 1905 Wood showed that the D lines of sodium could excite D line fluorescence in sodium vapour. Rayleigh (1922) showed that the resonance fluorescence of the 2537 Å line in mercury vapour was polarized, while Wood and Ellet (1923) showed that a small magnetic field would remove the polarization. In 1924 Hanle explained this depolarization of the resonance radiation in terms of the Zeeman effect and we now call this phenomenon the Hanle effect. Nowadays,

the Hanle effect has become one of the most important methods for the measurement of the lifetimes of the excited atomic energy levels. Before we go into more detail, a short review of lifetime and the related oscillator strength measurements will be helpful.

In the past few decades analyses of atomic spectra have succeeded in describing energy levels, fine structure and hyperfine structure and isotope shift of many atoms and ions. On the other hand, lifetimes of atomic levels and their related oscillator strengths remain of great interest to experimental and theoretical atomic physicists, because there are many unknowns and large discrepancies between the measured and calculated values. Oscillator strengths are widely used in the astrophysics for the study of stellar structure, and for the determination of ion densities and temperatures in plasma physics. More experimental data with greater accuracy is needed.

By definition, the lifetime of an excited atomic state is the average decay time of that state. All possible radiation transitions to lower energy states must be taken into consideration. If N_o represents the number of atoms in the excited state m at time t=0, then the number remaining at time t is given by

$$N_t = N_o \exp(-t/\tau_m) \tag{1}$$

where τ_m is the mean lifetime of the excited state m under investigation. The mean lifetime, τ_m, is the reciprocal of the sum of the

Einstein A coefficients (Mitchell and Zemansky 1934), so that,

$$\tau_m = 1/(\sum_n A_{mn}) \tag{2}$$
$$= \sum_n g_m m_e c^3 / (g_n 8\pi^2 e^2 \nu_{nm}^2 f_{nm})$$

Here the summation is taken over all possible transitions to the lower state n; g_m and g_n are the statistical weights of the upper and lower levels respectively; f_{nm} is the absorption oscillator strength related to the corresponding transition; ν_{nm} is the transition frequency; m_e and e are the rest mass and charge of the electron and c is the speed of light. Classically f_{nm} is equivalent to the number of classical oscillators in one atom in state n. The detailed explanation is given in Chapter II.

The lifetime of an excited level can be calculated from the measured values of the oscillator strength of transitions to lower levels, or can be measured directly. Various experimental methods have been developed and can be classified as 'relative methods' or 'absolute methods' depending upon whether or not the absolute density of atoms needs to be known.

Relative measurement

There are three principal relative methods, the emission method, the absorption method and the hook method. Results of these methods are proportional to the product of the absolute number of the

atoms per unit volume and the oscillator strength. Unless the density is known accurately, only the relative oscillator strengths can be determined with precision.

In the emission method the line intensities in the arc are measured by precise photographic techniques, and a temperature T is assumed for the arc core so that the excited state populations can be determined by Boltzmann's equation. The relative oscillator strengths of many lines in different spectra have been determined by this method. Eberhagen (1955) extended this method to the absolute measurement of oscillator strength by calculating the atom density in the arc from the Saha equation.

In the absorption method the equivalent widths of the absorption lines are measured. Continuous radiation is passed through an atomic vapour and the number of atoms in the ground level is calculated from the measured temperature and vapour pressure data. King (1940) has successfully used this method for relative oscillator strength measurements of many atoms.

The hook method, which was devised by Rozhdestvenskii and developed by Penkin, has been used to determine many relative oscillator strengths. A Jamin-Mach type interferometer, with a King furnace containing the vapour under investigation in one arm, and an accessory tube with a plane-parallel plate inserted in front of the

other arm, is used. The change of light path by the plate and by the gas leads to the formation of 'hooks' on either side of the spectrum lines. By determining the distance between the turning points of the hooks on either side of the spectral line and the length of the column of atoms, the product of the oscillator strength and the atomic concentration is obtained.

The methods described above have the advantage that the relative oscillator strength of a great number of lines can be obtained at the same time. However, the methods of estimating the atomic density may contain a serious error, which affects the absolute oscillator strengths calculated from these data.

Absolute measurement

The absolute methods are the ones which do not require the knowledge of the absolute number of atoms. They are the direct measurement method, the phase shift method, the optical double resonance method and the level crossing method.

The direct measurement method involves the observation of the intensity change along the path of the atomic beam beyond some point where excitation has occurred. The atoms can be excited electrically or optically, or by using the beam-foil technique. From equation (1), the population of the excited levels decays exponentially with the

time after excitation. Therefore, the emitted light intensity decreases exponentially with distance from the excitation region. This method is not accurate for lifetimes in the nano-second region because these excited atoms can travel only a short distance during their lifetime.

The phase shift technique uses modulated high frequency resonance radiation as an exciting pulse. The period of the exciting pulse is much greater than the lifetime to be measured. The fluorescent radiation has the same pulse shape as the exciting pulse, but lags in phase by an angle due to the finite lifetime of the excited level. By measuring the phase shift angle, the lifetime of the excited level can be determined.

The double resonance method involves exciting an atom with polarized resonance radiation. If the experiment has been arranged so that only one Zeeman state of the excited level is excited, an external rf oscillating magnetic field with the Larmor precession frequency will transfer the atom to another magnetic state. This modifies the polarization and direction of the fluorescent radiation. The lifetime can be calculated from the half width of the double resonance signal. In double resonance experiments the Doppler width of the rf signal is much smaller than the natural line width and can be neglected. But if the rf magnetic field is strong enough to induce many transitions between Zeeman states during the lifetime, power

broadening occurs and must be eliminated. This can be done by measuring the half width at several power levels of the rf oscillating field and extrapolating to zero field. However, for those excited states with lifetime shorter than 10^{-8} second, an rf magnetic field of magnitude about 100 gauss is required to saturate the resonance. The difficulty of the construction and stabilization of such high power rf sources limits the application of the double resonance method to measurements of relatively long lifetimes.

The level crossing method uses somewhat the same technique as the double resonance method, but the need of rf power is eliminated. When two levels of the excited state are tuned to degeneracy by an external magnetic field, interference effects change the spatial distribution of the scattered radiation. By analysing the scattered light signal during a level crossing, the lifetime of an excited state can be obtained accurately.

The most commonly used example of this method is the so called 'Hanle effect' or 'level crossing at zero magnetic field'. The Hanle effect is one of the most powerful methods for precise lifetime measurements. The reasons for this are multifold. First, only very simple equipment is required and no rf broadening, cascade problems and Doppler broadening have to be considered. Second, unlike the relative method, it does not require a direct knowledge of the atom density. Third, it is particularly suitable for lifetimes in the 10^{-8} to 10^{-9}

second range where other methods, also independent of absolute atom density, begin to lose their accuracy. Finally, if the excited level has more than one branch, detecting any one of the branches by the Hanle effect gives the lifetime of the excited level, so that convenient experimental choices can be made.

The history of the Hanle effect goes back to 1921 when Hanle worked a classical theory explaining the influence of a magnetic field on the polarization of resonantly scattered light. The observations were difficult before the photomultiplier tube was invented, and this technique was forgotten until the 1960's. In 1959 Colgrove et al. accidently found out that the level crossing effect can be explained by the Breit formula which was developed in the 1930's, and with this came a rediscovery of the Hanle effect, which is a special case of level crossing when the levels cross at zero magnetic field. In recent years, many accurate lifetimes for the excited levels of the group I and group II atoms, using the Hanle effect, have been reported. The same technique has also been applied succesfully to the group III elements and some diatomic molecules. Experiments for Hanle effect of excited ionic levels have been performed as well. Review articles discussing the use of the Hanle effect have been written by Budick (1967), zu Putlitz (1965), Happer(1968) and Series (1969).

The strontium atom

Atomic strontium has a $5s^2\ ^1S_o$ ground level. The singlet metastable level $5s4d\ ^1D_2$ is about 2.5 eV above the ground level. Like cadmium and barium, strontium also has doubly excited configurations of mdnp $^1P_1$ levels that are close in energy compared to the 5snp $^1P_1$ levels. The mixing of levels of the same parity may produce interesting results in the lifetimes of the $^1P_1$ levels and the related oscillator strengths. Prior to this work, Eberhagen (1955) studied the oscillator strengths for the $^1P_1 \rightarrow {}^1D_2$ transitions by the emission method. Ostrovskii and Penkin (1958, 1961b) determined the relative and absolute oscillator strengths for 5snp $^1P_1 \rightarrow {}^1S_o$ transitions by hook method. Their absolute values do not agree with the recent Hanle effect or phase shift experiments, but the hook method relative values should be reliable. These results show that the oscillator strengths for the principal series of strontium are not monotonic, and that a minimum value occurs at the second $^1P_1$ level. Except for the $5s5p\ ^1P_1 \rightarrow {}^1S_o$ transition, all the 5snp $^1P_1 \rightarrow {}^1S_o$ transitions have absorption oscillator strengths close to the forbidden transitions.

De Zafra et al. (1962), Lurio et al. (1964) and Hulpke et al. (1964) have determined the lifetime of the $5s5p\ ^1P_1$ level. Low atomic densities were employed in their experiments, but coherence narrowing, which is eliminated by extrapolation to zero atomic density to obtain true lifetimes, was not studied. Also, the lifetimes of $^1P_1$

levels higher than 5s5p were not determined. Prompted by this lack of information, the work described here has been undertaken to obtain further information about the lifetimes of the $^1P_1$ levels of the strontium atom and the related oscillator strengths. First of all, the true lifetime of the first $^1P_1$ level is obtained from coherence narrowing studies. This gives an accurate absolute oscillator strength for the first $^1P_1 \rightarrow {}^1S_o$ transition of wavelength 4607 Å. By coupling this with the accurate relative ratios given by Penkin (1961) from the hook method, the absolute oscillator strengths of the other $^1P_1 \rightarrow {}^1S_o$ transitions are calculated. The lifetimes of the 5s6p $^1P_1$, 5s7p $^1P_1$ and 5s8p $^1P_1$ levels are determined with the same technique, and using equation (2) the upper limit of oscillator strengths of the $^1P_1 \rightarrow {}^1D_2$ transitions are determined. As well, the collision broadening cross-section between Sr(5 $^1P_1$) and Sr(^1S_o) atoms is studied using the 4607 Å transition.

The levels which are involved in these experiments are shown in Figure 1.

The strontium ion

The singly ionized strontium atom has a 5s $^2S_{1/2}$ ground level. The energy levels involved in the present work are shown in Figure 2. The doublet separation between 5p $^2P_{1/2}$ and 5p $^2P_{3/2}$ is large enough to be resolved easily with our apparatus. Due to the large separation of the ^2P levels one may expect that the lifetimes of these two

levels will differ by a few percent. The excitation energy of the $5p\ ^2P_{3/2}$ is 3.04 eV above the ground level. This energy is close to the ionization energy of the neutral strontium atom in the $5s5p\ ^1P_1$ excited state, which is known to be 3.00 eV. This accidental resonance may cause interesting results in the collisions between strontium ions and strontium atoms. The Hanle effect is applied to study these two problems.

Yu. I. Ostrovskii and N. P. Penkin (1961a) have measured the absolute oscillator strengths for the doublet resonance lines of the strontium ion using the hook method. Gallagher (1967a) has measured the lifetimes of the $5p\ ^2P$ levels of the strontium ion and the collision cross section between ions in these levels and argon atoms. However, several extrapolations were made in the analysis of the data, and collisions between strontium ions and strontium atoms were not considered. The present work was undertaken to check the lifetimes and to obtain the information for collisions between strontium ions and strontium atoms utilizing a simpler approach.

Figure 1.

Energy level diagram for the singlet levels of neutral strontium.

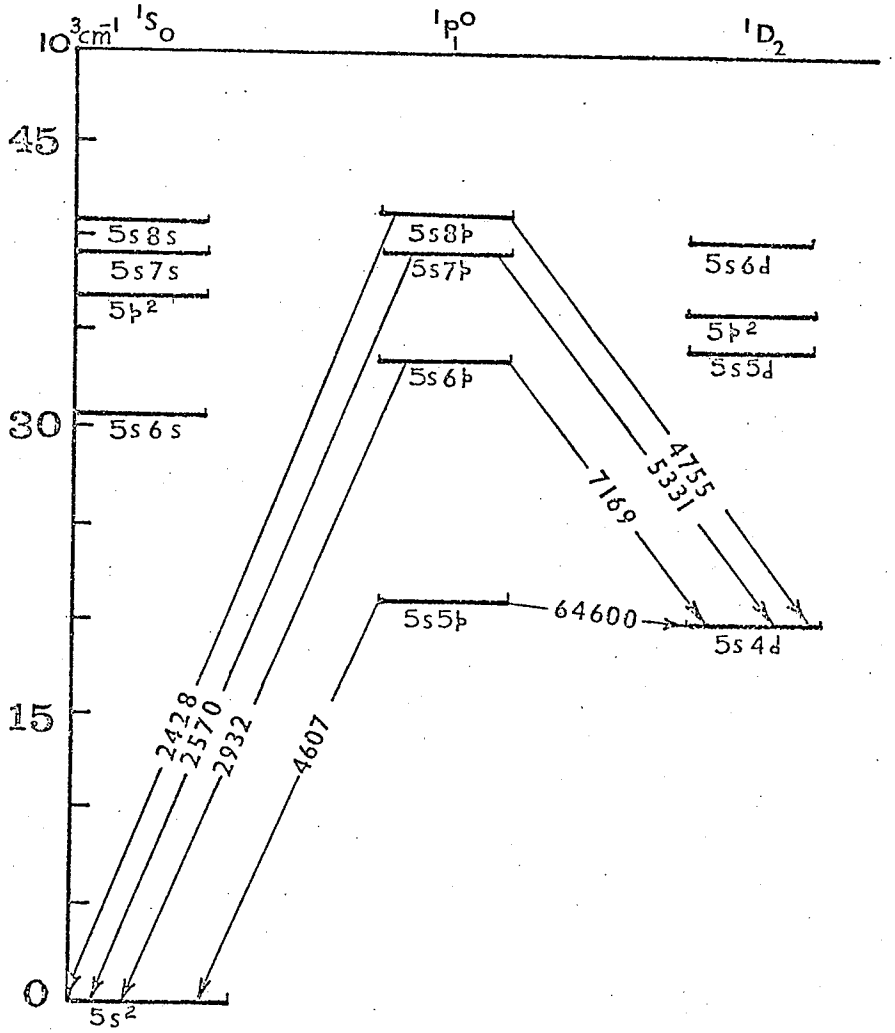
$10^3 cm^{-1}$
$^1S_0$
$^1P_1^o$
$^1D_2$
45
30
15
0
5s8s
5s7s
5p²
5s6s
5s8p
5s7p
5s6p
5s5p
5s²
5s6d
5p²
5s5d
5s4d
2428
2570
2932
4607
7169
4755
5331
64600

Figure 2.

Partial energy level diagram for the strontium ion.

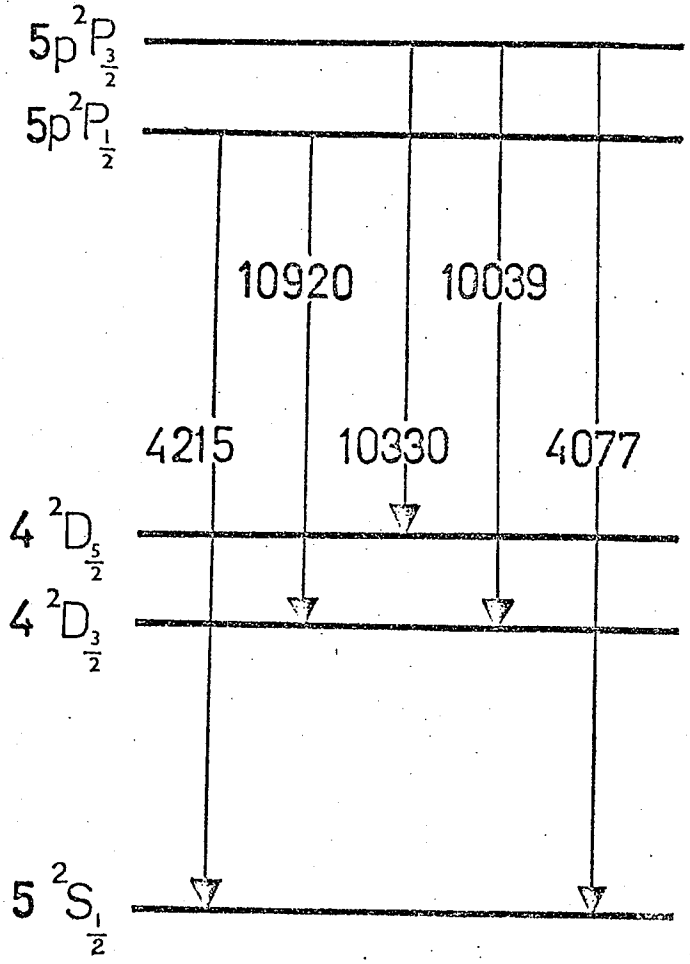
$5p\,^2P_{\frac{3}{2}}$
$5p\,^2P_{\frac{1}{2}}$
10920
10039
4215
10330
4077
$4\,^2D_{\frac{5}{2}}$
$4\,^2D_{\frac{3}{2}}$
$5\,^2S_{\frac{1}{2}}$

CHAPTER II THEORY

The theory of the Hanle effect based on the classical depolarization concept has been discussed in the book by Mitchell and Zemansky (1934). Quantum mechanically, the Hanle effect can be explained by interference effects, and the theory has been given in a form useful for atomic spectroscopy by Franken (1961) and Lurio et al. (1964).

Hanle effect in the ideal case

The essentials of the classical approach to the Hanle effect are shown in Figure 3. If the incident exciting radiation is polarized with its electric vector along the y axis, and if a sample atom located at the origin is acting as a classical oscillating dipole, after excitation it will vibrate parallel to the direction of polarization of the exciting light. At zero magnetic field this oscillating dipole gradually damps down due to radiation losses, but, the oscillation axis always points in the initial direction. Dipoles do not radiate along the axis of their oscillation, so that nothing will be observed if one looks along the oscillation axis for fluorescent light. However, if there is a magnetic field along the z axis, the dipole excited by the radiation will precess about the field direction at the Larmor precession frequency,

Figure 3.

Geometry of the Hanle experiment.

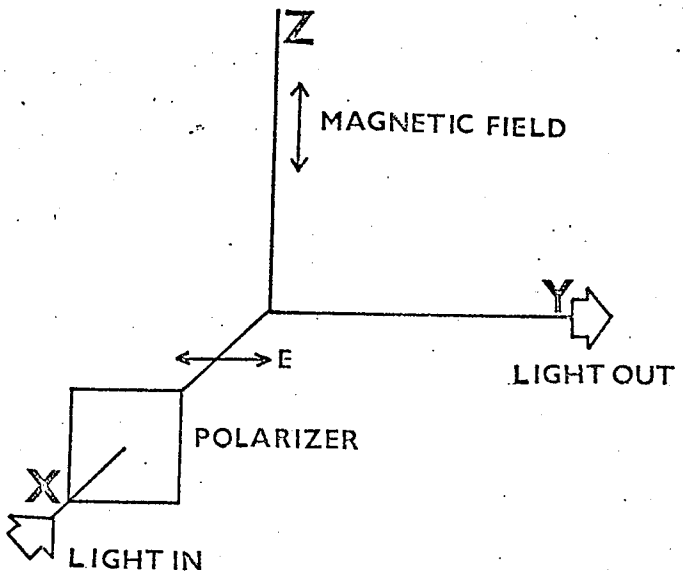
Z
MAGNETIC FIELD
Y
E
LIGHT OUT
POLARIZER
X
LIGHT IN

$\omega_L = \gamma H = g_j \mu_o H/\hbar$, where γ is the gyromagnetic ratio, μ_o is the Bohr magneton and g_j is the Landé g factor for the level. The radiation pattern in the x-y plane is determined by $\sin^2\theta$, where θ is the angle between the observation direction and the y axis. If the observer stays fixed, θ can be replaced by $\omega_L t$, where t is the time elapsed since excitation started. To obtain the observed intensity for a collection of atoms, a damping term $\exp(-t/\tau)$ must be included where τ is the mean lifetime of the level involved. For continuous excitation and observation, the intensity of the scattered radiation observed along y axis is given by :

$$(3) \qquad I = C\int_o^\infty \exp(-t/\tau)\sin^2\omega_L t \cdot dt$$

$$= I_o\{ 1 - \frac{1}{1 + (2\gamma\tau H)^2}\}$$

which is the inverted Lorentzian distribution. I_o represents the maximum observed intensity of the scattered radiation which depends on the incident light intensity, the beam density, the oscillator strength of the transition involved and also the geometry of the scattering chamber. When H takes the value such that $2\gamma\tau H = 1$, $I = I_o/2$. If we denote this H by $H_{1/2}$, we have

$$(4) \qquad 1/\tau = g_j \mu_o \Delta H/\hbar \qquad \text{sec}^{-1}$$

where $\Delta H = 2H_{1/2}$ and is the full width at half maximum of the Lorentzian curve. Therefore, in an experiment, one can determine the

lifetime of the excited level from equation (4) by measuring ΔH from the Hanle signal. In many simple atomic spectra the g_j values of excited levels are either well known from theoretical consideration or have been measured by the Zeeman effect or optical double resonance experiments.

Quantum mechanically, the Hanle effect can be described by the Breit-Franken formula (Franken 1961)

$$(5) \qquad R \sim \sum_{m,\mu,\mu',m'} \frac{f_{\mu m} f_{m\mu'} g_{\mu' m'} g_{m'\mu}}{1 + i\tau\omega(\mu,\mu')}$$

In the above equation R is the rate at which photons of polarization $\hat{f}$ are absorbed and photons of polarization $\hat{g}$ are emitted in the resonance fluorescence. The subscripts μ and μ' represent the magnetic states of the excited level which can be excited from the state with magnetic quantum number m of the initial level, and which can subsequently decay to the final state with magnetic quantum number m'. If m' does not belong to the same initial level as m, equation (5) is still valid provided that the summation over m is taken only over the magnetic states of the initial level, and the m' summation is over the magnetic states of the final level. The transition frequency $\omega(\mu,\mu') = (E_\mu - E_{\mu'})/\hbar$ is between the states μ and μ'. The f's and g's are the matrix elements for the absorption and re-emission process in electric dipole transitions; for

example, $f_{\mu m} = \langle \mu | \hat{f} \cdot \bar{r} \ | m \rangle$ and $g_{\mu' m'} = \langle \mu' | \hat{g} \cdot \bar{r}' \ | m' \rangle$.

Let us consider the simple J=0→J=1→J=0 transitions under the geometrical setting in Figure 3. Here, the final state is the same as the initial state and can be denoted by a. There are only two states corresponding to $m_j = \pm 1$ which can be populated and we will denote them as b and c. Then, m'=m=a and the sum over μ and μ' is taken by considering the two Zeeman states b and c. When the applied field is large enough to completely resolve the magnetic states of the excited level we have $\omega(\mu,\mu') \cdot \tau >> 1$ and equation (5) reduces to

$$R_1 = R_o \sim |f_{ab} g_{ba}|^2 + |f_{ac} g_{ca}|^2$$

The rate is just the sum of the individual rates and no interference term is present. When the applied field is near the cross-over point, the excited magnetic states are close to one another and cannot be resolved. Now, $\omega(\mu,\mu') \cdot \tau \leq 1$ and equation (5) becomes

$$R_2 \sim R_o + \frac{f_{ba} f_{ac} g_{ca} g_{ab}}{1 + i\tau\omega(b,c)} + \frac{f_{ca} f_{ab} g_{ba} g_{ac}}{1 + i\tau\omega(c,b)}$$

$$= R_o + \frac{A}{1 + i\tau\omega(b,c)} + \frac{A^*}{1 - i\tau\omega(b,c)}$$

where $A = f_{ba} f_{ac} g_{ca} g_{ab}$ and $A^* = f_{ca} f_{ab} g_{ba} g_{ac}$. The interference effect

occurs in the terms containing A and A*. In the case where the matrix product A is real, A*=A and we have

$$R_2 \sim R_o + \frac{2A}{1 + \tau^2\omega^2(b,c)}$$

which is the well known Lorentzian distribution. In the case where the matrix product A is imaginary, A*=-A, and we have

$$R_2 \sim R_o - \frac{2Ai\omega(b,c)}{1 + \tau^2\omega^2(b,c)}$$

which is a dispersion shaped distribution. In the case where the matrix product is a complex number, a mixed Lorentzian and dispersion distribution will be obtained. A is real, imaginary or complex depending upon the direction and the polarization of the incoming and outgoing light, and all three cases can be realized experimentally.

If any of the matrix elements in A or A* vanish, there will be no interference and $R_2=R_1$. This means that b and c must be populated coherently in an absorption process and also emit coherently for interference to take place in the cross over region. In other words, if the states are made degenerate by the magnetic field, a single photon can excite both states coherently and a finite phase relation exists between the wave functions representing the excited states. This is analogous to the classical phenomenon of a double slit interference pattern where the same photon can be shared by

both slits. Also, it should be noted that the total absorption cross section for the resonance radiation is independent of whether or not the levels are crossed. The only effect of the crossing is to modify the angular distribution of the re-emitted radiation. Furthermore, the Hanle effect is a crossing at zero field so that for this special case the matrix elements are all field independent.

Lurio et al. have considered the external static magnetic field to be along the z axis and have defined a set of complex unit vectors $\hat{e}$ with components

$$e_{\pm} = e_x \pm ie_y = (\cos\theta\cdot\cos\alpha \pm i\cdot\sin\alpha)\exp(\pm i\phi)$$

$$e_z = -\sin\theta\cdot\cos\alpha$$

to allow for arbitrary incident and observing directions. The incident light enters along a direction defined by (θ,ϕ) and with the electric vector $\hat{e}$ making an angle α with respect to $\hat{\theta}$. The scattered light is observed along (θ',ϕ') with its electric vector $\hat{e}'$ making an angle α' with respect to $\hat{\theta}'$ as shown in Figure 4. The general expression for the rate of scattering of resonance radiation can be written as

$$R \sim \sum_{\mu,\mu'} \frac{F_{\mu\mu'}G_{\mu'\mu}}{1 + i\tau\omega(\mu,\mu')} \tag{6}$$

where $F_{\mu\mu'} = \sum_m f_{\mu m} f_{m\mu'}$ and $G_{\mu'\mu} = \sum_m g_{\mu' m} g_{m'\mu}$ are the excitation and re-radiation matrices respectively. Lurio et al. (1964) have

Figure 4.

Coordinate and polarization system used in the calculation of the Hanle effect.

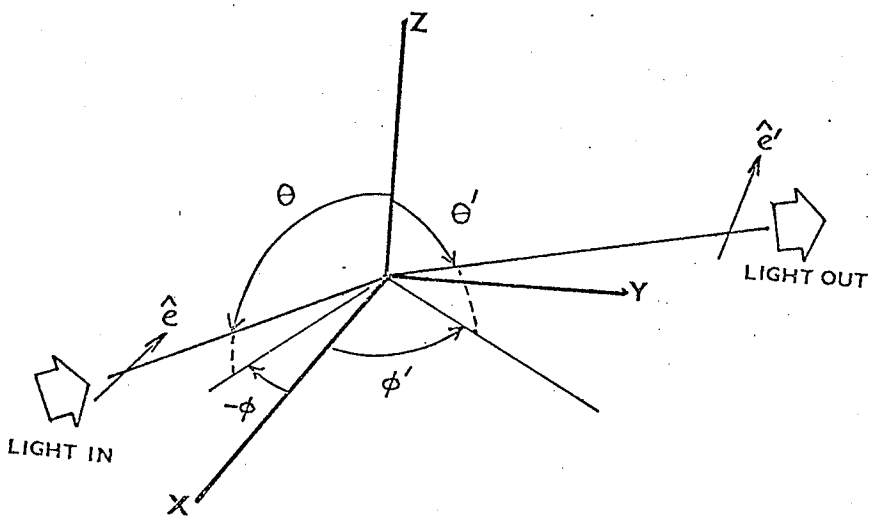
Z
θ
θ′
ê′
LIGHT OUT
Y
ê
LIGHT IN
-φ
φ′
X

calculated $F_{\mu\mu'}$ for the resonance scattering with J=0→J=1→J=0, and find,

$$(7) \qquad F_{\mu\mu'} = \begin{vmatrix} e_+e_-/2 & -e_-e_z/\sqrt{2} & -e_-^2/2 \\ -e_+e_z/\sqrt{2} & e_z^2 & e_-e_z/\sqrt{2} \\ -e_+^2/2 & e_+e_z/\sqrt{2} & e_+e_-/2 \end{vmatrix} \cdot C$$

where C represents the reduced radial matrix elements which can be absorbed into the constant term I_o in equation (3). For this case the re-emitted matrix $G_{\mu'\mu}$ is identical to equation (7) except that all quantities are primed. The matrix products can be collected into three groups according to Δμ=0,1,2 which leads to

$$R = R(\Delta\mu=0) + R(\Delta\mu=1) + R(\Delta\mu=2)$$

where

$$(8) \qquad R(\Delta\mu=0) \sim \frac{1}{2}(e_+e_-e'_+e'_-) + e_z^2e'^2_z$$

$$(9) \qquad R(\Delta\mu=1) \sim \frac{e_ze'_z}{2}\left[\frac{(e_-e'_+ + e_+e'_-) + i\tau\omega(1,0)(e_+e'_- - e_-e'_+)}{1+\tau^2\omega^2(1,0)} + \frac{(e_-e'_+ + e_+e'_-) + i\tau\omega(0,-1)(e_+e'_- - e_-e'_+)}{1+\tau^2\omega^2(0,-1)}\right]$$

$$(10) \qquad R(\Delta\mu=2) \sim \frac{1}{4}\cdot\frac{(e_-^2e'^2_+ + e_+^2e'^2_-) + i\tau\omega(-1,1)(e_+^2e'^2_- - e_-^2e'^2_+)}{1+\tau^2\omega^2(1,-1)}$$

These equations differ slightly from equation 10, 11 and 12 in Lurio's (1964) paper due to the correction of the sign in the denominator of the equation (6) pointed out by Stroke et al (1968). Among these components, $R(\Delta\mu=0)$ is magnetic field independent while the other two are field dependent.

For resonance scattering with $J=2\to J=1\to J=2$ transitions, we calculate that

$$(11)\qquad F_{\mu\mu'} = \begin{vmatrix} \frac{7}{2}e_+e_- + 3e_z^2 & (\sqrt{2}-\sqrt{18}/2)e_ze_- & -\frac{1}{2}e_-^2 \\ (\sqrt{2}-\sqrt{18}/2)e_ze_+ & 4e_z^2 + 3e_+e_- & (\sqrt{18}/2-\sqrt{2})e_ze_- \\ -\frac{1}{2}e_+^2 & (\sqrt{18}/2-\sqrt{2})e_ze_+ & \frac{7}{2}e_+e_- + 3e_z^2 \end{vmatrix} \cdot C$$

and $G_{\mu'\mu}$ is the same as $F_{\mu\mu'}$ except that all quantities are primed. A direct calculation shows that $R(\Delta\mu=1)$ and $R(\Delta\mu=2)$ are identical to the equation (9) and (10) except for a constant, $R(\Delta\mu=0)$ is different from equation (8) and is equal to

$$R(\Delta\mu=0) \sim 33(e_+e_-e_+'e_-' + e_+e_-e_z'^2 + e_+'e_-'e_z^2 + e_z^2e_z'^2) + \frac{1}{2}e_+e_-e_+'e_-' + e_z^2e_z'^2$$

For resonance scattering with $J=0\to J=1\to J=2$ transitions, the expression for $F_{\mu\mu'}$ is the same as equation (7) and the expression for $G_{\mu'\mu}$ is the same as equation (11) except that all quantities are primed.

Direct calculation again shows that expressions for $R(\Delta\mu=1)$ and $R(\Delta\mu=2)$ are similar to equation (9) and (10), but, $R(\Delta\mu=0)$ is equal to

$$R(\Delta\mu=0) \sim 3(e_+e_-e'_+e'_- + e_+e_-e'^2_z + e'_+e'_-e^2_z + e^2_ze'^2_z) + \frac{1}{2} e_+e_-e'_+e'_- + e^2_ze'^2_z$$

To check these results, let us assume $\theta=\theta'=\phi'=90^\circ$ and $\phi=0^\circ$. When substituting into equations (8), (9) and (10), we obtain

$$R \sim \sin^2\alpha\cdot\sin^2\alpha' + 2\cos^2\alpha\cdot\cos^2\alpha' + \frac{4\cos\alpha\cdot\cos\alpha'\cdot\sin\alpha\cdot\sin\alpha'\cdot\tau\omega}{1+\tau^2\omega^2(1,0)} - \frac{\sin^2\alpha\cdot\sin^2\alpha'}{1+4\tau^2\omega^2(1,0)}$$

If we further assume that $\alpha=90^\circ$ and integrate over all values of α', we have

$$R \sim 1 - \frac{1}{1+4\tau^2\omega^2(1,0)}$$

where $2|\omega(1,0)|=|\omega(1,-1)|$. This expression is identical to the classical result expressed by equation (3).

If we carry out the calculation for $J=0\rightarrow J=1\rightarrow J=2$ and $J=2\rightarrow J=1\rightarrow J=2$, the effect of the additional term from $R(\Delta\mu=0)$ is simply

the addition of a constant background to the inverse Lorentzian signal. This shows that the classical result given in equation (3) is true for the normalized Lorentzian signal obtained from $J=0\rightarrow J=1\rightarrow J=0$, $J=0\rightarrow J=1\rightarrow J=2$ and $J=2\rightarrow J=1\rightarrow J=2$ resonance scattering.

For the case of $J=1/2\rightarrow J=1/2\rightarrow J=1/2$, the Breit-Franken equation gives

$$F_{\mu\mu'} = \begin{vmatrix} e_+e_- + e_z^2 & 0 \\ 0 & e_+e_- + e_z^2 \end{vmatrix} .C$$

and $G_{\mu'\mu}$ is same as $F_{\mu\mu'}$ except all quantities are primed. From $F_{\mu\mu'}$ and $G_{\mu'\mu}$ we obtain

$$R \sim (e_+e_- + e_z^2)(e'_+e'_- + e'^2_z)$$

which is independent of the applied magnetic field. This shows that excitation with linearly polarized light cannot lead to any magnetic field dependence of the intensity or polarization of the scattered light. Since no off-diagonal elements occur in $F_{\mu\mu'}$ and $G_{\mu'\mu}$ no Hanle signal can be obtained.

Gallagher and Lurio (1962) have shown that if the excitation is by circularly polarized light and if the scattered light is analyzed for circular polarization, the Hanle effect can be

observed for a J=1/2→J=1/2→J=1/2 resonance scattering. Referring to Figure 4, and using the fact that circular polarization is the sum of two linear polarizations with a phase difference of 90°, the matrix $f_{\mu\mu'}$, etc. can be obtained by,

$$f_{\mu\mu'} = f_{\mu\mu'}(\alpha=0^{\circ}) \pm i \cdot f_{\mu\mu'}(\alpha=90^{\circ})$$

Again from the Breit-Franken equation we have

$$(12) \qquad F_{\mu\mu'} = \begin{vmatrix} 1 \pm \cos\theta & \pm\sin\theta \cdot \exp(-i\phi) \\ \pm \sin\theta \cdot \exp(i\phi) & 1 \mp \cos\theta \end{vmatrix}$$

and the expression of $G_{\mu'\mu}$ is the same as $F_{\mu\mu'}$, except all terms are primed. The scattering rate is equal to

$$(13) \qquad R \sim R(\Delta\mu=0) + R(\Delta\mu=1)$$

$$\sim 1 + (\pm)(\pm)'\cos\theta \cdot \cos\theta'$$

$$+ \frac{(\pm)(\pm)'\sin\theta \cdot \sin\theta' \cdot \Gamma\cos(\phi'-\phi)}{\Gamma^2 + \omega^2}$$

$$- \frac{(\pm)(\pm)'\sin\theta \cdot \sin\theta' \cdot \omega\sin(\phi'-\phi)}{\Gamma^2 + \omega^2}$$

where the primed terms refer to the scattered light and the unprimed terms to the incident light, and $\Gamma=1/\tau$. Equation (13) is the same as equation 6 of Gallagher and Lurio (1962) except the last term has an opposite sign due to the correction of the sign in the denominator of the Breit-Franken equation. If $\theta=\theta'=90^{\circ}$ and $\phi-\phi'=90^{\circ}$, equation (13) reduces to

$$R \sim 1 - \frac{\omega}{\Gamma^2 + \omega^2}$$

which is a dispersive shaped distribution.

For a $J=1/2 \rightarrow J=3/2 \rightarrow J=1/2$ resonance scattering, direct calculation shows that both linearly polarized light and circularly polarized light lead to occurrence of an observable Hanle effect. The formulas are similar to those already discussed above.

In summary, the $J=0 \rightarrow J=1 \rightarrow J=0$, $J=0 \rightarrow J=1 \rightarrow J=2$, $J=2 \rightarrow J=1 \rightarrow J=2$ and $J=1/2 \rightarrow J=3/2 \rightarrow J=1/2$ Hanle effect can be excited with linearly polarized light and analysis can be effected without polarization. The magnetic states of the excited level which enter the experiment and which cross over at the zero field are those states for which $\Delta\mu=2$. On the other hand, excitation with circularly polarized light and circular analysis must be employed for the $J=1/2 \rightarrow J=1/2 \rightarrow J=1/2$ case. The magnetic states of the excited level which cross over at zero field are $m_j=\pm 1/2$ and $\Delta\mu=1$.

Departure from the ideal case

The theory of the Hanle effect described in the previous section is for ideal cases. In actual experiments there are a number of difficulties which can cause considerable systematic

error. These difficulties arise from the width of the incident resonance radiation, hyperfine structure, departures from strict 90° geometry, and the important coherence narrowing and collision broadening effects. Not all these difficulties can be avoided, but once they are recognized it is not hard to make the necessary corrections.

The Hanle experiment requires that the width of the exciting resonance radiation be larger than the largest Zeeman splitting of the excited levels of the atom being illuminated. This means that the incident radiation must have a uniform intensity over a frequency range sufficiently large to excite all the Zeeman states in the range of the magnetic fields used in the experiment. If this is not so, distortion will occur and the scattered signal will no longer have a standard Lorentzian distribution. This requirement can be justified by the following argument. The Zeeman splitting in a field H is given to the first order by $\Delta E_z = g_j \mu_o H$. On the other hand, the natural width of the resonance line is given by $\Delta E_n \simeq \hbar/\tau$. The theory of the Hanle effect shows that the Lorentzian shape reaches half-maximum at a field $H_{1/2}$ which is related to the lifetime τ by $\tau = \hbar/(2g_j \mu_o H_{1/2})$. This implies that at the field strength $H_{1/2}$, $\Delta E_z \simeq \Delta E_n/2$. Thus, in Hanle effect experiments the Zeeman splitting, ΔE_z, is of the same order of magnitude as the natural width ΔE_n. Doppler broadening in the source of the incident resonance light generally yields a line

width $E_D >> E_n$, and we can safely assume that the Zeeman splitting of the atoms in the scattering region is located within a constant intensity region of the line profile of the incident radiation from a hollow cathode lamp.

A second source of difficulty arises from the presence of isotopes having non-zero nuclear spin. The effect of this can be two-fold. (i) The nuclear angular momentum I alters the total angular momentum of the scattering atoms, and hence affects the angular distribution of the scattered resonance radiation, leading to a level crossing signal of different width and depth from that for the I=0 case. (ii) The presence of the hyperfine structure splitting may lead to non-zero magnetic field level crossing at fields small enough to cause a distortion of the normal zero field level crossing line shape.

In the present experiment, natural strontium which contains 82.56% of Sr^{88} and 9.86% of Sr^{86}, both of which have zero nuclear spin, is used. The odd isotope Sr^{87} has a nuclear spin I=9/2 but only a 7.02% abundance and the effect of the hyperfine structure of this will be insignificant on the Hanle line width. It can be shown from the Breit-Franken formula that the effect of the odd isotope on the measured Hanle width in Sr and Sr^+ is less than 1% even with the assumption of equal lamp intensity exciting all isotopes. So we will neglect the effect of the presence of the odd isotope, Sr^{87}, and

treat the results as zero nuclear spin in the analysis process. A similar result was justified by Dickie (1971) during experiments employing natural isotopic barium which also has odd isotopes.

Geometrical departures from the ideal case can arise from the non-zero solid angle subtended by the detecting system. If we assume $\alpha=\alpha'=90^{\circ}$, equation (8), (9) and (10) give us

$$(14) \qquad R \sim (2-\sin^2\theta') + \frac{\sin^2\theta'\cdot\cos(\phi'-\phi)}{1 + 4\tau^2\omega^2(0,1)} + \frac{2\tau\omega(0,1)\sin^2\theta'\cdot\sin 2(\phi'-\phi)}{1 + 4\tau^2\omega^2(0,1)}$$

$$= R(1) + R(2) + R(3)$$

where θ', ϕ and ϕ' are the angles shown in Figure 4 and R(1), R(2) and R(3) represent the first, second and the third term in the above equation. If the incoming and outgoing light spreads over a non-zero solid angle , symmetric with respect to the x axis and y axis, say, $\theta'\rightarrow 90^{\circ}\pm\delta$, $\phi\rightarrow 0^{\circ}\pm\xi$, $\phi'\rightarrow 90^{\circ}\pm\beta$, $\theta\rightarrow 90^{\circ}\pm\gamma$, and if we define $d\Omega=\sin\theta'\sin\theta d\theta d\theta' d\phi d\phi'$ then the average R can be obtained, following Fry and Williams (1969)

$$\overline{R} = \int R d\Omega \;/\; \int d\Omega$$

Direct calculations show that:

$$\int d\Omega = 16\xi\beta\sin\gamma\cdot\sin\delta$$

$$\int R(1) d\Omega = 16\xi\beta\sin\gamma\cdot\sin\delta\cdot(1 + \frac{1}{3}\sin^2\delta)$$

$$\int R(2)d\Omega = \frac{-1}{1 + 4\tau^2\omega^2(0,1)} 4\sin\gamma\cdot\sin\delta\cdot\sin2\xi\cdot\sin2\beta(1-\frac{1}{3}\sin^2\delta)$$

$$\int R(3)d\Omega = 0$$

Adding these together we have

$$R \sim \frac{\sin2\xi\cdot\sin2\beta(3-\sin^2\delta)}{4\xi\beta \cdot 3}\left[\frac{2\xi2\beta\cdot(3+\sin^2\delta)}{\sin2\xi\cdot\sin2\beta(3-\sin^2\delta)} - \frac{1}{1+4\tau^2\omega^2(0,1)}\right]$$

Two conclusions can be drawn from the above results. First, if ξ, β and δ approach zero, R reduces to a standard inverse Lorentzian distribution. If all quantities are non-zero, a bigger solid angle subtended symmetrically with respect to the y axis will reduce the signal to background ratio for the detecting system, since it creates a constant background. Second, R is independent of the incident angle θ so that a broad light source can be used provided that the source is symmetric about the x axis.

If θ' and ϕ' are spread into angles which are not symmetric about y axis, say, θ' from $\pi/2 - \theta_1$ to $\pi/2 + \theta_2$, ϕ' from $\pi/2 - \phi_1'$ to $\pi/2 + \phi_2'$, then direct calculations lead to

$$(15) \qquad \bar{R} \sim \frac{\sin2\xi[1 - (1/3)(\sin^2\theta_1 - \sin\theta_1\sin\theta_2 + \sin^2\theta_2)]}{4\xi(\phi_1' + \phi_2')} \cdot$$

$$\cdot\left[\frac{4\xi(\phi_1'+\phi_2')[1+\frac{1}{3}(\sin^2\theta_1 - \sin\theta_1\sin\theta_2 + \sin^2\theta_2)]}{\sin2\xi\cdot[1-\frac{1}{3}(\sin^2\theta_1 - \sin\theta_1\sin\theta_2 + \sin^2\theta_2)]}\right.$$

$$\left. - \frac{(\sin2\phi_1' + \sin2\phi_2')}{1+4\tau^2\omega^2(0,1)} + \frac{2\tau\omega(0,1)(\cos2\phi_2' - \cos2\phi_1')}{1+4\tau^2\omega^2(0,1)}\right]$$

This can be rewritten as

$$R \sim A - \frac{B}{1 + 4\tau^2\omega^2(0,1)} + \frac{C\tau\omega(0,1)}{1 + 4\tau^2\omega^2(0,1)}$$

where A, B and C are the constants dependent on the experimental situation. It is clear that not only is the signal to background ratio decreased, but a dispersive component which depends on ϕ' only is introduced. In the experiments, if the detecting slit is used with its long axis parallel to the z axis, ϕ' corresponds to the width of the slit. If wider slits are used it is possible that ϕ_1' and ϕ_2' are not equal to each other and in such case, the Hanle signal must be analyzed with equation (15) where a dispersion component which must be taken into account is present.

If circular polarization is used in both the incident and scattered light and if one assumes that the angles are spread as follows: θ from $\pi/2 - \alpha$ to $\pi/2 + \alpha$, ϕ from $0^\circ - \beta$ to $0^\circ + \beta$, θ' from $\pi/2 - \gamma_1$ to $\pi/2 + \gamma_2$ and ϕ' from $\pi/2 - \delta_1$ to $\pi/2 + \delta_2$, equation (13) yields

(16)
$$R \sim 1 + \left[\frac{(\pm)(\pm)'\Gamma \sin\beta(\alpha + \sin\alpha\cdot\cos\alpha)}{4\beta\sin\alpha(\Gamma^2 + \omega^2)} \cdot \frac{(\gamma_1 + \gamma_2 + \sin\gamma_1\cos\gamma_1 + \sin\gamma_2\cos\gamma_2)(\cos\delta_2 - \cos\delta_1)}{(\delta_1 + \delta_2)(\sin\gamma_1 + \sin\gamma_2)} \right] - \left[\frac{(\pm)(\pm)'\omega \sin\beta(\alpha + \sin\alpha\cdot\cos\alpha)}{4\beta\sin\alpha(\Gamma^2 + \omega^2)} \cdot \frac{(\gamma_1 + \gamma_2 + \sin\gamma_1\cos\gamma_1 + \sin\gamma_2\cos\gamma_2)(\sin\delta_1 + \sin\delta_2)}{(\delta_1 + \delta_2)(\sin\gamma_1 + \sin\gamma_2)} \right]$$

The last term is the main dispersive distribution while the second term is the Lorentzian distribution. The results again shows that if the angle subtended at the detecting system, δ_2 is not equal to δ_1, then there is always a Lorentzian shaped component added to the main dispersion shape distribution. The ratio of their magnitude is approximately equal to $(5/2)(\cos\delta_2 - \cos\delta_1)/(\sin\delta_2 + \sin\delta_1)$, which is usually less than 10% provided that δ_2 and δ_1 do not exceed 10° and their difference is smaller than 5°. This also shows that the peak position of the dispersive shape distribution will not be altered by the occurrence of the small Lorentzian component, although the shape may depart from the ideal case.

So far no consideration had been given for the effect of atomic density on the Hanle signal. However, in the experiments we do not measure the lifetime of a single atom, but an ensemble average relaxation time. There is always some collision depolarization of the excited atoms and trapping of the fluorescent light. If the measured width for the Hanle signal is plotted against the density of the sample atoms, at low densities, the width is inversely proportional to the density. In the intermediate density range, the width remains nearly constant while at high densities the width increases rapidly with the density. These density ranges are usually called the coherence narrowing region, the saturated region and the collision broadening region.

In the low density region, radiation trapping is the main effect and results in a narrowing of the Hanle signal width. The narrowing increases with atom density and can approach 3/10 the natural width. This can be understood from the following arguments. If the excited atom is precessing about the applied magnetic field, and emits a photon after rotating through a certain angle the emitted light will be depolarized. Then, if this depolarized emitted light is reabsorbed by a neighbouring atom, the second excited atom will reflect the orientation of the first excited atom and will also precess in the magnetic field. As a result, a smaller magnetic field is required to depolarize the net radiation pattern and the resultant Hanle effect line width is narrowed.

In the present experiment, we will study the case where linearly polarized incident light is employed and the $J=0 \rightarrow J=1 \rightarrow J=0$ transition is involved. Consequently, we will pay more attention to this special case. Since the $J=0$ ground level is nondegenerate, we will express the $J=1$ excited atom as a set of three mutually perpendicular one-dimensional dipoles. Only the one whose axis is parallel to the polarization direction of the incident light can be excited. When such aligned excited atoms decay, the resultant radiation field can be analysed in terms of the linear polarization of the electric vector parallel to and perpendicular to the alignment axis. D'Yakonov and Perel(1965a) have shown that the relevant fractions of

the radiated energies are 8/10 for the parallel polarization and 1/10 for each of the perpendicular polarizations. Thus, in a recapture process, the newly excited atom will have a probability of 8/10 of being aligned parallel to the original alignment direction and 1/10 of being along either of the perpendicular directions. This result can be re-expressed as a probability of 3/10 for an isotropic distribution of alignment and 7/10 for excess alignment along the original direction. Roughly speaking, if we define N_e as the number of excited atoms, N_g as the number of atoms in the ground level, A as the Einstein spontaneous emission coefficient, and x as the probability of recapture, then the rate equation for alignment atoms is approximately

$$dN_e/dt = -AN_e + AN_e \cdot x \cdot (7/10)$$

$$= -A(1 - \frac{7}{10} \cdot x)N_e$$

This leads to

$$N_e(t) = N_e(0) \cdot \exp[-A(1 - 0.7x)t]$$

$$= N_e(0) \cdot \exp[-\Gamma_o(1-0.7\ x)t]$$

where $\Gamma_o = A = 1/\tau_o$ is the natural width at zero beam density. The above expression gives the width at non-zero beam density as $\Gamma = \Gamma_o(1-0.7x)$. This width varies from Γ_o to $0.3\Gamma_o$ as x varies from zero to unity.

A more complete semi-classical treatment has been given by Deech and Baylis (1971). Transitions which occur among the

dipoles due to emission and reabsorption of photons can be described by the rate equation

$$dn_i/dt = -\sum_j \gamma_i^j n_j \qquad i,j=x,y,z$$

where n_i represents the density of the dipoles along the i axis and γ_i^j are elements of a real symmetric matrix γ and are given by

$$\gamma_i^j = \Gamma_o(\delta_i^j - \omega_i^j)$$

Here ω_i^j is the average probability that a photon emitted by a j dipole is absorbed by an i dipole. In an isotropic medium

$$\omega_i^j = \begin{cases} 0.8x & \text{if } i=j \\ 0.1x & \text{if } i\neq j \end{cases}$$

where x is the average reabsorption probability of a photon. According to this definition, the off-diagonal elements of γ are not zero and the matrix can be diagonalized to give three real eigenvalues, which are the characteristic decay constants for the system. The corresponding eigenvectors yield the linear combination of the n_i, each of which decays with a single decay constant. Their result shows that

$$\gamma = \Gamma_o \begin{vmatrix} 1-x & 0 & 0 \\ 0 & 1-0.7x & 0 \\ 0 & 0 & 1-0.7x \end{vmatrix}$$

with eigenvectors $n_o=(n_x+n_y+n_z)/3$, (n_x-n_z) and (n_y-n_o). When substituted into the rate equation, we have

$$n_o(t) = n_o(0)\exp[-\Gamma_o(1-x)t]$$

$$n_x(t)-n_z(t) = (n_x(0)-n_z(0))\exp[-\Gamma_o(1-0.7x)t]$$

$$n_y(t)-n_o(t) = (n_y(0)-n_o(0))\exp[-\Gamma_o(1-0.7x)t]$$

In our experiment, at time t=0, the dipole densities are $n_x(0)=n_z(0)=0$ and $n_y(0)=3n_o(0)$. The detector which is fixed in y direction can only record signals proportional to the radiation emitted by $n_x(t)+n_z(t)$, which from the above result is

$$n_x(t)+n_z(t)= n_o(0)[2e^{-\Gamma_o(1-x)t} - 2e^{-\Gamma_o(1-0.7x)t}]$$

The alignment lifetime which is the inverse of the width $\Gamma=\Gamma_o(1-0.7x)$ will be detected in Hanle effect experiments and corresponds to the coherence narrowing effect. The so called 'overall' decay constant given by $\Gamma_o(1-x)$ in the first term cannot be detected in the Hanle effect experiment and just contributes to a constant background.

D'Yakonov and Perel(1965a) have treated this problem quantum mechanically using a density matrix formalism. By transforming the density matrix $\rho(t)$ into the Liouville space, one has the expansion coefficients

$$f(\bar{r},\bar{p},t)= \frac{1}{(2\pi)^3} \int d^3\bar{K}\ e^{i\bar{K}\cdot\bar{r}} f(\bar{p},\bar{K},t)$$

where $f(\bar{p},\bar{K},t)$ is the matrix elements of $\rho(t)$ in Liouville space and $f(\bar{r},\bar{p},t)$ is analogous to the classical distribution function of the atoms. If $f_e(\bar{r},\bar{p},t)$ is the projection of $f(\bar{r},\bar{p},t)$ on the excited state and if the atom traverses a short distance while $f_e(\bar{r},\bar{p},t)$ remains unchanged during the time of the emission, then provided that no external field is present, the rate of $f_e(\bar{r},\bar{p},t)$ can be expressed as the following

$$\frac{\partial}{\partial t} f_e(\bar{r},\bar{p},t) = -\Gamma f_e(\bar{r},\bar{p},t) + \Gamma \int d^3\bar{p}' \int d^3\bar{r}' K(\bar{r}-\bar{r}',\bar{p},\bar{p}') f_e(\bar{r}',\bar{p}',t)$$

In this equation the kernel $K(\bar{r}-\bar{r}',\bar{p},\bar{p}')$ describes the excitation of a system at $(\bar{r},\bar{p})$ due to the decay of another system at $(\bar{r}',\bar{p}')$. D'Yakonov and Perel(1965a) further assume that the excited atoms have a Maxwellian momentum distribution and obtain the rate equation for the excited atom density as

$$\frac{\partial}{\partial t} n(\bar{r},t) = -\Gamma n(\bar{r},t) + \Gamma[\int d^3\bar{r}' \int d^3\bar{p}' \int d^3\bar{p}\; n(\bar{r}',t) \cdot K(\bar{r}-\bar{r}',\bar{p},\bar{p}')(2\pi mKT)^{-3/2} \exp(-\frac{\bar{p}'^2}{2mKT})]$$

To solve the above equation, it is convenient to expand the density matrix in terms of irreducible tensor operators as $n = \sum_L \sum_M T_L^{-M} n_L^M (-1)^M$. The expansion coefficients represent the multipole moments of the system and satisfy

$$\frac{\partial}{\partial t} n_L^M = -\Gamma_L n_L^M$$

where $\Gamma_L = \Gamma_o(1 - \alpha_L x)$, x is the trapping probability for photon and α_L is an angular factor. Each multipole component n_L^M decay exponentially and is independent of other components. When L=0, $\tau_{oo} = 1/\Gamma_{L=0}$ is called the overall relaxation time which characterizes the decay of the excited state. When L=1, $\tau_1 = 1/\Gamma_{L=1}$ is called the orientation relaxation time which is the decay time of the magnetic moment. When L=2, $\tau_2 = 1/\Gamma_{L=2}$ is called the alignment relaxation time which is the

decay time of the plane polarization. All these three relaxation times approach the natural lifetime $\tau_o = 1/\Gamma_o$ at zero atomic density. To detect or excite the L=1 component, circular polarized light is required. The L=0 and L=2 components are excited by any light beam.

In our experiment, the atoms are excited by plane polarized resonance light, so that only L=0 and L=2 components are present. Moreover, since the polarization axis is perpendicular to the magnetic field, only M=0 and M=2 components are excited. If we assume that the system has spherical symmetry and the detected light is not analyzed for polarization, only the (L,M)=(0,0),(2,0),(2,2) components of n_L^M can be observed. These are given by

$$n_{oo} \sim n_o = (n_x + n_y + n_z)/3$$

$$n_{20} \sim n_y$$

$$n_{22} \pm n_{2,-2} \sim n_x - n_o,\ n_z - n_o$$

The first one decays with constants $\Gamma_{oo} = \Gamma_o(1 - x\alpha_o)$ while the rest decay with $\Gamma_2 = \Gamma_o(1 - x\alpha_2)$. For J=1→J=0, α_2 is equal to 7/10 and α_o is equal to 1. These results are consistent with the semi-classical results.

When there is branching from the excited level, Saloman and Happer (1966) have extended the theory by separating $\rho(t)$ into the sum $\rho^{(L)}(t)$. They obtain $\Gamma = \Gamma_o(1 - \sum_i x_i \alpha_i \beta_i)$ for every component of L. x_i and α_i have the same meaning as before except n is changed to n_i and $\beta_i = \Gamma_i/\Gamma$ is the branching ratio of the i^{th} branch. In special

cases, when most of the branches are weakly trapped, but one is strongly trapped, the above expression can be employed to determine the branching ratio of that strongly trapped branch.

Collision broadening is caused either by collisions with foreign atoms or by collisions with atoms of the same kind. In the former case, the colliding atom may give or lose some kinetic energy to the excited atom. This may lead to a redistribution of the population of the Zeeman states, which in turn changes the polarization of the scattered light. If the excited atom is in a coherent mixture of states, the coherence can be partially destroyed. The effective cross section is large compared to the gas kinetic cross section. When the collision is between the same kind of atoms, beside the phenomena described above, another important process 'resonance transfer of the excitation' occurs. By exchanging the excitation energy between the colliding atoms without radiation, the natural width of the original excited state is broadened. The effective cross section for such collisions can be extremely large and can exceed the cross section for foreign atoms by several orders.

For our experimental situation, only collisions between the same kind of atoms are possible. Classically, this broadening has the typical Holtzmark form which takes place when the pressure of the absorbing gas is increased (Mitchell and Zemansky 1934).

The line width is given by $\Gamma = \frac{1}{2\tau} + 4\sigma_H^2 N(\pi RT/M)^{1/2}$, where N is the density of the absorbing atoms, σ_H^2 is the effective cross section associated with Holtzmark broadening and $(4\pi RT/M)^{1/2}$ is the average speed of the atoms.

Quantum mechanically, according to D'Yakonov and Perel (1965b) if $f_{mm'}$ represents the density matrix of the excited atom A before collision, the change of density matrix of the excited atom in one collision is

$$\Delta f_{mm'} = f_{mm'} - f^A_{mm'} - f^B_{mm'}$$

where $f^A_{mm'}$ is the projection of the density matrix of atom A on the excited state after collision, and $f^B_{mm'}$ is the corresponding quantity for the colliding ground state atom B. The subscripts m and m' number the Zeeman states of the excited level. The increment of the density matrix per unit time referred to one excited atom is

$$\frac{\partial}{\partial t} f_{mm'} = -n\int \Delta f_{mm'} \zeta \cdot d\zeta v^3 dv \Phi(v) d\Omega$$

where $d\Omega = \sin\theta d\theta d\phi d\chi$, n is the concentration of normal atoms, θ and ϕ are the polar angles of the relative velocity v, $\Phi(v)$ is the distribution function of the relative velocity, and χ is the azimuthal angle of the impact parameter ζ in a plane perpendicular to v. By assuming a Maxwellian momentum distribution for the excited atoms and by expanding the density operator into the irreducible tensor as done in the coherence narrowing case, one has

$$\frac{d}{dt} n_L^M = -\gamma_L n_L^M$$

where γ_L is the self-broadening associated with different orders of L which has the same meaning as in the narrowing case. If the interaction between the normal and excited atoms is assumed to be the dipole-dipole interaction

$$\hat{V}(t) = r^{-5}[3(\hat{d}_A \cdot \vec{r})(\hat{d}_B \cdot \vec{r}) - (\hat{d}_A \cdot \hat{d}_B)\vec{r}^2]$$

where d_A and d_B are the operators of the dipole moments of A and B and $\vec{r} = \vec{\zeta} + \vec{v}t$ is the radius vector drawn from one atom to the other. Then γ_L can be written as

$$\gamma_L = n\pi(\frac{\lambda}{2\pi})^3 \Gamma_o \int_o^\infty \frac{d\alpha}{\alpha^2} \tau_L(\alpha)$$

where $\alpha = (\frac{\lambda}{2\pi})^3 \Gamma_o/(\zeta^2 v)$ and the function $\tau_L(\alpha)$ depends on α and the angular momentum of the ground and excited states. D'Yakonov and Perel(1965b) have carried out the solution of $\int_o^\infty [d\alpha/(\alpha^2)]\tau_L(\alpha)$ for the J=1→J=0 transition. Their result shows

$$\gamma_{L=0} = 0$$
$$\gamma_{L=1} = 0.035 n\lambda^3 \Gamma_o$$
$$\gamma_{L=2} = 0.028 n\lambda^3 \Gamma_o$$

Among these, only γ_2 can be observed under our experimental set up. In the literature, γ is usually expressed as $\gamma = n\sigma\bar{v}$, where σ is the effective collision cross section. Comparing with the above equation, we have

$$\sigma_2 = \frac{0.028\lambda^3 \Gamma_o}{\bar{v}}$$

for the J=1→J=0 transition. Various authors give various expressions

for σ_2, differing because of the various collision theory approximations applied.

The inclusion of coherence narrowing and collision broadening formulas for branching, results in a general expression,

$$\Gamma = \Gamma_o - \sum_i x_i \alpha_i \beta_i \Gamma_o + \sum_j N_j \beta_j \sigma_j \bar{v} \tag{17}$$

where i and j are summed over all possible decay channels. Theoretically, when an experiment has covered the narrowing, saturated and broadening regions, one should be able to obtain the values of Γ_o, β, x and σ. In practise, Γ_o and σ can be determined easily from the slope of the narrowing and broadening region of the overall experimental curve. But, β and x are usually very hard to estimate because the saturated region is not always well defined and because the experimental cell is not always spherically symmetric.

Note on oscillator strength

The concept of oscillator strength has its origin in classical electromagnetic dispersion theory. In the theory, the optical behaviour of N_n atoms per unit volume are considered to be equivalent to N_c classical oscillators. Mitchell and Zemansky (1934) have given the classical absorption cross section for each oscillator as $a_c=\pi e^2/(m_e c)$, where m_e and e are the rest mass and charge of the

electron. The classical atomic absorption coefficient for N_c oscillator is

$$\frac{dI \cdot d\Omega}{I \cdot d\Omega} = - \frac{e^2 \pi}{m_e c} N_c$$

where I is the incident light intensity.

The corresponding quantum atomic absorption coefficient can be expressed by the Einstein B coefficient. Using n to describe the lower state and m the upper state, Foster (1964) has given this as

$$\frac{dI d\Omega}{I d\Omega} = - \frac{1}{4\pi} B_{nm} N_n h\nu_{nm}$$

Equating these two equations, we have

$$f_{nm} = \frac{N_c}{N_n} = \frac{m_e c}{4\pi^2 e^2} B_{nm} h\nu_{nm}$$

In this equation, f_{nm} is defined as the ratio of N_c/N_n which can be regarded as the number of classical oscillators equivalent to one atom in state n and is named as the 'absorption oscillator strength' and usually just called 'oscillator strength'.

It is well known (Condon and Shortley 1936) that

$$g_n B_{nm} = g_m B_{mn}$$

$$A_{mn} = \left(\frac{2h\nu^3}{c^2}\right) B_{mn}$$

where B_{mn} is the induced emission coefficient and A_{mn} is the Einstein spontaneous emission coefficient and g_n and g_m are the statistical weights of the lower and upper state respectively. We then have

$$f_{nm} = \frac{m_e c^3 g_m}{8\pi^2 e^2 \nu^2 g_n} A_{mn} \tag{18}$$

$$= 1.499\lambda^2 \frac{g_m}{g_n} A_{mn}$$

Equation (18) is the basic equation which we employ to calculate the oscillator strength from experimental data in this work.

The calculation of oscillator strengths is equivalent to the calculation of the dipole matrix element $\langle \gamma SLJ | P | \gamma' SL'J' \rangle$ where $P = \sum_i r_i$ is the electric dipole moment operator. This can be reduced to (Shore and Menzel 1968)

$$\langle \gamma SLJ | P | \gamma' SL'J' \rangle \sim L(SLJ, SL'J') R(\gamma L, \gamma' L') \langle nl || r || n'l' \rangle$$

Here $L(SLJ, SL'J')$ is the line factor which gives the relative strength of the lines within a multiplet and $R(\gamma L, \gamma' L')$ is the multiplet factor. Both the line factor and the multiplet factor are readily evaluated for simple cases and are given in the book by Shore and Menzel (1968). The reduced matrix element $\langle nl || r || n'l' \rangle$ which depends on the quantum numbers of the jumping electron and the radial wave function is given by

$$I(nl,n'l') = \langle nl||r||n'l'\rangle$$

$$= \begin{cases} (-1)^{l-l_>}\sqrt{l_>}\,P_{nl}(r)P_{n'l'}(r)r\cdot dr & \text{if } l'=l\pm 1 \\ 0 & \text{if } l'\neq l\pm 1 \end{cases}$$

where $l_>$ is the larger value of l and l', and, $P_{nl}(r)$ and $P_{n'l'}(r)$ are the radial wave functions of the jumping electron. Once I(nl,n'l') is known, f can be calculated. The calculation of I involves the determination of the wavefunctions and the evaluation of the radial integrals. The wavefunctions can be obtained by the Hartree-Fock method or from various of semi-empirical methods.

The evaluation of the radial integral can be approached in three different forms, which are: (a) the dipole-length form, (b) the dipole-velocity form, and (c) the dipole-acceleration form. For one electron atoms, the three expressions yield identical results because the exact wave function can be obtained. For atoms which contain more than one electron, various approximate methods are employed to obtain the approximate wave functions, and the three expressions above give different results. This is due to the fact that different ranges of the value of r give the principal contribution to the radial integral in different forms. In the dipole-length form, the contribution to the radial integral from region of large r is important, whereas in the acceleration form, the region near the nucleus is important. The velocity form lies between these two cases. Which of the forms is the appropriate one depends on the type of the approximate

wave function which is used. The theoretically predicted f values for SrI and SrII from various methods are compared with the experimental values obtained in the present work and are collected in Chapter four.

CHAPTER III EXPERIMENTAL DETAILS

The basic components of the Hanle effect experimental equipment discussed in this thesis are: (1) a source of resonance radiation, (2) an atomic beam, (3) a magnetic field, (4) a scattering chamber and (5) the detecting system. The outline of the apparatus is shown in Figure 5.

The light emitted from the hollow cathode lamp is reflected into the optical entry tube by a plane mirror. Because nonpolarized light can always be considered as the superposition of two perpendicular linear polarized components, a polarizer is not necessary for those states that can be excited by linear polarized light. However, to increase the signal to background ratio for the Hanle effect, a Polaroid HN38 (or HN37) polarizer is placed at the front of the entry tube. These polarizers have a total luminous transmittance of about 38%, and the axis of polarization can be carefully adjusted to be perpendicular to the applied field direction. The linearly polarized light is then focussed by a quartz lens at the geometrical centre of the scattering chamber, where the resonance radiation meets the atomic beam and the Hanle effect takes place.

Light scattered at an average angle of 90° with respect to both the incident light and magnetic field direction is observed.

Figure 5

Schematic diagram of the experimental apparatus; the direction of observation is perpendicular to the plane of the diagram.

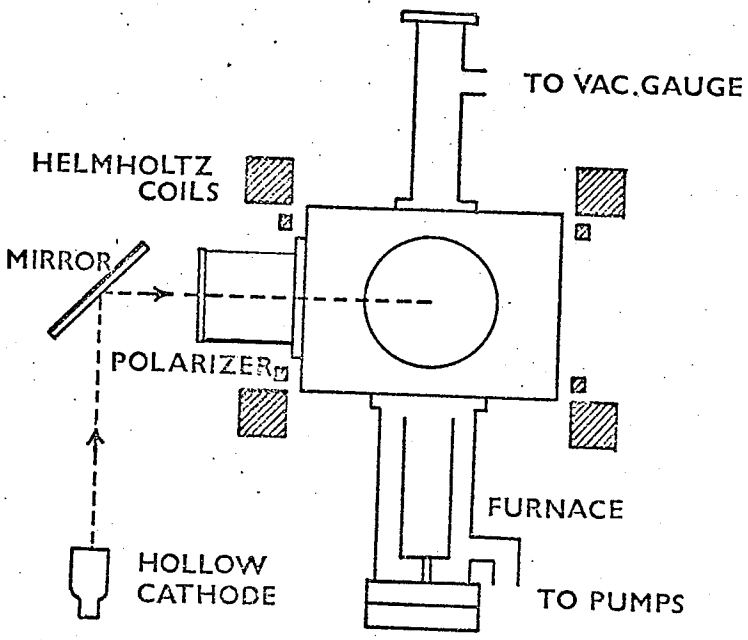
TO VAC.GAUGE
HELMHOLTZ
COILS
MIRROR
POLARIZER
FURNACE
HOLLOW
CATHODE
TO PUMPS

The exit tube surrounding the optical axis contains two quartz lenses. The first is fixed with its first focal point at the centre of the scattering chamber while the second one is moveable so that the scattered light for a selected wavelength can be exactly focussed on the entrance slit of the monochromator.

A single photon counting system is used to analyse the fluorescent light selected by the monochromator. To avoid a further decrease in light intensity, no polarizer is used in the exit arm, except when circular analysis is necessary. The inner walls of the entire scattering chamber and the entry and exit tubes are blackened to prevent unwanted reflection of light at the walls of the system. More details of the individual components are given in the following sections.

The hollow cathode lamp

A good Hanle effect light source is one that provides stable intense spectral lines which are free of self-reversal. An ideal source requires a minimum amount of sample material and affords an easy control of the output intensity of the resonance lines. It is well known that hollow cathode sources are especially suitable for the above conditions.

In the hollow cathode lamp, the discharge is maintained in a rare gas such as He, Ne, Ar or Kr. The material under investigation is imbedded in the walls of the cathode or forms the hollow cathode itself. Rare gas ions, formed in a dc discharge between the anode and the cathode, are accelerated by the electric field, strike the cathode and sputter atoms out of the cathode into the gas. Once in the vapour phase, the atoms under investigation are excited by collisions and subsequently radiate spectral lines. The width of the lines is determined by the Doppler broadening and some self-absorption.

The lamp used in this work, which has been described by Dickie (1971) in his thesis, is shown in Figure 6. The lamp is made from two standard conical glass joints. The anode is a thin sheet of aluminium rolled into a hollow cylinder and inserted into the vertical glass tube. A quartz lens which has a focal length equal to the length of the vertical glass tube forms the exit window of the light source. The cathode is a cylindrical copper block tapered at the top to match a standard conical glass joint and is hollowed at the other end. Copper is chosen for good heat conduction. The sample material is placed in the copper block in the form of a closely fitting cylinder. Then, a hole is drilled into the sample to form the hollow of the hollow cathode. Both the copper block and the quartz lens are sealed to the conical glass envelope with laboratory black wax.

Figure 6

Hollow cathode lamp used in this work.

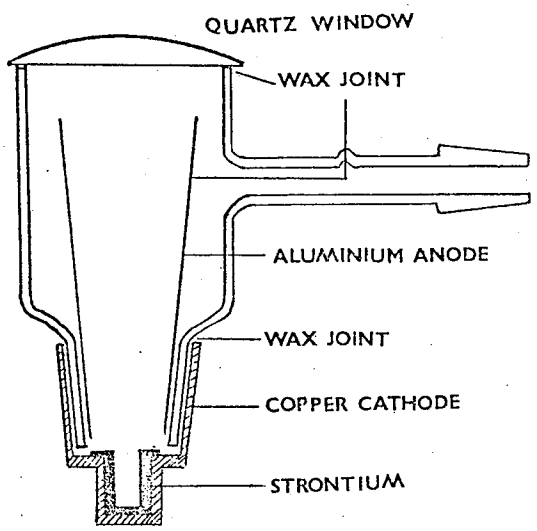
QUARTZ WINDOW
WAX JOINT
ALUMINIUM ANODE
WAX JOINT
COPPER CATHODE
STRONTIUM

The gas handling system of the lamp is shown schematically in Figure 7. The lamp is joined to the gas handling system and pumped continuously for several days. After outgassing, pure neon gas at a pressure of a few mm Hg is introduced into the system through the stopcocks. The pressure of the gas is monitored by measuring the length of the dark space in a discharge tube. During operation a dc power supply provides 200 to 400 V across a series combination of the lamp and a variable ballast resistance. The current in the lamp is controlled by adjusting the supply voltage. For strong lines the current should not exceed 75 mA to prevent self-reversal. For weak lines where self-reversal is not important, the current employed may be greater than 100 mA. The temperature of the gas and thus the Doppler broadening of spectral lines is controlled by cooling the cathode with an ice water bath. Since the separation of the anode and the cathode is less than the length of the dark space, the positive column of the discharge is suppressed. At a suitable pressure, the discharge consists of a negative dark space close to the inner wall of the cathode and a very bright negative glow which fills the hollow cathode. However, it is found that the sputtered material deposits on the glass envelope, and if the distance between the anode and the cathode is too small, arcing occurs and the life of the lamp is shortened. The presence of small quantities of impurities with low ionization potentials quenches the resonance lines and must be avoided. A liquid nitrogen-cooled charcoal trap is used to remove such impurities from

Figure 7

Gas handling system for the hollow cathode lamp.

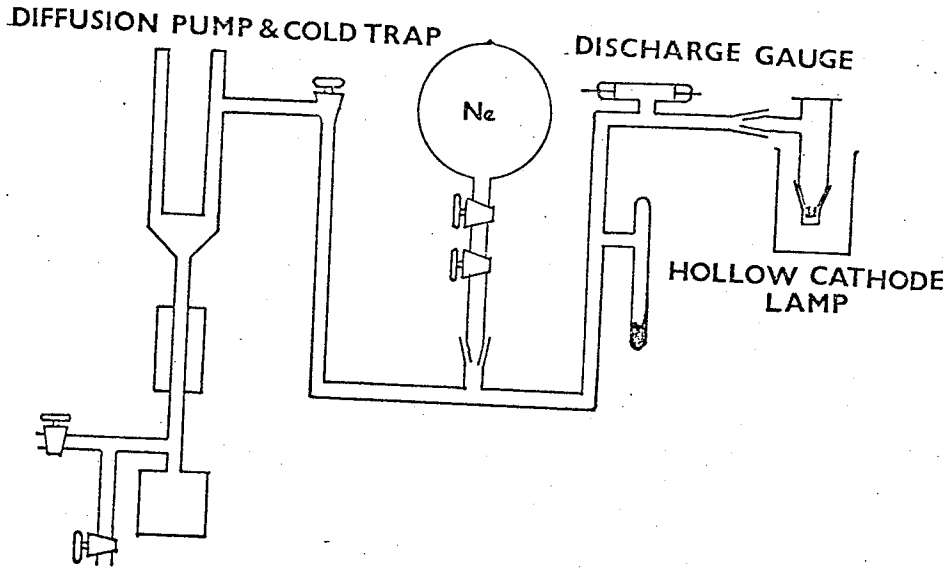
DIFFUSION PUMP & COLD TRAP
Ne
DISCHARGE GAUGE
HOLLOW CATHODE LAMP

the system. After the cathode temperature and the gas pressure have stabilized, the lamp output remains steady for an hour or more and the lamp current serves as an indicator of the spectral line intensity. In this work, the first and second spectra of strontium are produced by the same lamp with a high intensity.

Scattering chamber and atomic beam

The design of the vacuum chamber is shown in Figure 8. The central scattering region is made with four aluminium plates sealed with O-rings on the frame. The top plate holds a brass tube with an air inlet valve and an ionization vacuum gauge. The bottom plate, made from brass, supports the furnace. Copper tubing is soldered to the furnace chamber, and tap water is circulated through the tubing to cool this section. Aluminium, brass and copper are chosen because they are non-magnetic. The whole chamber is evacuated by a 4 inch oil diffusion pump backed by a two stage rotary pump. The operating pressures are less than 10^{-5} mm Hg.

The furnace is made from a 1 inch diameter steel rod with a 7/8 inch hole bored in it. A thin layer of boron nitride is placed on the outside and a spiral of nichrome wire is wound on it. Magnetic fields, which are produced by this high furnace current, and which would interfere with our observations are avoided by using

a bifilar winding. This provides two equal windings but with opposite currents so that the magnetic field is small enough to be neglected. The ends of the windings are secured by wrapping them around screws insulated with ceramic beads. A coating of boron nitride about 3 mm thick is then applied to insulate the windings. Metallic strontium in the form of a rod with a diameter of 3/4 inch is used to fill the furnace. The whole unit is held in place by means of an insulated stand mounted on the bottom plate of the vacuum chamber. The power for the furnace is controlled from a dc supply. Typical operating voltage across the furnace range from 20 to 35 volts with current from 7.5 to 12 amperes. The furnace temperature can be varied by changing the voltage, but about two hours are needed to reach a stable condition. Beyond this stabilization period the furnace yields beams which are adequately steady over periods which are long compared to the time required for individual measurements. The furnace used in this work has a useful life of about 120 hours.

The velocity distribution of the strontium atoms inside the furnace is Maxwellian and given by (Saplakoglu 1972)

$$\frac{dN}{dv} = \frac{4Nv^2 \exp(-v^2/\alpha^2)}{\sqrt{\pi}\cdot\alpha^3}$$

where $\alpha=(2KT/M)^{1/2}$ is the most probable atom velocity. Since the flow of the atom from the furnace mouth is proportional to the velocity, the beam intensity becomes

$$I(v) = \frac{2I_o v^3 \exp(-v^2/\alpha^2)}{\alpha^4}$$

The melting point of strontium is 1040 $^{\circ}$K and the vapour pressure increases to 1 mm of Hg at 1170 $^{\circ}$K. We find that a typical operating temperature is near 1000 $^{\circ}$K, so that the most probable velocity of the strontium atoms is between 10^4 to 10^5 cm/s. At these temperatures nearly all atoms are in the ground state, because the thermal energies of the atoms are much smaller than the energy of the first excited level. Even if some strontium atoms are excited by a discharge at the furnace mouth to the 5snp $^1P_1$ levels, none of these excited atoms can reach the scattering region as they travel only a very short distance during their lifetime. However, the metastable 5s4d $^1D_2$ and 5s5p $^3P_{2,0}$ levels cannot decay by electric dipole radiation and atoms in these levels may get to the scattering chamber.

The furnace mouth and the cylindrical tube BC, as shown in Figure 8, form a beam collimating system. The aperture at the top of the collimating system can be changed by replacing the tube BC with different sized central holes when necessary. The circular cross section of the beam is less than 2 cm^2 at the scattering region. After passing the scattering region the beam is condensed on the top plate of the upper tube which is at room temperature. A liquid nitrogen trap has been used to lower the temperature of the top plate but not

Figure 8

Scattering chamber and furnace.

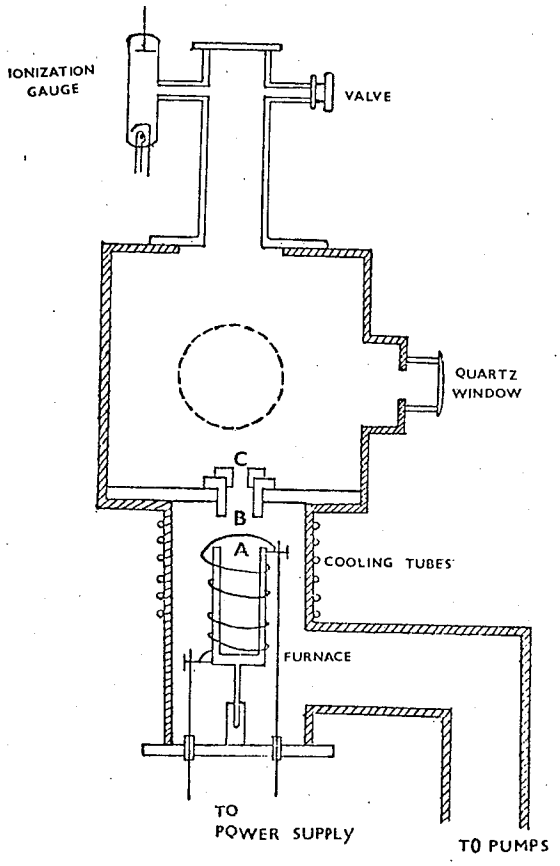
IONIZATION GAUGE
VALVE
QUARTZ WINDOW
C
B
A
COOLING TUBES
FURNACE
TO POWER SUPPLY
TO PUMPS

much improvement is observed.

The temperature of the furnace could be reliably measured by several means. However, the rate of evaporation depends on surface contamination so that an estimate of beam density from temperature and vapour pressure would not be reliable. Fortunately, when we are interested only in the lifetime measurements, the absolute atomic density is not required. A relative density can be obtained from comparisons of the output Hanle signal intensity. When absolute density is needed, a simple method coupled with the collision broadening theory is employed and has led to reasonable results. This will be discussed in the next chapter.

The magnetic field

The vertical homogeneous magnetic field at the scattering chamber is generated by two pairs of Helmholtz coils, both fixed horizontally. The outer one, 40 cm in diameter, is in series with a 0.1 Ω standard resistor and is supplied by a regulated dc source. The standard resistor is monitored by a digital voltmeter accurate to 0.01%, and gives the current flowing in the outer coils. Changing the direction of the current reverses the field direction. The current-field relation is measured with a Rawson-Lush rotating coil gaussmeter with an accuracy of better than 0.01%. Table 1 shows one set of calibration data. The

TABLE 1

Calibration of Helmholtz coils

Volts across 0.1 Ω	Magnetic field in gauss
+ 0.8006	+ 248.502
0.7006	217.439
0.6003	186.326
0.5001	155.232
0.4006	124.314
0.3009	93.361
0.2002	62.117
- 0.2022	- 62.753
- 0.3007	- 93.349
- 0.4005	- 124.306
- 0.5005	- 155.359
- 0.6004	- 186.436
- 0.7004	- 217.446

Least squares fit to a straight line gives:

Slope equal to 30.78 ± 0.01 G/A

result is linear from 0 to about 200 gauss, which is more than enough to cover the saturation magnetic field range for the Hanle effect experiment in the present work. Also, it is found that the uniform field is spread over a cube with sides up to 3 cm. This is determined with a constant current, and by moving the probe of the gaussmeter to different positions.

The Hanle signal can be observed as the scattered light intensity is measured while the magnetic field is changed in a sequence of steps from a maximum in the positive z direction to a maximum in the negative z direction. This has been a common technique for Hanle effect experiments. However, the parameters of an experimental situation vary with time, and it is better to obtain the information for the whole magnetic field range within a short period, so all data points of the Hanle Lorentzian distribution are taken under the same conditions. The inner pair of Helmholtz coils is introduced for this purpose. These coils have a 30 cm diameter and are in series with a 0.6Ω standard resistor and are supplied by a ramp generator with a symmetric saw-tooth output voltage. The period of the ramp can be selected from a range of 0.5 to 10 seconds. The output voltage is adjusted so that the maximum potential drop across the 0.6Ω standard resistor is not greater than -4 V, to match the multi-channel analyzer requirement. A potentiometer which controls the baseline is available on the power supply. Another potentiometer is provided to adjust the wave form

until an exact symmetric triangular ramp wave with constant slope on both sides is obtained. The sweep field produced by the inner coils varies from 0 to about -200 gauss. This together with the steady field of the outer coils results in a net range of -100 to +100 G in the scattering region, varying with the period of the ramp. This net variable field sweeps the Zeeman states of the level under investigation through the zero field cross over point.

The scattered light intensity is recorded by a 512 channel analyzer. Each channel has a counting time interval approximately equal to $T/(2*512)$, where T is the period of the ramp. This time interval, about $3*10^{-3}$ s, is much larger than the lifetime, about 10^{-9} s, of the level under investigation. Also, the shift in energy of the Zeeman states due to the variation of magnetic field in each counting time interval is much smaller than the natural width of the level. Thus, the variable net field we are using in the work has the advantage that it can scan the whole Hanle spectrum in just a few seconds and provide enough time for storing the counts in the appropriate channel. During every switching period, the conditions of the system remain constant so that the Hanle signal, taken in this way, is more accurate than the ones obtained by changing the field in a sequence of discrete steps during which parameters of the system may change.

The earth's field is about 0.5 G. The vertical component is added to the applied field and merely shifts the zero of the Hanle signal. This does not influence the results as we determine the width of the Hanle signal. The horizontal component of the earth's field means that the total applied field is not quite at 90° to the optical axis. Dickie (1971) used another Helmholtz coil to balance out the horizontal field but found that the experimental results remained unchanged as the horizontal component is under 0.1 G.

Data taking and analysis

The single photon counting technique is used to obtain the distribution of the scattered light intensity as a function of the magnetic field. Figure 9 is a block diagram of the electronic system employed.

The scattered light is selected by a 0.25 meter Ebert monochromator and is focused on the photomultiplier (PMT). In the early experiments, an EMI 6265B PMT was used. This tube has a relatively high dark current when operated at room temperature, and prevents us from detecting the low intensity scattered light when very low atomic beam densities are used or when the decays are from higher excited levels. The EMI tube was later replaced by an RCA C31034 PMT with a cooling system to overcome the above difficulties. Tap water is circulated through

Figure 9

Block diagram of the electronic system employed in this work.

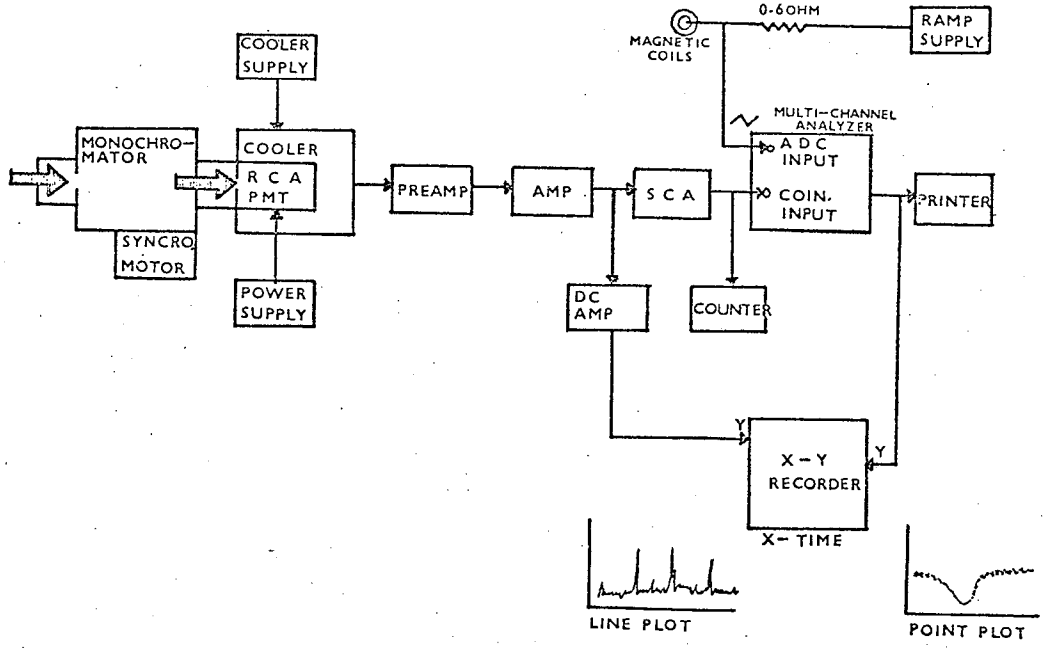
COOLER SUPPLY
MONOCHRO-MATOR
COOLER
R C A PMT
SYNCRO MOTOR
POWER SUPPLY
PREAMP
AMP
S C A
DC AMP
COUNTER
MAGNETIC COILS
0-60HM
RAMP SUPPLY
MULTI-CHANNEL ANALYZER
A D C INPUT
COIN. INPUT
PRINTER
Y
Y
X - Y RECORDER
X- TIME
LINE PLOT
POINT PLOT

the cooling system and the temperature of the PMT is maintained at about 15 degrees below the water temperature. This reduces the thermal noise and improves the signal to noise ratio.

Single photon pulses from the PMT are fed into the preamplifier and the linear amplifier, and passed to the single channel analyzer. Low energy noise or high energy pulses which are not due to single photon interactions are 'discriminated' by the SCA. The output from the SCA is fed into a counter and also into the coincidence input of the multichannel analyzer. The voltage across a standard resistor in series with the ramp coils is applied to the direct input of the multichannel analyzer. The channel number of the analogue to digital converter on the multichannel analyzer is controlled by the height of the direct input voltage. A single photon pulse arriving at the coincidence input will cause the analyzer to sample the voltage on the direct input and store the count in the appropriate channel.

As described in the previous section, the ramp is used to sweep the magnetic field. Thus, each channel in the multichannel analyzer corresponds to some fixed magnetic field strength at the scattering region. The multichannel analyzer stores the spectrum of the light intensity in counts versus channel numbers. The period of ramp is a few seconds but the counts can be accumulated over a few minutes to a few hours. The final spectrum can be plotted on a

Hewlett-Packard x-y recorder or printed out.

All data, except the 5p $^2P_{1/2}$ level of the strontium ion, are taken using the following procedures. First of all, the excitation resonance radiation is identified from the spectrum of the hollow cathode lamp. This can be done by setting a mirror in the scattering region to reflect the incident light into the detecting system. The reflected pulses are amplified by a dc amplifier and fed into the x-y recorder. The intensity is plotted as a function of time on the recorder while the grating in the monochromator is rotated synchronously with the drive time of the recorder. One of the calibrated spectra is shown in Figure 10. The light scattered from the beam is recorded in the same manner as the spectrum from the hollow cathode lamp, but with a fixed magnetic field in the saturation region and without the reflecting mirror. Although the scattered signals are weak, the lines of the scattered spectrum can be identified and assigned to the appropriate transitions in the strontium spectra. Once the Hanle signal for a certain transition is confirmed in this way, the widest possible slit is chosen for the monochromator such that no overlap with signals from other transitions is present, and the maximum possible intensity of the scattered light is obtained. After identification of the transition, the pressure of the neon in the hollow cathode, the grating monochromator and the polarizer axis are kept unchanged throughout the experiment for the same transition.

Figure 10

Spectrum of the hollow cathode lamp.

80.91 Å/cm

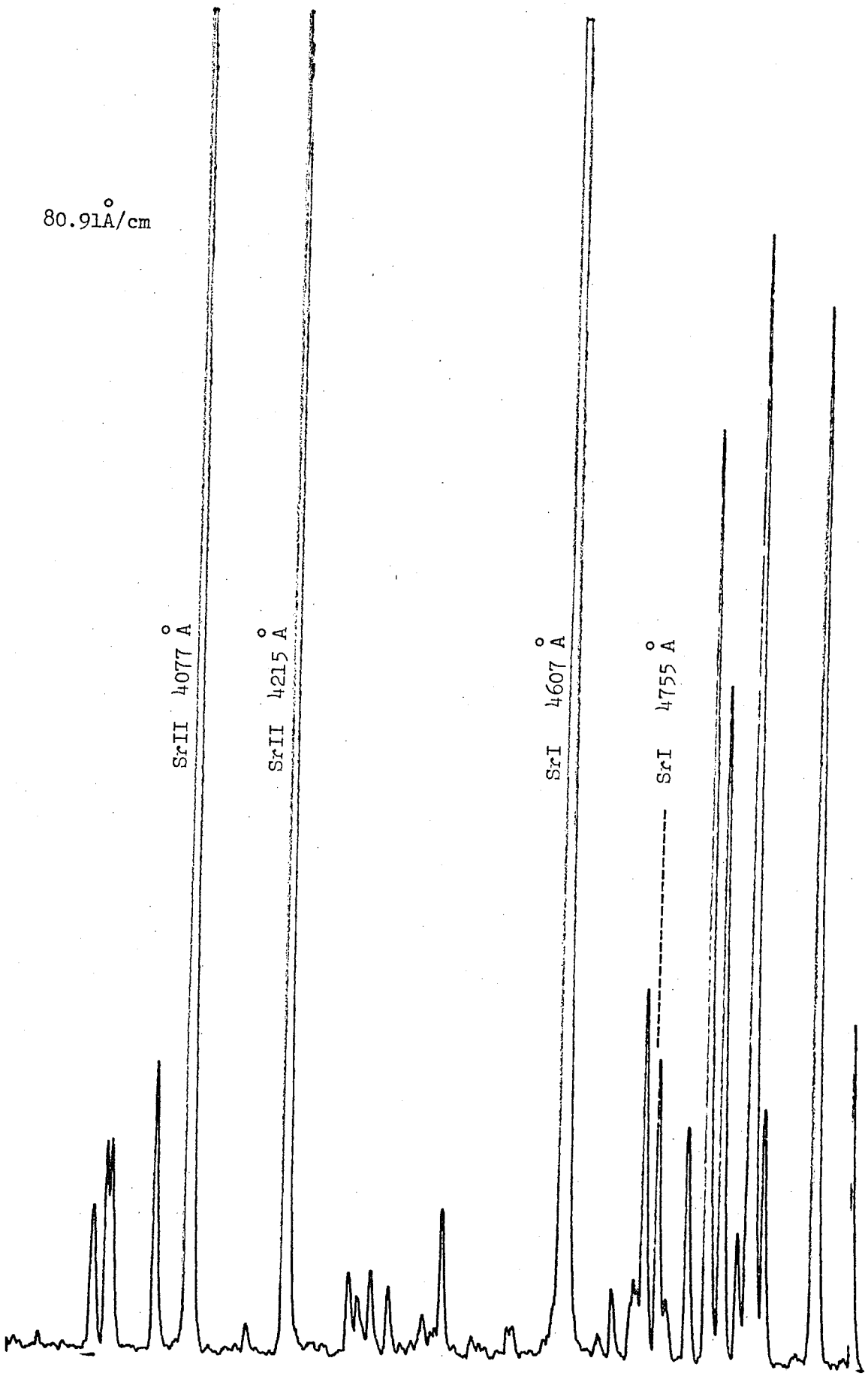
80.91Å/cm
SrII 4077 Å
SrII 4215 Å
SrI 4607 Å
SrI 4755 Å

163.07Å/cm
SrII 4077 Å
SrII 4215 Å
SrI 4607 Å
SrI 4755 Å
SrI 5331 Å
NeI 5853 Å

163.07Å/cm

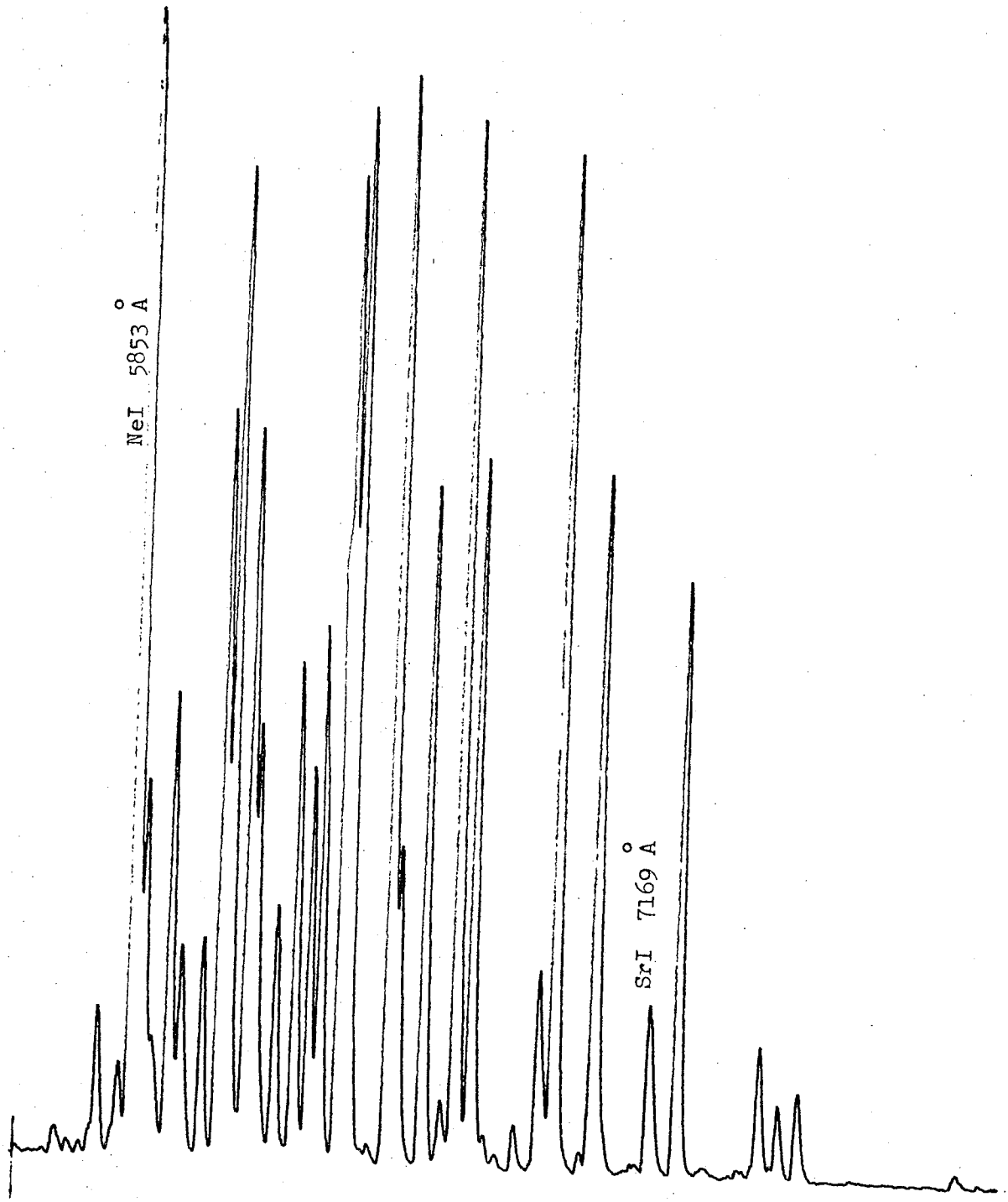

The magnetic field strength that is needed to saturate the Hanle effect for the transition is obtained by changing the steady field in discrete steps while the counts are recorded. This makes certain that the net switching field is sufficiently large for the Hanle signal under investigation. Also, before starting the runs, the output wave form of the ramp generator is plotted on the x-y recorder and is adjusted until there is a symmetric saw-tooth wave with a constant slope on both sides. Because the count rate of Hanle signal at the cross over point is much less than that at the saturated field, the count rate for strong lines, such as 4607 Å of SrI, is kept low to ensure that the dead-time of the multichannel analyzer is not important.

Since the information stored in the multichannel analyzer is a count number against a channel number, a conversion factor which changes channel number to magnetic field strength is required. It is known that the peak of the Hanle spectra corresponds to a net zero applied field. This in turn is dependent on the magnitude of the steady field. A change in the steady field will also change the peak position of the spectrum stored in the multichannel analyzer. If several runs with different steady field current are taken, and the peak positions in channel numbers are plotted against field strengths in amperes, we can get a factor C_2=(field current)/(channel number) from the slope. Table 2 gives one such result using the 4607 Å line. The points in the table are fitted to a straight line using the least squares method.

TABLE 2

Calibration of multichannel analyzer

Volts across the 0.1Ω resistor in series with the main coils	Channel number of center of Hanle resonance for 4607 Å line of SrI
0.1800	244
0.1900	251
0.2000	262
0.2100	277
0.2200	289
0.2000	263
0.1700	228
0.1700	228
0.2200	288
0.1800	243

Least squares fit to a straight line gives:

Slope equal to 0.00825 A/Channel ± 0.00001

Table 1 already gives us the factor C_1=(gauss/field current). By multiplying C_1 by C_2 we get the required conversion factor C=(gauss/channels). When this factor is known, the runs are kept at a constant steady field such that the peak of the Hanle curve is near channel number 256.

4607 Å, 7169 Å, 5331 Å and 4755 Å of SrI and 4077 Å of SrII have been studied in this way. The output data is fitted to the Lorentzian distribution given by equation (15) by a computer program run on the University of Manitoba IBM system 360. The program gives the full width at half intensity and other parameters for the best fit.

For 4215 Å of SrII, circular polarization of the incident light and circularly analysis of the scattered light is required to produce a Hanle effect. For this line the light intensity is extremely weak, and the Hanle line shape is dispersive rather than Lorentzian. For these reasons, which will be discussed further in the next chapter, we have taken the data by changing the steady field step by step and have observed counts accumulated for a fixed period of time on the counter. The result is in counts versus steady magnetic field intensity, so only the factor C_1 is needed. The data is fitted by another program according to equation (16). The program gives the width between the maximum and minimum and other information for the best fit.

In both cases the lifetime of the excited level is calculated from equation (4), where for 4215 Å observations, ΔH is

equal to half of the width between the maximum and minimum intensity, and ΔH is equal to the full width at half intensity for all the other transitions.

CHAPTER IV RESULTS AND DISCUSSION

The neutral strontium atom

The Hanle effect for the singlet principal series of SrI was observed for the $5s5p\ ^1P_1$ level using the transition to the $5s^2\ ^1S_o$ ground level at the 4607 Å, while the $5s6p\ ^1P_1$, $5s7p\ ^1P_1$ and $5s8p\ ^1P_1$ levels were observed by the transitions to the $5s4d\ ^1D_2$ metastable level, at 7169 Å, 5331 Å and 4755 Å respectively.

$5s5p\ ^1P_1$ level

The $5s5p\ ^1P_1$ level of the strontium atom decays to the $5s^2\ ^1S_o$ ground level by the emission of a 4607 Å photon or to the $5s4d\ ^1D_2$ metastable level with a photon of wavelength 64,600 Å. This later wavelength is calculated from the table of Moore (1952).

Measurements were first made at low atomic beam density using the EMI 6256B photomultiplier. The level was populated by optical excitation with linearly polarized light and the scattered resonance light was observed at 90°, as shown in Figure 3. The results are shown in table 3. All runs are taken under identical conditions except that the steady magnetic field is changed to determine the gauss-channel conversion factor. By taking the average width of these

TABLE 3

Hanle effect of $5s5p\ ^1P_1$ excited level of the neutral strontium atom.

Run number	Full width at half height
2	83.62 channels
3	83.00
4	84.11
5	81.31
7	82.38
8	83.59
9	83.14

Average ΔH=83.02 channels = 21.48 G

Lifetime τ=5.29 ± 0.10 ns

seven runs and the theoretical value g_j=1.0, we obtain a lifetime equal to 5.29±0.10 ns for the 5s5p $^1P_1$ level. The related absorption oscillator strength calculated from equation (3), is f(4607)=1.80±0.03. The Hanle signal of a typical run plotted in number of counts versus magnetic field intensity is shown in Figure 11. The count rate becomes independent of magnetic field at about ± 50 G. We shall call this portion of the curve the saturated region of the Hanle curve. The counts at the minimum of the Hanle curve show that the total background counting rate from the entire system is about 1/7 of the maximum counting rate. The fact that no $\Delta m=0$ transitions occur under this experimental set up, means that the saturated scattered intensity I_o is proportional to the difference of counts at the saturated field and the zero field.

Although the effective widths of the individual runs agree very well, and the lifetime and oscillator strength are comparable to the previous work reported in literature, two weak points still exist. First, the EMI 6256B PMT has a relatively high background which prohibits observation at lower atomic beam densities. Second, effects due to the 64,600 Å transition to the $^1D_2$ level cannot be ruled out, and if there is a branching ratio of even a few percent the value of f(4607) will be changed.

To overcome these difficulties, we have modified our experimental apparatus as described in Chapter III. The Hanle width,

Figure 11

Hanle resonance curve for 4607 Å transition. Dots are experimental points. The solid line is the fitted Lorentzian.

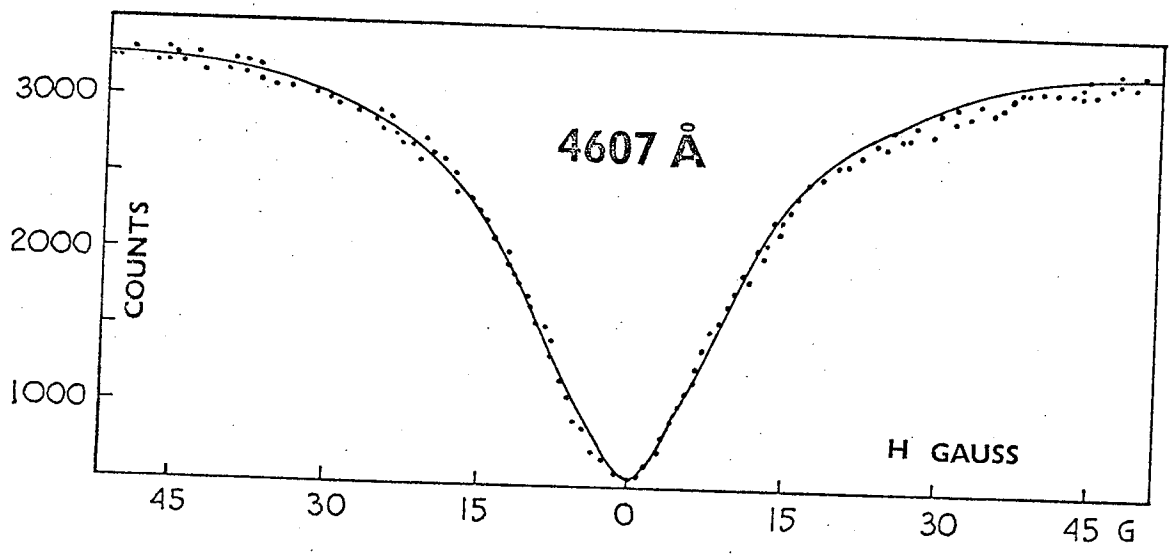
4607 Å
3000
2000
1000
COUNTS
45
30
15
0
15
30
45 G
H GAUSS

and thus the lifetime of the $5s5p\ ^1P_1$ level, has been studied as the density of the strontium atomic beam is changed over a wide range. The new runs are shown in table 4. During these observations only the atomic density is varied by changing the heating current in the furnace. The other parameters, such as the hollow cathode lamp current and the amplitude of the ramp magnetic field, are kept constant.

According to Franken (1961), the saturated intensity I_o of a Hanle signal detected in a fixed direction is proportional to both the beam density and the lamp intensity. Since I_o and the lamp intensity are known for every run, we can define an atomic density parameter ρ in arbitrary units as

$$\rho = \frac{\text{Maximum counts in the wings - Counts at H=0}}{(\text{accumulation time})\ (\text{lamp current})^2}$$

This definition is valid only for a certain constant slit width on the monochromator. If slits of different width are used, a geometric factor must be determined to convert the value of ρ to a constant slit width.

Figure 12 shows a plot of the measured Hanle width in channels against the density parameter over a wide range. The solid curve is obtained when the full spectrum of strontium from the hollow cathode lamp irradiates the strontium beam, whereas the broken curve is obtained when the incident ultraviolet lines are cut off by placing

TABLE 4

Hanle effect of $5s5p\ ^1P_1$ excited level of neutral strontium atom.

Ultraviolet included		Ultraviolet cut off	
ΔH (channels)	ρ(arb. unit)	ΔH(channels)	ρ(arb. unit)
100.18	19	85.80	79
102.12	36	81.50	94
95.19	38	85.36	280
89.78	52	89.50	390
93.95	61	91.80	760
90.51	67	97.90	13,250
92.43	86	108.10	34,750
91.07	94	118.30	45,070
94.02	125	148.35	163,600
92.05	129		
94.47	156		
95.63	248		
97.19	297		
99.70	361		
100.50	531		
100.52	855		
100.26	1,868		
105.13	5,330		
113.05	12,050		
118.23	28,800		
129.65	49,320		
137.64	66,760		
144.10	88,040		

Figure 12

The variation of the Hanle width of 4607 Å with atomic density.

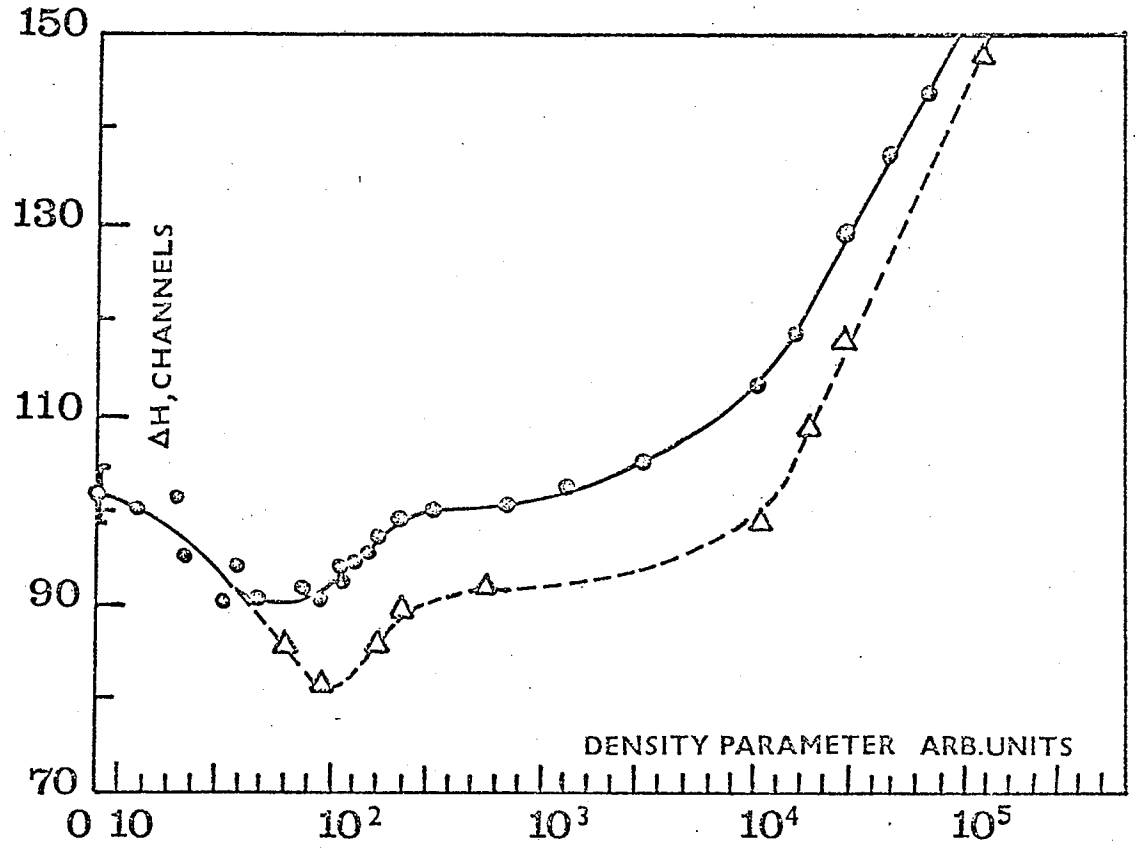
150
130
110
90
70
ΔH, CHANNELS
DENSITY PARAMETER ARB.UNITS
0 10
10^2
10^3
10^4
10^5

a sheet of glass in the incident light beam. Both curves show coherence narrowing in the region of the very low densities and a collision broadening region at the high atomic densities. At intermediate densities a not well defined saturation region exists.

When ρ is small, the Hanle signal is weak but the noise remains the same. To improve the signal to noise ratio, wider entrance and exit slits on the monochromator are used. This is found to introduce a slight skewness into the Hanle signal. The skewness indicates the presence of a dispersive component which in turn is traced to the fact that the region of irradiation of the atomic beam is not completely symmetrical about the optical axis of the system. The image of the hollow cathode source formed with resonance radiation, 4607 $\mathring{A}$, scattered from the beam, and focussed on the slit of the monochromator is pear shaped with a sharpened end. When a narrow slit is used only a small section of this image is admitted to the monochromator. However, with a wide slit the illumination is no longer angularly symmetric about the optical axis, and the skewness results. This has been proved in Chapter II by integrating over the total radiation region seen by the detecting system. A computer program based on equation (15) is used to eliminate the effect of the dispersive component on the width of the Hanle signal. Narrow slits are used on the monochromator for observations at medium and high densities and this problem does not arise.

For runs with $\rho<80$ the data were accumulated over a period of 30 minutes to an hour. The coherence narrowing region is easily identified in Figure 12 but the statistics in this region are not good.

For the case under consideration at low beam densities, equation (17) reduces to

$$\Gamma = \Gamma_o(1 - \alpha_1 x_1 \beta_1 - \alpha_2 x_2 \beta_2)$$

where the subscript 1 refers to the ground level ^1S_o and the subscript 2 refers to the $^1D_2$ metastable level. Since the branching, the probability of the reabsorption and the α value for the metastable level are much smaller than for the ground level, we can rewrite the above equation as

$$\Gamma = \Gamma_o(1 - Ax)$$

where A is a constant and x is the probability of reabsorption of 4607 $\mathring{A}$ photon by the ground level atoms. The probability depends on the density in a complicated manner. However, over these low densities x can be treated as a linear function of ρ , so that the variation of Hanle width with ρ can be fitted by a straight line and the extrapolation to $\rho=0$ gives the natural width. A least squares fit gives a value $\Delta H=24.29 \pm 0.54$ gauss at $\rho=0$. The lifetime calculated from this width is 4.68 ± 0.10 ns, where the error is the standard deviation. From Figure 12 our previous value of 5.29 ns corresponds to $\rho =80$ and thus contains a 10% systematic error due to coherence narrowing.

When ρ increases, the reabsorption probability x approaches unity. If decays to the 5s4d $^1D_2$ metastable level can be neglected, then, in the J=1→J=0 transition, the Hanle width at x=1 can be expressed as $\Gamma = \Gamma_o(1 - A)$ and A is equal to 7/10 (Saloman and Happer 1966). This means the Hanle width can be reduced to 3/10 of the natural width. This does not occur in our data. Instead, from the solid curve we have a ratio Γ_{min}/Γ_o=0.91 at ρ=100. DeZafra and Kirk (1967) have pointed out that different sized bulbs will show different widths at non-zero beam density due to different optical path lengths through the vapour. The value A=7/10 is calculated for a spherically symmetric scattering region. In our case the scattering region is not spherically symmetric, so A may not be equal to 7/10. This lack of spherical symmetry may help to explain why Γ_{min} does not reach $0.3\Gamma_o$, but cannot explain the shape of the solid curve near ρ=100, indicating that the $^1D_2$ level must be taken into account in the intermediate density region.

The $^1D_2$ metastable level may be populated by transitions from the optically excited $^1P_1$ levels or excited by the discharge in the vicinity of the furnace mouth. The optical excitation of $^1P_1$ levels above the 5s5p $^1P_1$ level is entirely by ultraviolet lines. Therefore, if we place a glass plate in the input arm to block these lines the population of atoms in the $^1D_2$ level should be reduced. The results with the ultraviolet lines excluded are shown by the dashed curve in Figure 12. The incident intensity of 4607 Å is adjusted to be the same as without

glass plate. Γ_{min}/Γ_o decreases to 0.77, but this ratio is still considerably larger than 0.3, the theoretical value. This implies that collision broadening due to atoms in the $^1D_2$ level is important in the intermediate region.

When ρ is in the high range, equation (17) becomes

$$\Gamma = K_1 + N_1\sigma_1\bar{v} + N_2\sigma_2\bar{v}$$

where the subscripts 1 and 2 represent the ground level and the metastable level respectively and K_1 is a constant. N_1 and N_2 are the densities of atoms in ground level and in the $^1D_2$ level, σ_1 and σ_2 are the related collision broadening cross sections between the atoms in the corresponding levels with atoms in the 5s5p $^1P_1$ level. In the present experiment, the intensity of the incident excitation light is maintained at a constant value and the $^1D_2$ level is mostly populated by decays from the $^1P_1$ levels. Under these conditions, N_2 reaches a maximum value but N_1 will continue to increase as ρ increases. Thus, at the highest densities we can write

$$\Gamma = K_2 + N_1\sigma_1\bar{v}$$
$$= K_2 + b\rho\sigma_1\bar{v}$$

where K_2 is the sum of K_1 and $N_2\sigma_2\bar{v}$. The width of the Hanle resonance is now proportional to the density parameter ρ, and b is the proportionality constant. This simple result allows us to make an estimate of the ratio of our density parameter ρ and the absolute number of atoms

per unit volume in the scattering region. Byron et al. (1964) have discussed the fact that, when the related oscillator strength is larger than one, the broadening cross section due to collisions between like atoms is velocity independent. Moreover, for a J=1→J=0 transition, D'Yakonov and Perel(1965b) have shown that $\Gamma_2=\Gamma_o \cdot 0.028N\lambda^3$ where Γ_2 is the contribution to the Hanle width for like atom collision broadening. If we equate Γ_2 to $b\rho\sigma_2\bar{v}$, then

$$\Gamma = K_2 + \Gamma_o \cdot 0.028N_1\lambda_1^3$$

A least squares fit of straight line in our curve beyond $\rho = 10^4$ gives us the relation

$$N_1 = 1.64 \cdot 10^9 \cdot \rho$$

and we are now able to convert our arbitrary density parameter ρ to absolute density N_1 for further discussions.

D'Yakonov and Perel(1965b) have pointed out that when $N\lambda^3 \simeq 1$, collision broadening becomes an important factor in the width of the Hanle resonance. For collisions between atoms in the $5s5p\ ^1P_1$ level and the ground level, λ=4607 Å, so we can expect collision broadening to occur around $N_1=(1/\lambda)^3=10^{13}$ atoms per cm^3. This density corresponds to $\rho=6 \cdot 10^3$ and agrees very well with our observation in Figure 12. On the other hand, if we apply the same condition, $N\lambda^3 \simeq 1$ to collisions between atoms in the $5s5p\ ^1P_1$ and $5s4d\ ^1D_2$ levels, λ_2 is 64,600 Å, and we obtain $N_2=4 \cdot 10^9$ atoms per cm^3 in the metastable level. There is no simple way to estimate the population of $^1D_2$ atoms relative

to ρ. However, the branching ratios for the two possible transitions from the excited 5s5p $^1P_1$ level are known to be related by

$$\beta_2/\beta_1 = g_2 f_2 \lambda_1^2 / (g_1 f_1 \lambda_2^2)$$

In this expression $g_1=1$, $g_2=5$ and $(\lambda_1/\lambda_2)^2$ is in the order of 0.005. If we assume that the incident resonance light of 4607 Å is strong enough to excite most of the ground state atoms to the 5s5p $^1P_1$ level in the intermediate density region, then at ρ =100, $N_2 \doteq 1.64 \cdot 10^{11} \cdot 0.005$ and is approximately equal to 10^9 atoms per cm^3 in the $^1D_2$ level. Thus, collisions of the excited 5s5p $^1P_1$ atoms with metastable $^1D_2$ atoms will become effective at much lower densities than collisions with ground level atoms. The dip in our curve near ρ=100 may be due to this effect.

When the observed lifetimes for various densities are calculated from the Hanle widths in channel numbers as shown in Figure 12, the slope of the broadening curve at high densities yields the product of collision broadening cross section and the relative average velocity $\bar{v}$. From our experimental solid curve we calculate

$$\sigma_{\bar{v}} = 5.2 \cdot 10^{-7} / \bar{v} \quad cm^2$$

for the collision between atoms in the 5s5p $^1P_1$ excited level and atoms in the ground ^1S_o level. This result is 2 to 3 orders greater than the collision broadening cross section with atoms of a foreign gas. This is reasonable since we are dealing with resonance type collisions between like atoms. Penkin and Shabanova (1968) have studied the broadening cross section of 4607 Å line for SrI with He, Ne, Ar and Kr gas. Their

results vary from $7.5 \cdot 10^{-15}$ cm^2 for He to $2.69 \cdot 10^{-14}$ cm^2 for Kr with an operating temperature of 750 °K. This gives

$$\sigma_{\bar{v}} = 1.5 \cdot 10^{-9}/\bar{v} \ cm^2 \quad \text{for He}$$

$$\sigma_{\bar{v}} = 1.7 \cdot 10^{-9}/\bar{v} \ cm^2 \quad \text{for Kr}$$

Penkin and Shabanova (1969) also studied the broadening effect of Sr-Sr collisions by the hook method. The operating temperature was 820 °K. The cross section for 4607 Å is found to be $5.8 \cdot 10^{-12}$ cm^2. This gives $\sigma_{\bar{v}} = 3.7 \cdot 10^{-7}/\bar{v}$ cm^2, and if corrected with our lifetime, this becomes

$$\sigma_{\bar{v}} = 4.7 \cdot 10^{-7}/\bar{v} \ cm^2$$

The difference between this result and ours is 10% which is smaller than the combined errors of the measurements.

Byron and Foley (1964) have given a theoretical expression for the broadening cross section as

$$\sigma_{\bar{v}} = \lambda^3 \Gamma_o/(10\pi\bar{v})$$

$$= 0.032\lambda^3\Gamma_o/\bar{v} \quad cm^2$$

D'Yakonov and Perel (1965) have modified the above equation for the alignment depolarization case and obtained

$$\sigma_{\bar{v}} = 0.028\lambda^3\Gamma_o/\bar{v} \ cm^2$$

With our measured lifetime this yields a value of $\sigma_{\bar{v}} = 5.6 \cdot 10^{-7}/\bar{v}$ cm^2. This also agrees very well with our experimental value. Another theoretical formula has been given by Omont (1966) and results in $\sigma_{\bar{v}} = 4.4 \cdot 10^{-7}/\bar{v}$

cm^2. The agreement is not as good as the former one but still within the experimental error.

A good absolute value of the oscillator strength of 4607 Å transition is very important for the strontium spectrum. Penkin and Shabanova (1962) have measured the relative oscillator strengths of $5snp\ ^1P_1$ transitions for n=5 up to n=17. If the absolute oscillator strength of 4607 Å transition can be determined accurately, all the others can be converted from the relative value to the absolute value. Also, once the absolute oscillator strengths of the principal lines are known, the oscillator strengths of the diffuse lines can be calculated from the lifetimes of the excited levels. In the present case with numerical substitution in equation (18) we obtain

$$\frac{1.499}{4.68\cdot10^{-9}} = \left\{ \frac{f(4607)}{3\cdot4607^2} + \frac{5f(64,600)}{3\cdot64,600^2} \right\} \frac{1}{10^{-16}}$$

where f(64,600) is the oscillator strength of the $5s5p\ ^1P_1 \rightarrow 5s4d\ ^1D_2$ transition. No information about f(64,600) either experimental or theoretical is available. However, if the branching ratio β's are known, then

$$f(64,600) = \frac{\beta(64,600)f(4607)\cdot64,600^2}{5\beta(4607)\cdot4607^2}$$

When this is subsitituted into the above expression, we have

$$f(4607) = \frac{1.499\cdot3\cdot4607^2\cdot10^{-16}}{4.68\cdot10^{-9}[1+\beta(64,600)/\beta(4607)]}$$

$$= \beta(4607)\cdot[1.499\cdot3\cdot4607^2\cdot10^{-16}/(4.68\cdot10^{-9})]$$

since $\beta(64,600)+\beta(4607)=1$. These branching ratios could, in principle, be measured directly. But due to the greatly different wavelengths, such a measurement is nearly impossible. Thus, we have to obtain information from Figure 12.

As discussed before, in the coherence narrowing region, the observed width is $\Gamma=\Gamma_o(1-Ax)=\Gamma_o[1-\beta(4607)x(4607)\alpha(4607)]$, where $\alpha(4607)$ equal to 7/10 as mention earlier.The trapping probability for a photon is

$$x=1-\exp(-\bar{k}/l_o)$$

where

$$\exp(-\bar{k}/l_o)=\frac{1}{\sqrt{\pi}}\int_{-\infty}^{\infty}\exp(-\omega^2)\exp(-Le^{-\omega^2}/l_o)\cdot d\omega$$

This integral is tabulated by Mitchell and Zemansky (1934) in their book. L is the characteristic cell length which can be adjusted to different values even for the same experiment to get the best fit. The mean free path of the photon with $\lambda=4607$ Å is defined as

$$l_o=\frac{3\cdot 8\cdot \pi^{3/2}\cdot \bar{v}\cdot \tau_o\cdot 10^{24}}{N\cdot(4607)^3\cdot\beta(4607)}$$

by D'Yakonov and Perel (1965a). In this equation, N represents the density of ground state atoms and $\bar{v}$ is their average velocity. For $\rho<70$, if we take $\bar{v}$ equal to $5\cdot10^4$ cm/s and L=1 cm, we find that the best fit is obtained when $\beta(4607)=0.95$. For example when $N=10^{10}$ atoms/cm^3, or $\rho=6.1$, we have $\Gamma=99.6$ channels; when $N=10^{11}$ atoms/cm^3, or $\rho=61$, we have $\Gamma=89.5$ channels. These calculated values are

quite close to the experimental values. Therefore, we adopt $\beta(4607)=0.95$ to calculate $f(4607)$, and the final result is

$$f(4607) = 1.94 \pm 0.06$$

where the error has been increased by 50% to allow for uncertainties in the branching ratio estimate. If the decay to the metastable level is neglected the f value is 2.04.

The calculation that $\beta(4607)=0.95$ means that $\beta(64,600)=0.05$. This means that the oscillator strength $f(64,600)$ is equal to $3.8^{+0.2}_{-3.0}$. The uncertainty in this is large as the change in f is large for small changes in the branching ratio. Kim and Bagus (1972) in a theoretical paper assume a branching ratio of 4% for the 64,600 Å transition. It is also of interest to compare this result with the Ba atom where the branching of the transition $6s6p\ ^1P_1$ to $6s5d\ ^1D_2$ at 15,000 Å has been estimated from 4% to 7% (Hulpke et al. (1964), Lurio (1964) and Dickie (1971)).

In Table 5 we have collected lifetime measurements and oscillator strengths calculated from experiments and from theory for the $5s5p\ ^1P_1$ level. The agreement of the recent lifetime measurements (references 5, 6 and 8 in the table) is excellent. The disagreement between the hook method and recent Hanle effect and phase shift measurements is likely due to the uncertainty in atomic density used in the hook method calculation.

TABLE 5

Lifetime of the $5s5p\ ^1P_1$ level of SrI and the related oscillator strength.

	Lifetime in ns	f(4607)	Method	Ref
Experiment	8	1.2	Dispersion	(1)
	6.4	1.5 ±0.2	Hook	(2)
	6.2	1.54±0.05	Hook	(3)
	6.1 ±0.6	1.56±0.16	Hanle	(4)
	4.97±0.15	1.92±0.05	Hanle	(5)
	4.56±0.21	2.09±0.10	Phase	(6)
	5.29±0.10	1.80±0.03	Hanle	(7)
	4.68±0.10	1.94±0.06	Hanle	(8)
		2.20±0.70	Emission	(9)
Theory		1.90	B & D	(10)
		3.18	RPA	(11)
		2.12	NBC	(12)
		2.45	SE	(13)
		2.53	HF*	(13)
		2.39	CPC	(14)
		2.46	HF*	(15)
		1.95	MCHF	(15)

Ref. (1) Prokofev (1928); (2) Ostrovskii et al. (1958); (3) Ostrovskii and Penkin (1961); (4) De Zafra et al. (1962); (5) Lurio et al. (1964); (6) Hulpke et al. (1964); (7) Dickie et al. (1973); (8) This work; (9) Eberhagan (1955); (10) Bates and Damgaard (1949); (11) Random Phase Approximation. Altick and Glassgold (1964); (12) Nodal Boundary Condition. Helliwell (1964); (13) Semi-emperical Method. Zilitis (1970); (14) Core Polarization Correction. Hameed (1972); (15) Multi-configuration Hartree-Fock. Kim and Bagus (1972).

* HF=Single configuration Hartree-Fock Method.

The Hartree-Fock approximation using a single configuration for the ground level and the excited level has been used to calculate the oscillator strength for the 4607Å transition by Zilitis (1970) and also by Kim and Bagus (1972). The value 2.53 given by Zilitis and 2.46 given by Kim and Bagus are much higher than the experimental values. This is not unexpected, for the wavefunctions given by the Hartree-Fock method are known to be inaccurate at large values of radial distance, and this is the region which is important for oscillator strength calculations. Hameed (1972) has added core polarization corrections to the simple Hartree-Fock method and obtained f=2.39 for the 4607 Å transition, but there still remains a large discrepancy with the experimental value.

Recently, Kim and Bagus (1972) have reported the calculated f value for this transition by the multi-configuration Hartree-Fock method. Their multi-configuration Hartree-Fock wave function contains two configurations for both the ground level and the excited level. They use

$$\Psi(^1S_o) = a\Phi(ns^2) + b\Phi(np^2)$$

$$\Psi(^1P_1) = a'\Phi(nsnp) + b'\Phi(npn'd)$$

where n'=n-1 and a, b, a' and b' are the configuration mixing coefficients. They obtained a value of 1.95 for f(4607). This value gives the best agreement between the theoretical and experimental results. Another result given by Altick et al. (1964) by extending the Hartree-

Fock theory by the random phase approximation method gives a value 3.18, which is really poor.

Semi-emperical methods usually give satisfactory results. The Bates and Damgaard (B & D) method (1949) is based on the assumption that the valence electron moves in a pure Coulomb field, and the experimental energy terms are used as the energy eigenvalues of the electron. From their table we calculate f(4607) equal to 1.90. This result agrees quite well with the present experimental result. Helliwell (1966) has developed a semi-emperical method called 'Nodal boundary condition method' for atoms and ions having two valence electrons. His calculated value for f(4607) is 2.12, not as good as the B & D method but is still within the calculation error. Zilitis (1970) has used another semi-emperical method for calculations of the oscillator strengths. From the tables given in his paper we calculate f(4607) equal to 2.45. The agreement is not good in this case.

$5s6p\ ^1P_1$ level

The $5s6p\ ^1P_1$ level of strontium can decay to the ground level by emitting a photon of 2932 Å, or to the $^1D_2$ metastable level by emitting a photon of 7169 Å. Another transition to the $5s6s\ ^1S_o$ level with a wavelength of 28,517 Å, calculated from the energy level tables of Moore (1952), is also allowed.

The $5s6p\ ^1P_1$ level is populated by optical excitation either from the ground level or from the metastable level. Since the incident resonance light is plane polarized perpendicular to the magnetic field, and since electric dipole transitions only are considered, the selection rule $\Delta m=\pm 1$ is valid in the excitation process. During the re-emission process both $\Delta m=0$ and $\Delta m=\pm 1$ transitions are allowed. But, the Hanle effect requires that the Zeeman states of a level under investigation and which cross to give a Hanle signal, must be excited coherently from the same initial state, and must also emit coherently to the same final magnetic state, otherwise no interference occurs. In the present case, it does not matter whether the final level is ^1S_o or $^1D_2$ as only the a and b σ components take part in the Hanle signal as shown in Figure 13. The difference between the observation of the transition to the $^1D_2$ level and the transition to the ^1S_o level is a field independent π component background superimposed on the inverse Lorentzian distribution, as already discussed in Chapter II. The transition at 7169 $\mathring{A}$ to the $^1D_2$ level is observed in this experiment for the lifetime of the $5s6p\ ^1P_1$ level.

A search for the transition at 2932 $\mathring{A}$ to the ground level has been undertaken, but due to the weak oscillator strength for this transition and absorption of the ultraviolet light in the components of the system, this scattered signal is too weak to be separated from the background.

Figure 13

Zeeman structure of upper and lower levels for $^1P_1 — ^1D_2$ transition.

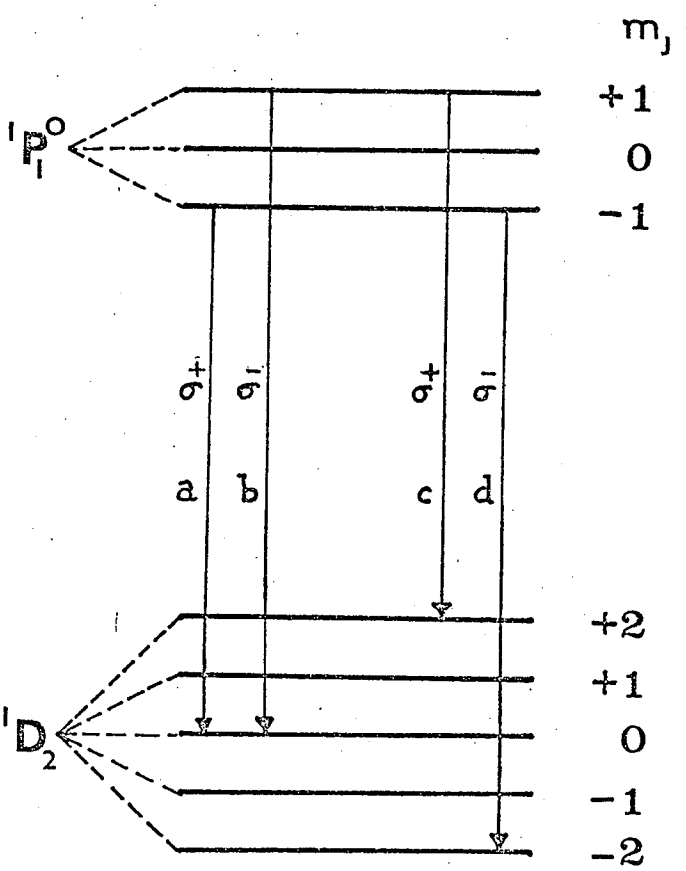
m_J
+1
0
−1
$^1P_1^o$
σ^+
σ^-
σ^+
σ^-
a
b
c
d
+2
+1
0
−1
−2
$^1D_2$

Ten independent runs, each with accumulation times of about 100 minutes have been made. Several values of the heating current for the furnace and thus several values of beam density have been employed. We did not discover a significant trend in the value of the widths of the Hanle resonance which can be connected to coherence narrowing. Also the beam densities used do not reach the collision broadening region. The fluctuations in widths seem to be random so we take the mean value of ΔH for the ten runs, 31.2±1.2 G. From this the lifetime of the 5s6p $^1P_1$ level is

$$\tau = 3.64 \pm 0.14 \quad \text{ns}$$

When numerical values are substituted into equation (18), we have

$$\frac{1}{\tau} = \frac{10^7}{1.499}[38.76f(2932) + 32.43f(7169) + 0.41f(28,517)]$$

The above expression shows that the omission of the last term produces an error which is smaller than the other errors in the experiment. The remaining oscillator strengths f(2932) and f(7169) can be calculated in several different ways.

Penkin and Shabanova (1962) obtained the relative oscillator strength ratio f(4607)/f(2932)=1000/3.40. Coupling this ratio with our experimental value, f(4607)=1.94, gives

$$f(2932) = (6.60 \pm 0.22)\cdot 10^{-3}$$

The error is estimated from a 0.3% error in the ratio and a 3.2% error in f(4607). Substituting these values into the $1/\tau$ equation, we calculate the absolute oscillator strength of f(7169) to be 1.22±0.05. Here the error arises from the error in the lifetime measurement.

Meggers et al. (1961) give the ratio of the intensities for SrI lines which have been observed from the arc emission spectrum. The intensity ratio of 4607 Å to 2932 Å is 650/2.0. If we use the relation

$$I_1/I_2 \simeq f_1 g_1 \lambda_2^3/(f_2 g_2 \lambda_1^3)$$

where f's and g's are the absorption oscillator strengths and the statistical weights of the levels, f(2932) is equal to $1.54 \cdot 10^{-3}$. The result is of the same order as that calculated from the hook method ratio and supports a small value of f(2932). The corresponding value of f(7169) is 1.23. On the other hand, if we use I(2932)/I(7169)=2.0/2.5 from the same table, we obtain f(2932)/f(7169)=0.274. With this ratio, our lifetime gives f(2932)=0.26 and f(7169)=0.96. The agreement is poor for f(2932).

Eberhagen (1955) has determined the absolute oscillator strengths of the diffuse series of SrI by the arc emission method. He obtained f(7169)=0.13, a much smaller value than all those calculated above. If we take Meggers's value $f(2932)=1.54 \cdot 10^{-3}$ into account,

Eberhagen's value gives the ratio, f(2932)/f(7169), 23 times smaller than the one obtained by Meggers et al. (1961).

There are large discrepancies between the f(7169) experimental values determined by the emission method and other methods. The reason is due to the fact that in the emission method intensities cannot be measured accurately due to the self-absorption of the spectral lines and to the non-linearities in the detecting system considering the wide range of wavelengths, and the temperature of the arc which Eberhagen used to determine the absolute oscillator strengths may not be measured accurately. Therefore, the f(7169) values from emission methods which depends strongly on these factors can contain systematic errors of several hundred percent.

A few theoretical methods have been used to predict the oscallator strength of 2932 $\mathring{A}$, but also leads to totally different magnitudes. The B & D method, which gives an extremely good value for f(4606), predicts f(2932)=0.02. This value is about 3 times larger than the experimental value of $(6.60)10^{-3}$. During this calculation, we have extrapolated the B & D tables to obtain the required values for the higher excited levels, and this, of course, restricts the accuracy. Helliwell (1964) with the nodal boundary condition method obtained f(2932)=0.356, much larger than the experimental value. Zilitis (1970) finds $f(2932)=(4.4)10^{-3}$. This calculation is the closest to our experimental value.

Table 6 gives the oscillator strengths for 2932 Å and 7169 Å as obtained from various methods. Among these, we believe that the most reliable values are those shown in the fourth line. These values are obtained by combining our experimental f(4607) value, our measured lifetime of the $5s6p\ ^1P_1$ level and the relative ratio f(4607) to f(2932) from hook method.

An experimental observation of Hanle resonance for the 7169 Å transition is shown in Figure 14.

$5s7p\ ^1P_1$ level

The lifetime of this level has been measured using the 5331 Å transition to the $^1D_2$ metastable level. The geometry and the signal averaging technique are the same as in 7169Å except the standard resistor in series with the ramp generator is replaced by a larger one to keep the counts in convenient channels. The count-rate is low and the signal to noise ratio is reduced to about 3:1. Ten individual runs with the same incident light intensity but different steady fields are taken to get the channel-gauss conversion factor as well as the width of the Hanle resonance curve. Counts for each run are accumulated for about two hours but the statistics are still not good. The average width at half height is 96.2±2.7 channels, which leads to ΔH=23.02±0.64 G

TABLE 6

Lifetime of the $5s6p\ ^1P_1$ level of neutral strontium and the related oscillator strengths.

$$\tau = 3.64 \pm 0.14 \quad ns$$

	f(2932)	f(7169)	Method	Ref
Experiment	$1.54 \cdot 10^{-3}$	1.23	Intensity	(1)
	0.26	0.96	Intensity	(1)
		0.13	Emission	(2)
	$(6.60 \pm 0.22) 10^{-3}$	1.22±0.05	Hanle-Hook	(3)
Theory	0.02		B & D	(4)
	0.356		NBC	(5)
	$4.4 \cdot 10^{-3}$		SE	(6)
	0.228		RPA	(7)

Ref:
(1) Megger et al. (1961). Our calculations.
(2) Eberhagen (1955)
(3) This work and Penkin and Shabanova (1962)
(4) Bates and Damgaard (1949). Our calculations.
(5) Helliwell (1964)
(6) Zilitis (1970). Our calculations.
(7) Hameed (1972)

Figure 14

Hanle resonance curve for $5s6p\ ^1P_1$ level for neutral strontium. Dot points are the experimental data and the solid line is the fitted Lorentzian.

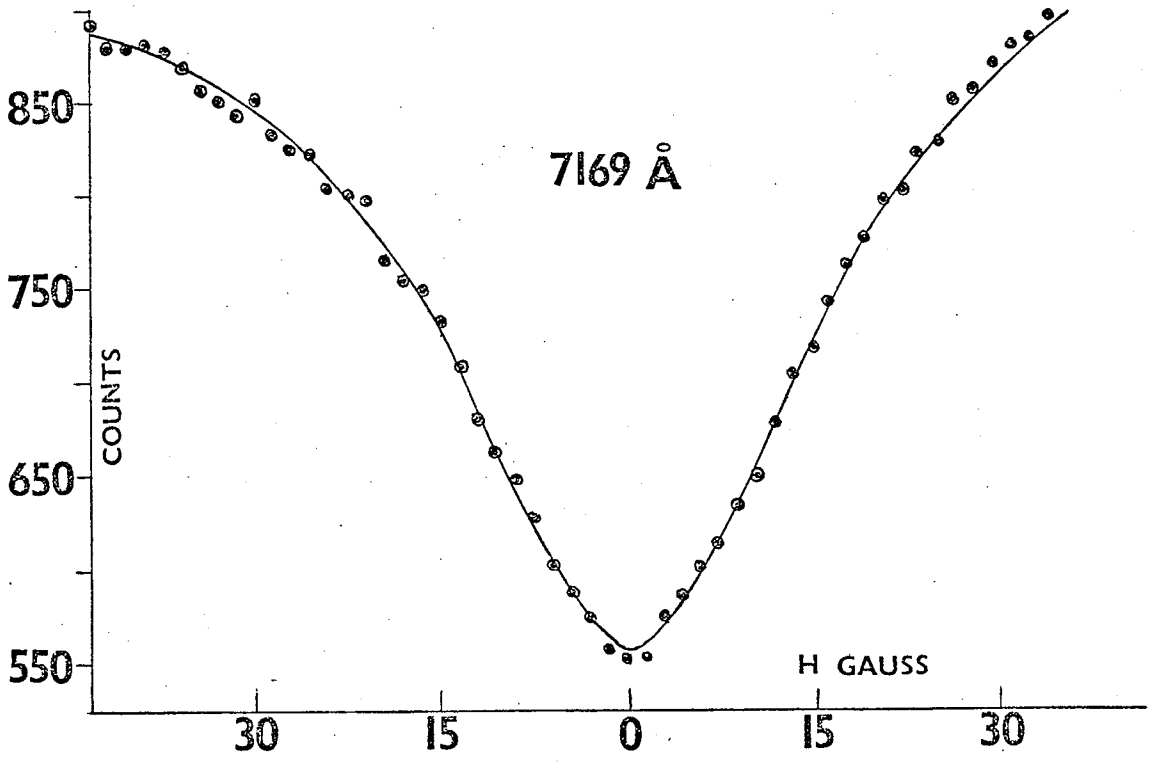
7169 Å
850
750
650
550
COUNTS
H GAUSS
30
15
0
15
30

and a lifetime τ=4.93±0.14 ns. The error is the standard deviation.

To improve the statistics, a computer program is used to add the number of counts of the individual runs by shifting the counts to the appropriate channels with respect to the zero field channel. The composite curve obtained in this way has a width at half height of 89.3 channels and the statistics are improved. But, the process of shifting the counts to the appropriate channels may introduce an extra error, so we consider the value 96.2 channels to be better and increase the error to 7% to include the difference between the average value and the composite value. We thus take

$$\tau = 4.93 \pm 0.35 \quad \text{ns}$$

as the best value of the lifetime of the $5s7p\ ^1P_1$ level. Figure 15 shows the composite Hanle curve for 5331 Å.

During the runs, the atomic density is kept at a value such that collision broadening is not important. Also chance of trapping 5331 Å is insignificant since the population of atoms in the metastable level tends to be small compared with the population of atoms in the ground level.

There are seven allowed transitions from the $5s7p\ ^1P_1$ level to the lower levels. Among these only 5331 Å and 2570 Å are important for oscillator strength calculations. The remaining transitions are

Figure 15

Composite Hanle curve for 5331 Å.

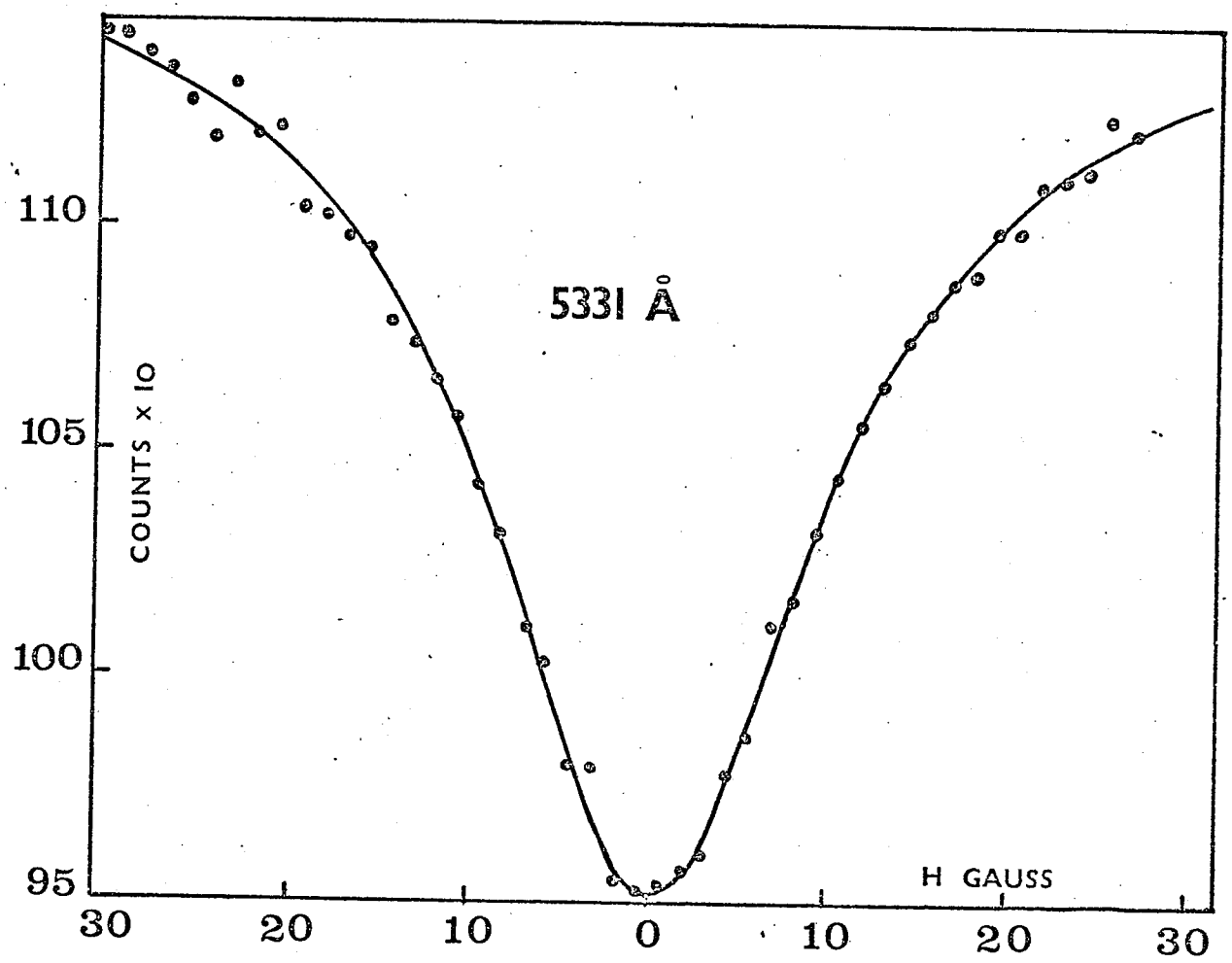
5331 Å
COUNTS x 10
110
105
100
95
30
20
10
0
10
20
30
H GAUSS

all of very long wavelength and can be neglected unless some of them are associated with unusually large f values. The hook method by Penkin and Shabanova (1962) yields f(4607)/f(2570)=1000/7.15. Using f(4607)=1.94 we have f(2570)=$(1.38)10^{-2}$. This gives f(5331)=0.49, if we neglect all but the transitions to the ground level and the metastable level. If we assume that each of the neglected transitions has an f value equal to 0.1, the calculated value of f(5331) becomes equal to 0.48, instead of 0.49. Thus, we make f(5331)=0.485±0.040. The error comes almost entirely from the error in the measured lifetime.

The arc intensity ratio gives I(4607)/I(2570)=650/1.2 (Meggers et al. 1961). From this we get f(2570)=$(6.6)10^{-4}$ and f(5331) is equal to 0.52. This supports a small f(2570) and a large f(5331). From the same table I(2570)/I(5331)=1.2/3.5, which gives f(2570)=0.085 and f(5331)=0.45. This again supports a small f(2570) and a large f(5331).

Eberhagen (1955) obtained f(5331)=0.12 from the emission method. This value is not in good agreement with any of the values discussed above, due to the same reasons discussed for the $5s6p\ ^1P_1$ level.

No theoretical f value for 5331 Å has been reported. For 2570 Å, our calculation with the B & D method gives f(2570)=0.0012,

which is small compared to our experimental value. Zilitis (1970) has given f(2570)=0.011, which is in good agreement with our experimental value, 0.0138. Altick and Glassgold (1964) from the random phase approximation method gives f(2570)=0.057, which is large compared to other values.

Table 7 collects the oscillator strengths for 2570 Å and 5331 Å. We consider the values in the fifth line to be the most reliable. The errors are estimated from the measured lifetime.

$5s8p\ ^1P_1$ level

The lifetime of this level is determined from the Hanle effect in the 4755 Å transition. Since the gauss-channels calibration factor has been already determined from the $5s7p\ ^1P_1$ level, all the runs for 4755 Å are taken with the identical steady field. The signal is even weaker than 5331 Å. Each run needs a period of more than three hours to obtain a discernible Lorentzian distribution. For five individual runs, the average FWHM is 86.2±2.6 channels. The composite data of these five runs gives a value 87.0 channels. The agreement between these two values is excellent. The zeros of the Lorentzian curves are all at the same channel number for each individual run, and no shifting of counts to other channels is required for the composite curve. Thus, we use the composite FWHM value for lifetime calculation since the

TABLE 7

Lifetime of $5s7p\ ^1P_1$ level of neutral strontium and the related oscillator strengths.

$$\tau = 4.93 \pm 0.35 \quad ns$$

	f(2570)	f(5331)	Method	Ref
Experiment		0.12	Emission	(1)
	0.0110		Hook	(2)
	0.0007	0.52	Intensity	(3)
	0.085	0.45	Intensity	(3)
	$(1.38\pm0.04)10^{-2}$	0.485±0.04	Hanle-Hook	(4)
Theory	0.0012		B & D	(5)
	0.011		SE	(6)
	0.057		RPA	(7)

Ref:

(1) Eberhagen (1955)
(2) Penkin and Shabanova (1962)
(3) Meggers et al. (1961). Our calculations.
(4) This work and Penkin and Shabanova (1961)
(5) Bates and Damgaard (1949). Our calculations.
(6) Zilitis (1970). Our calculations.
(7) Hameed (1972)

statistics are much improved. This gives $\Delta H=20.8\pm0.6$ G and the related lifetime is

$$\tau = 5.47 \pm 0.17 \text{ ns}$$

The larger error from the standard deviation error of the individual runs has been used to allow for unknown systematic errors. Figure 16 shows the composite curve for 4755 Å.

Nine transitions from $5s8p\ ^1P_1$ level are allowed. But, for oscillator strength calculations only 2428 Å and 4755 Å are important. Penkin and Shabanova (1962) give the relative value f(4607)/f(2428) equal to 1000/20.9. From this we obtain $f(2428)=(4.10\pm0.13)10^{-2}$. If all the other branches except 4755 Å are neglected, we obtain $f(4755)=0.34\pm0.02$. If we assume that each of the neglected transitions has an f value equal to 0.08, f(4755)=0.329, in place of the upper limit 0.34. Thus, we make the value of f(4755) equal to 0.33 ± 0.02.

From the Meggers et al. (1961) intensity ratio, we have I(4607)/I(2428)=650/1.2 which gives $f(2428)=(5.1)10^{-4}$ and f(4755)=0.37. These values for 4755 Å transition are again in contrast with the emission result of f(4755)=0.075 given by Eberhagen (1955).

In table 8 we have collected the experimental and theoretical f values for both 2428 Å and 4755 Å. We again suggest that the values in the fourth line are the most reliable.

Figure 16

Composite Hanle curve for 4755 Å. Dot points are the experimental data and the solid line is the fitted Lorentzian.

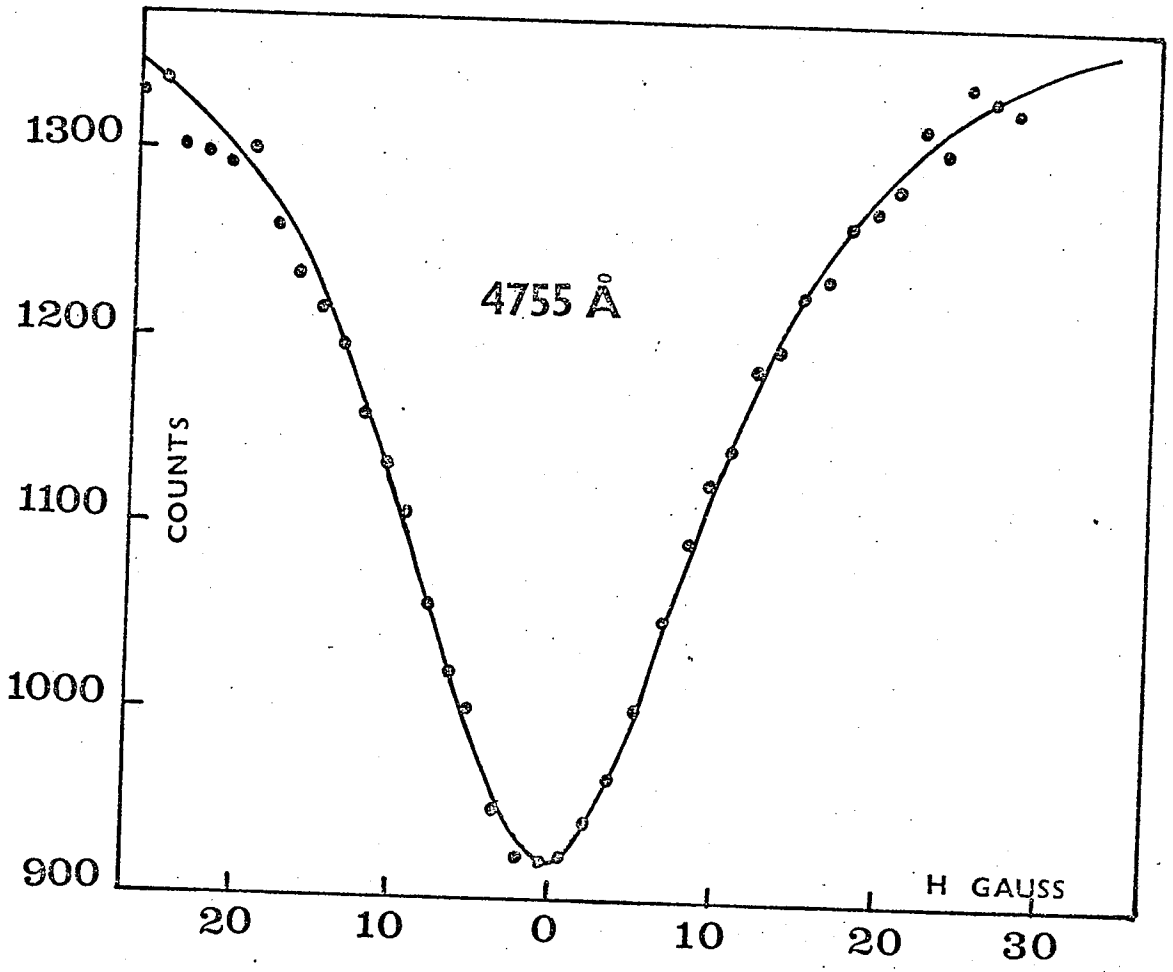
4755 Å
COUNTS
1300
1200
1100
1000
900
20
10
0
10
20
30
H GAUSS

TABLE 8

Lifetime of $5s8p\ ^1P_1$ level of neutral strontium and the related oscillator strengths.

$$\tau = 5.46 \pm 0.17 \quad \text{ns}$$

	f(2428)	f(4755)	Method	Ref
Experiment		0.075	Emission	(1)
	0.032		Hook	(2)
	0.005	0.37	Intensity	(3)
	0.041±0.0013	0.34±0.02	Hanle-Hook	(4)
Theory	0.033		B & D	(5)
	0.030		SE	(6)

Ref:
(1) Eberhagen (1955)
(2) Penkin and Shabanova (1962)
(3) Meggers et al. (1961). Our calculations.
(4) This work and Penkin and Shabanova (1962)
(5) Bates and Damgaard (1949). Our calculations.
(6) Zilitis (1970). Our calculations.

The strontium ion

The extension of the Hanle effect from neutral atoms to free ions has two main difficulties. First, ions of thermal velocity have to be produced at a sufficiently high density in the scattering region; second, the motion of charged particles in a magnetic field introduces an extra uncertainty in the beam density.

Various types of ion sources have been used in experiments in atomic spectroscopy. The ionization process during contact of neutral atoms with a heated surface is known as surface ionization or thermal ionization. The degree of ionization is given by the equation derived by Langmuir and Kingdom (1923) as

$$N^+/N_o = (g^+/g_o)\exp[-11{,}600(I-\phi)/T]$$

where N^+/N_o is the ratio of positive ions to neutral atoms, g^+ and g_o are the statistical weights of the ground levels of the ions and the atoms respectively, I is the ionization potential of the atom in volts, ϕ is the work function of the heated surface in volts and T is the absolute temperature. The high ionization potential of the strontium atom, 5.692 eV, makes it difficult to select another metal whose work function is high enough to make the quantity $(I-\phi)$ negative or even close to zero. Therefore, this type of source is not practical for the present experiment. Initially, attempts were made to develop a electron bombardment source for this work. An electron gun assembly

with tungsten coated filaments and an anode on the opposite side of the beam were used but found unsatisfactory.

Another type of source which is widely used is a plasma source. Ions are extracted from the plasma that is produced by an electrical discharge. The discharge can be carried by a foreign gas (Smith and Gallagher 1966, Weber et al. 1973a, b.) or just by the material under investigation(Penkin and Redko 1964). In the experiment reported here we have found that when the furnace is operated with a high current, a discharge is maintained in the vapour at the furnace mouth from the electric field due to the potential difference across the terminals of the bifilar winding of the furnace. No foreign gas is needed to carry the discharge and the density of the strontium ions can be changed by changing the current in the furnace windings and thus the temperature of the strontium vapour at the furnace mouth.

Ostrovskii and Penkin (1960) have studied the processes of atomic excitation and ionization by a discharge in a heated oven. They have shown that the atoms are distributed among energy levels according to Boltzmann's law, and the degree of ionization follows Saha's equation (Saha 1921). The equation is given by Ostrovskii and Penkin (1960) in the following form

$$N_i \cdot N_e = N_a \left(\frac{2\pi mk}{h^2}\right)^{3/2} \frac{g_i g_e}{g_a} T^{3/2} \cdot 10^{-5040 V_a/T}$$

where N represents the concentrations and g represents the statistical weights. The subscripts are i for ion, e for electron and a for atom. V_a is the atomic ionization potential in volts, T is the absolute temperature, h and k are Planck's and Boltzmann's constants, and m is the rest mass of the electron. There are no foreign ionizing impurities and if we assume that the number of electrons from thermal emission is small compared to the number from ionization of the strontium atoms, we can assume $N_i = N_e$. For alkaline earth atoms and ions, $g_a = 1$ and $g_i = g_e = 2$. The operating temperature in the present experiment is about 1000° K. The substitution of numerical values into Saha's equation gives

$$N_i \sim 1.3 N_a^{1/2}$$

This means that for our experiments the ion density will be close to the square root of the number of the atoms.

In our study of collision broadening of strontium atoms, we have found that N_a does not exceed 10^{17}. Thus, the upper limit of the density of ions in this experiment will be near $4 \cdot 10^8$ ions per cc. For the investigation of excited levels which are connected with the ground level with oscillator strength between 1 and 10^{-3}, this is the lowest density that suffices for the Hanle effect as described by

Bucka (1969). At such low ion density the measured lifetime can be considered as the natural lifetime provided that no collision effects occur.

The plasma created in this way has the advantage that no strontium ion radiation background originating from the discharge itself is in the scattering region, and it is not necessary to operate the discharge on a pulsed basis. When Sr^+ resonance radiation is produced by the discharge in the scattering region, the discharge must be pulsed and the Hanle signal is observed only when the discharge is off as done by Gallagher (1966). The disadvantages are that the ion density is low and can be varied only over a very narrow range.

It has been found that the ion density at the scattering region changes with the applied field. We have checked the variation of ion density by observing the scattered π polarized radiation at different magnetic field intensities while the furnace current and the hollow cathode intensity are kept constant. The results show that the scattered π light intensity, and thus the ion density, remains constant at field strengths below 25 G and then increases and reaches a maximum value at about 40 G. The distortion of the normal Lorentzian Hanle signal due to this effect is easily seen and for this reason we limit the amplitude of the variable magnetic field to about ± 20 G. This effect has been mentioned by Smith and Gallagher (1966) and by Ackermann et al. (1967).

$5p\ ^2P_{3/2}$ level

The lifetime of this level is observed by the Hanle effect of the 4077 Å transition to the ground $5s\ ^2S_{1/2}$ level of the ion. The geometry of the experiment is the same as in the atomic case.

Ten independent runs were taken with different densities of the strontium atoms. The strontium atom density is varied approximately from 10^{14} to 10^{15} atoms per cc. Below this range of atom densities the ion density is too low and the scattered resonance light cannot be resolved from the background. Above this range of temperature for the furnace we observe a decrease in ion density.

For each observation of 4077 Å of the ion spectrum, a counting rate for 4607 Å, the singlet resonance line of the neutral atom, at a saturated value of the magnetic field is determined with undisturbed experimental condition. The number of Sr atoms, expressed as a beam density parameter ρ, in arbitrary units, is defined earlier on page 76. ρ can be converted to the number of strontium atoms per cc by $N=(1.85)10^{12}\rho$ in this case. The results are given in Table 9. The variation of the full width at half maximum of the 4077 Å Hanle curve with respect to the atomic beam density parameter ρ is plotted in Figure 17.

TABLE 9

Hanle effect of $5p\ ^2P_{3/2}$ level of the strontium ion.

FWHM of 4077 Å in channels ΔH	Density parameter of Sr atom in arbitrary unit ρ
67.14	201.1
68.67	221.4
69.87	306.4
72.39	366.5
76.75	396.2
77.76	434.5
76.30	453.2
80.65	492.7
77.08	504.1
80.09	510.3

Figure 17

Hanle effect line widths for 4077 Å in channel numbers plotted against the density of strontium atoms in arbitrary units.

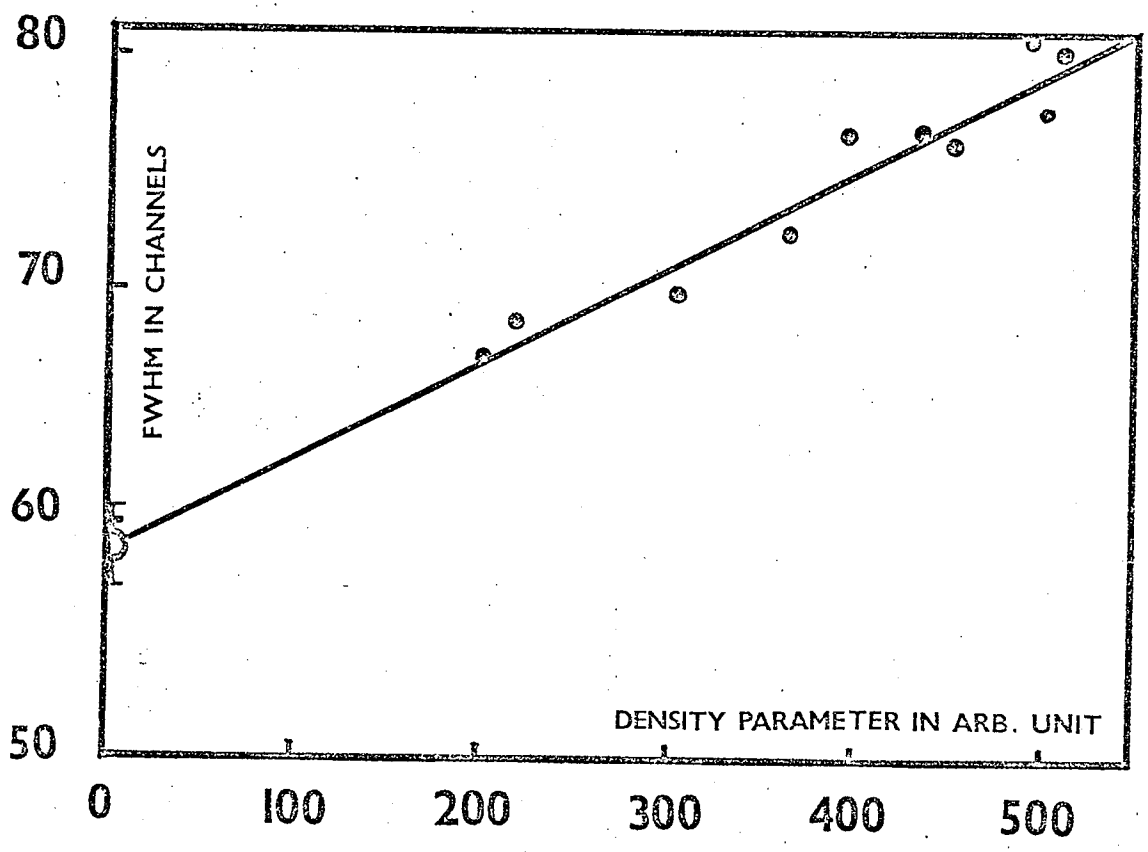
80
70
60
50
FWHM IN CHANNELS
DENSITY PARAMETER IN ARB. UNIT
0
100
200
300
400
500

According to Saha's equation, the number of Sr^+ ions is approximately equal to the square root of the number of strontium atoms. At these low densities, broadening due to the Sr^+-Sr^+ collisions can be completely neglected, and coherence narrowing will be very small. The increase in Hanle widths shown in Figure 17 must be due to collisions between strontium atoms and strontium ions.

The relation between the observed lifetime, τ, the lifetime at zero density, τ_o, and the depolarization cross section, σ, is given by

$$1/\tau = 1/\tau_o + N\bar{v}\sigma$$

where N is the number of strontium atoms per cc, and $\bar{v}$ is the mean relative speed of the colliding particles, and is equal to $[16RT/(\pi M)]^{1/2}$. From a least squares fit for a straight line, we obtain $\Delta H = 15.15 \pm 0.45$ G at zero atomic density and the lifetime of $5p\ ^2P_{3/2}$ is found to be

$$\tau_o = 5.63 \pm 0.17 \quad \text{ns}$$

This value is 14% smaller than the value of Gallagher (1967). The discrepancy is discussed later.

If the transitions to the ^2D levels are neglected, we have $f(4077)=0.88\pm0.03$ as an upper limit. If we use a branching ratio of 94% (Gallagher 1967), our lifetime gives $f(4077)=0.83\pm0.03$. Gallagher (1967) using his lifetime and the 94% branching ratio found $f(4077)=0.71 \pm0.03$. The difference between these results is due to the difference in the observed lifetime.

Ostrovskii and Penkin (1961), using the hook method, find f(4077)=0.75±0.03. The hook method results depend directly on a determination of the value for the density of the atoms in the absorption chamber. The hook method value for the singlet resonance line, 4607 Å, of the neutral strontium atom is lower than that determined by Hanle effect. If our value of f(4607) is used to correct the density measurements in the hook method, the Ostrovskii and Penkin result gives f(4077)=0.85. This same adjustment has been made by Gallagher (1967a). The agreement between our value for f(4077) and the corrected hook method result is good.

The only available theoretical prediction for f(4077) of SrII is from the B & D method. From their tables we calculate f(4077) =0.74, which agrees within errors with all the experimental values discussed above.

In Gallagher's (1967) experiments there were three variables to control during the lifetime measurements, the pressure of the argon, the current in the argon discharge used to produce the strontium ions and the temperature of the oven used to produce the strontium vapour. The natural lifetime of the $5p\ ^2P_{3/2}$ level is obtained by extrapolating the Hanle width to zero ion density at a fixed argon pressure to remove any effect of coherence narrowing. The results are then extrapolated again to zero argon pressure to remove the broadening

due to collisions between argon atoms and strontium ions. However, collisions between strontium atoms and strontium ions have not been taken into account. This last effect may account for the difference between his and our result for the lifetime of the $5p\ ^2P_{3/2}$ level of Sr^+.

For ion-atom collisions, which are non-resonant, the excess charge of the ion adds an additional term to the perturbation potential of atom-atom collisions. However, Smith and Gallagher (1966) and Gallagher (1967a)have shown that this term does not directly produce changes in the density matrix of the excited level of the ion. Therefore, the cross section for ion-atom collisions should be about the same magnitude as nonresonant atom-atom collisions.

The depolarization cross-sections for the Sr^+ $5p\ ^2P_{3/2}$ level with foreign gas atoms have been determined by several authors (Gallagher 1967a,Weber et al. 1973). Some of the results are collected in Table 10. Neutral Rb atoms have the same electronic structure as strontium ions, and Sr atoms have the same closed electronic shells as Sr^+. Their depolarization cross sections with foreign gases are also collected in the same table.

TABLE 10

Depolarization cross sections of collisions between strontium ions, strontium atoms and rubidium atoms with the foreign gases.

Depolarization cross section in $\mathring{A}^2$	He	Ne	Ar	Kr	Xe	Ref
$\sigma(Sr^+ 5p\ ^2P_{3/2})$	72 ± 9	80 ± 10	124±15 120±25	148±18	196±23	(1) (2)
$\sigma(Rb\ 5p\ ^2P_{3/2})$	98	100 100	203 210	283	305	(1) (3)
$\sigma(Sr\ 5s5p\ ^1P_1)$	75	85	221	269		(4)

Ref:

(1) Weber et al. (1973a, b)

(2) Gallagher (1967a)

(3) Gallagher (1967b)

(4) Penkin and Shabanova (1968)

A comparision of the results given in Table 10 shows that the ionic charge has no strong influence on the cross section of the $^2P_{3/2}$ level. $Sr^+(^2P_{3/2})$-$Sr(^1S_o)$ collisions do occur in our experiment, but we expect that the depolarization cross section is about the same as those given in Table 10, and not as large as the $Sr(^1P_1)$-$Sr(^1S_o)$ collision cross section which we have measured in the study of 4607 Å transitions of SrI.

From the slope of the straight line in Figure 17, and the conversion factor given on page 112 to find the number of atoms per cc, we obtain the depolarization cross section for collisions between the neutral strontium atoms and the strontium ions to be

$$\sigma = (8.4)10^{-13} \text{ cm}^2$$
$$= 8400 \text{ Å}^2$$

This value is very large compared to the data in Table 10.

The strontium atoms are produced by evaporation from a furnace and the ions from an electrical discharge in the strontium vapour at the furnace mouth. Any neutral atom in a $^1P_1$ excited level will decay to the ground level before it reaches the scattering region. However, in this work, the scattering region is irradiated with the complete strontium spectrum including the strong singlet resonance line, 4607 Å, of the neutral atoms. Consequently, the scattering region contains neutral atoms in the ground ^1S_o level and the excited 5s5p $^1P_1$ level, and

ions in the ground $^2S_{1/2}$ level and the excited ^2P levels. The cross section, σ, which we are measuring is a weighted sum of a cross section, σ_1, for collisions between atoms in the ground level and ions in the excited $^2P_{3/2}$ level, and a cross section, σ_2, for collisions between atoms in the first excited $^1P_1$ level and the excited ions in the $^2P_{3/2}$ level. There will be other cross sections for collisions between the excited ions and atoms in other excited levels, but the population of these other excited levels will be much smaller than that of 5s5p $^1P_1$ and consequently their contributions to the broadening may be neglected.

The excitation energy of $Sr^+(^2P_{3/2})$ is 3.04 eV. There are no excited levels of the strontium atom with this energy so that we can conclude that resonance collisions do not contribute to σ_1. On the other hand, the energy of $Sr(5s5p\ ^1P_1)$ is 2.69 eV. The sum of this energy and the energy of $Sr^+(^2P_{3/2})$, 3.04 eV, is 5.73 eV which is just larger than the ionization energy, 5.69 eV, for the strontium atom. As a result, resonant nonradiative collisions, may occur between $Sr^+(^2P_{3/2})$ and $Sr(5s5p\ ^1P_1)$ which produce two ions in the ground state of the ion and a free electron. These collisions can be treated analogously to the imperfect-resonance-collisions between two neutral atoms (Mott and Massey 1965). Hence the order of σ_2 can be same as that of exact resonance collisions between two identical Sr atoms, which is equal to $10^{-12}cm^2$. Such resonant collisions will cause the consequent removal of the ions from the excited $^2P_{3/2}$ level and this will result in the broadening

of the Hanle signal and alarge depolarization cross section for the $^2P_{3/2}$ level of strontium ions can be expected.

A further experiment is under consideration to check this argument by placing a monochromator in the optical input arm, so that all the incident light from the hollow cathode, except 4077 Å, can be blocked. This will stop the excitation of neutral atoms to the $5s5p\ ^1P_1$ level and remove the possibility of $Sr(5s5p\ ^1P_1)$-$Sr^+(5p\ ^2P_{3/2})$ collisions in the scattering region. If the above suggestion is correct the only collisions will be those between $Sr^+(^2P_{3/2})$ ions and Sr normal atoms. The depolarization cross section for this collision should be about the same as those in Table 10.

$5p\ ^2P_{1/2}$ level

The lifetime of this level is measured by the Hanle effect of the 4215 Å resonance transition. As already proved in chapter II, circularly polarized light must used in the excitation and the analysis. The 70% absorption in each of the two polarizers results in a much weaker signal compared to the signal for the $^2P_{3/2}$ measurements. The current in the furnace windings, therefore, is kept near its optimum value for the production of a dense beam of strontium ions, and no significant change of density of strontium atoms for observing the effect of collisions on the Hanle signal widths can be made. Fortunately, the ion density

is so low that the coherence narrowing effect should be very small. Moreover, Gallagher (1967b,errata 1967) has shown from the theoretical point of view that the depolarization of a J=1/2 state is zero, so the collision broadening effect for collisions between ions and atoms can be eliminated. Experimentally, several authors (Gallagher 1967a, Weber et al. 1973) have reported non-zero collision cross sections between ions in J=1/2 level and foreign gas atoms, but the magnitudes are usually much smaller than for the $^2P_{3/2}$ level. Also, the energy of a excited $^2P_{1/2}$ Sr^+ is 2.94 eV, which is energetically not able to produce the resonance type of collision as in the $^2P_{3/2}$ level. Therefore, if there exists a broadening by collision between ions in the $^2P_{1/2}$ level and the normal strontium atoms, the effect on the lifetime should be small and within the experimental errors.

The Hanle signal shape is not Lorentzian for this case, and changes as $1 - [y/(1+y^2)]$, where $y=g_J\mu_o H\tau/\hbar$, as already discussed in chapter II. In this case, we have not used the ramp field. Instead, the uniform magnetic field is varied in regular steps of about 1.5 G from -25 G to +25 G. At each value of the magnetic field about 30s are allowed for conditions to become steady. Then several readings of the counts, each accumulated over 10s are taken. With everything else undisturbed, the incident beam of light is shut off, and several readings of the background counts are taken with the same accumulation times for each of the readings. The difference between these two count rates is

the signal count rate. Thirty-five sweeps of the magnetic field from -25 G to +25 G have been made and the average counts corresponding to each fixed value of the magnetic field are obtained. The results are shown in Table 11. The computer fitted curve with the experimental points is shown in Figure 18.

From the computer fitted result, the points of inflection, or the points where y= ±1 are determined to be ±22.6 G. Substituting this into the equation $\tau=\hbar/(\mu_o g_j H)$ gives the value

$$\tau = 6.74 \pm 0.20 \text{ ns}$$

where the error has been doubled to include a possible systematic error for a collision broadening effect.

This value of the lifetime is 8% smaller than Gallagher's (1967) value, 7.35±0.30 ns. Gallagher stated that the uncertainty in the lifetime measurement is large due to a gradual dependence of the ion density on field intensity which resulted in a distortion of the $^2P_{1/2}$ line width. In our experiment we have attempted to eliminate this effect by restricting the field intensity to ±25 G.

If we ignore the transition to $^2D_{3/2}$ level, the upper limit of f(4215) is equal to 0.395 from our lifetime measurement. If we use the branching ratio of 93% for the 4215 Å transition from Gallagher's (1967a) result, we obtain

TABLE 11

Hanle effect for 5p $^2P_{1/2}$ level of strontium ion

Steady magnetic field intensity in amperes	Experimental counts	Fitting counts
+ 0.85	652	673.7
0.80	676	674.4
0.75	693	674.8
0.70	681	674.9
0.65	742	674.5
0.60	708	673.7
0.55	703	672.2
0.50	668	669.9
0.45	679	666.9
0.40	662	662.8
0.35	667	657.7
0.30	635	651.5
0.25	629	644.1
0.20	605	635.5
0.15	583	625.9
0.10	567	615.5
0.05	567	604.4
0.00	555	592.9
- 0.05	564	581.5
- 0.10	543	570.4
- 0.15	564	559.9
- 0.20	558	550.4
- 0.25	560	541.8
- 0.30	543	534.4
- 0.35	557	528.1
- 0.40	550	523.0
- 0.45	551	518.9
- 0.50	540	515.9
- 0.55	510	513.7
- 0.60	528	512.2
- 0.65	495	511.3
- 0.70	469	510.9
- 0.75	512	511.1
- 0.80	500	511.5
- 0.85	537	512.2

Figure 18

Hanle curve for 4215 Å plotted in counts versus field intensity in amperes. Dot points are experimental data and the dashed curve is the fitting curve according to the equation (16).

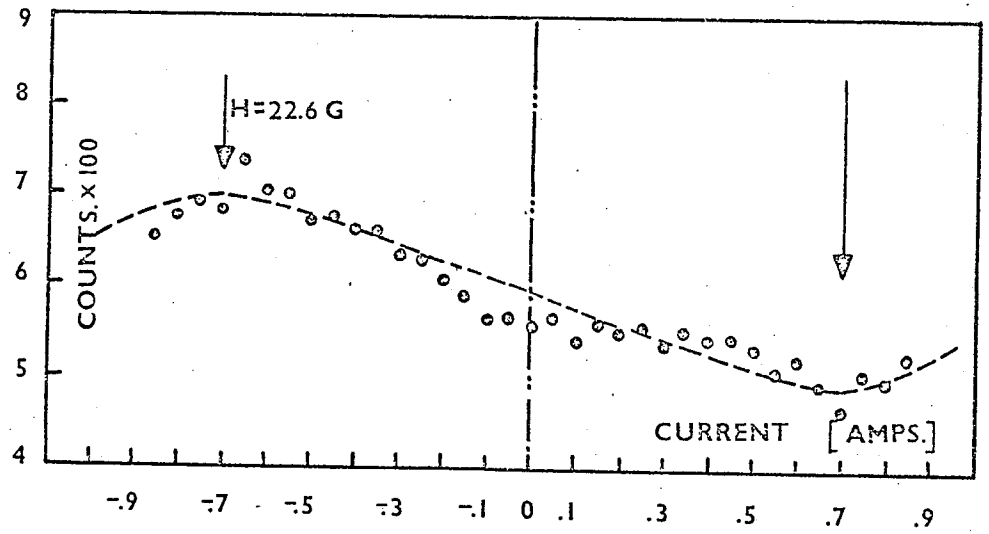
9
8
7
6
5
4
H=22.6 G
COUNTS. x 100
CURRENT [AMPS.]
-.9
-.7
-.5
-.3
-.1
0
.1
.3
.5
.7
.9

$$f(4215)=0.37 \pm 0.02$$

where the error is estimated from the lifetime error.

We have used the theory of B & D to calculate a theoretical value of $f(4215)=0.36$. The agreement between experiment and theory is good.

Table 12 shows the various experimentally measured f values for 4077 Å and for 4215 Å. The agreement between the experimental values and the theoretical values is better than the agreement for the Sr atom.

TABLE 12

Lifetimes for $5p\ ^2P$ levels of strontium ions and the related oscillator strengths.

Method	$\tau(^2P_{3/2})$ in ns	$\tau(^2P_{1/2})$ in ns	f(4077)	f(4215)	$\frac{f(4077)}{f(4215)}$	f(4077) + f(4215)	Ref
B & D			0.74	0.36	2.06	1.10	(1)
Hook			0.85	0.43	1.98±0.02	1.28	(2)
Hanle	6.53±0.2	7.35±0.3	0.71±.03	0.34±.015	2.09±.18	1.05±.05	(3)
Hanle	5.63±.17	6.74±.20	0.83±.03	0.37±.02	2.2±0.2	1.20±.05	(4)

Ref:

(1) Bates and Damgaard (1949). Our calculations.

(2) Ostrovskii and Penkin (1961)

(3) Gallagher (1967)

(4) This work

CHAPTER V CONCLUSIONS

Our measurements of the lifetime of the $5s5p\ ^1P_1$ level of the strontium atom include a survey of the observed Hanle widths over a wide range of density of the atoms in the scattering region. Such a survey has not previously been done. The lifetime of the $5s5p\ ^1P_1$ level extrapolated to zero density agrees well with other Hanle measurements but has a smaller assigned error. This determination of an accurate lifetime together with the precise relative measurements of oscillator strengths by the hook method leads to accurate absolute oscillator strengths for the $5s^2\ ^1S_o$- $5snp\ ^1P_1$ transitions of neutral strontium.

The effect of the transition to the metastable $5s4d\ ^1D_2$ level from the $5s5p\ ^1P_1$ level has been shown to be important in depolarization collisions in the intermediate range of density. Our value of the collision cross section for depolarization of the $5s5p\ ^1P_1$ level in the higher density range is in agreement with those of other authors using different methods.

The new measurements of the lifetimes of the 5s6p, 5s7p and $5s8p\ ^1P_1$ levels have enabled us to extend the determination of absolute oscillator strengths to the transitions to the $5s4d\ ^1D_2$ level.

The Hanle resonance of the levels higher than $5s8p\ ^1P_1$ cannot be observed although these lines were seen with a low intensity in the spectrum of the hollow cathode lamp. Two changes might make these resonances observable: (1) excite the atoms to the $5s4d\ ^1D_2$ metastable level by electron collisions, and (2) increase the hollow cathode lamp current. The excitation of atoms to the $^1D_2$ level would enable absorption from this level to the higher $5snp\ ^1P_1$ level, using transitions with higher oscillator strengths than the transitions to the ground state. Increasing the lamp current increases the intensity of most lines in the spectrum as the current squared.

A high population of the $^1D_2$ metastable level obtained by a discharge in a pure strontium vapour as reported by Brinkmann (1969) seems to be the preferable way for the further development in this work. The same system should also be satisfactory for the study of the lifetimes of the triplet levels of the strontium atom. More efficient polarizers would also help. At present the polarizers absorb almost 70% of the incident light.

Our measurements of the lifetimes of the $5p\ ^2P_{3/2,\ 1/2}$ levels of the ionized strontium atom are smaller by 14% and 8% than those reported by Gallagher (1967a) The difference is just beyond the combined experimental error. Our measurements of the lifetime of the $^2P_{3/2}$ level include an extrapolation to zero strontium atom density

and the determination of an unusually large and previously unreported cross section for collisions between $^2P_{3/2}$ ions and 5s5p $^1P_1$ atoms. This effect was not considered by Gallagher and may account for the difference in the $^2P_{3/2}$ results.

However, the measurement of the lifetime of the 5p $^2P_{1/2}$ level requires two polarizers and consequently the signals from 4215 Å have poor statistics. Due to the intensity limitation we are unable to study any collision broadening of this Hanle width, and the poor statistics lead to a lower confidence in the $^2P_{1/2}$ measurement.

In SrII, the sum of f(4077) and f(4215) is greater than unity which does not agree with the theoretical sum rule (Condon and Shortley 1936). We note that similar experimental results were obtained for BaII and for RbI (Penkin 1961, Gallagher 1967 b)

The much larger f($^1P_1$-$^1D_2$) values compared to f($^1P_1$-^1S_o) values for strontium atom indicate that configuration mixing is important. Doubly excited configurations are present in the Sr atom. If the nsmp $^1P_1^o$ excited levels are mixed with mp(n-1)d $^1P_1^o$ levels, one would expect that the probability for a transition to the $^1D_2$ metastable level is greater than for a decay to the ^1S_o ground level. This latter transition needs a two electron jump for the mp(n-1)d $^1P_1^o$ mixed component and this is forbidden for electric dipole transitions while the mixed

component can decay to 5s4d $^1D_2$ level with a single electron jump. Kim and Bagus (1972) have obtained a value of f(4607) very close to the experimental result by taking into account the configuration mixing of the excited level. These authors also plan to extend the calculation to higher 5snp levels (Priv. Comm. 1973) and this may lead to interesting results.

The present work has demonstrated that the Hanle effect is a powerful technique for the lifetime measurement of higher excited levels, particularly for those which can be optically excited from the ground level. It also showed that the inclusion of solid angle contributions in a Hanle effect experiment can introduce distortion in the output signal. For transitions with strong f values, the atomic beam can be used to study depolarization cross sections. At high beam density, the collision broadening effect can be used to estimate the absolute atomic density in the scattering region.

Reports on lifetimes and related oscillator strength for excited levels of neutral strontium atoms have been published in the Journal of Canadian Physics (Dickie et al. 1973, Kelly et al. 1973a, b; 1974a) and in Spectroscopy Letters (Mathur et al. 1974). Reports of Sr^+ will appear shortly (Kelly et al. 1974b).

References

Ackermann, H. , zu Putlitz, G. and Weber, E. W. Phys. Lett. 24A, 567 (1967)

Altick, P. L. and Glassgold, A. E. Phys. Rev. 133, A632 (1964)

Balmer, J. J. Ann. d. Physik. 25, 80 (1885)

Bates, D. R. and Damgaard, A. Phil. Trans. 242, 101 (1949)

Breit, G. Rev. Mod. Phys. 5, 71 (1933)

Brinkmann, U. Z. Physik. 228, 440 (1969)

Bucka, H. Journal de physique. 30, 3 (1969)

Budick, B. Advan. At. Mol. Phys. 3, 73 (1967)

Byron, Jr, F. W., McDermott, M. N. and Novick, R. Phys. Rev. 134, A615 (1964)
and Foley, H. M. Phys. Rev. 134, A625 (1964)

Colgrove, F. D., Franken, P. A., Lewis, R. R. and Sands, R. H.
Phys. Rev. Lett. 3, 420 (1959)

Condon, E. U. and Shortley, G. H. The theory of atomic spectra.
Cambridge University Press, London (1936, 1963)

Deech, J. S. and Baylis, W. E. Can. J. Phys. 49, 91 (1971)

De Zafra, R. L., Goshen, R. J., Landman, A. and Lurio, A.
Bull. Am. Phys. Soc. 7, 433 (1962)
— and Kirk, W. Am. J. Phys. 35, 573 (1967)

Dickie, L. O. Thesis (The University of Manitoba) (1971)
and Kelly, F. M., Koh, T. K., Mathur, M. S., Suk, F. C.
Can. J. Phys. 51, 1088 (1973)

D'Yakonov, M. I. and Perel, V. I. Sov. Phys. JETP 20, 997 (1965a)
Sov. Phys. JETP 21, 227 (1965b)

Eberhagen, A. Z. Physik. 143, 392 (1955)

Foster, E. W. Repts. Prog. Phys. 27, 469 (1964)

Fry, E. S. and Williams, W. L. Phys. Rev. 183, 81 (1969)

Gallagher, A. Phys. Rev. 157, 24 (1967a)
— Phys. Rev. 157, 68 (1967b)
— Erratum: Phys. Rev. 163, 206 (1967c)
and Lurio, A. Phys. Rev. Lett. 10, 25 (1962)

Hameed, S. J. Phys. B: At. Mol. Phys. 5,746 (1972)

Hanle, W. Z. Physik. 30, 93 (1924)

Happer, W. Beam-foil spectroscopy. ed. Bashkin, S.
(Gordon and Breach, New York) (1968)
— and Saloman, E. B. Phys. Rev. 160,23 (1967)

Helliwell, T. M. Phys. Rev. 135, A325 (1966)

Hulpke, E., Paul, E. and Paul, W. Z. Physik. 177, 257 (1964)

Kelly, F. M., Koh, T. K. and Mathur, M. S. Can. J. Phys. 51, 1653 (1973a)
— Can. J. Phys. 51, 2295 (1973b)
— Can. J. Phys. 52, (1974a)
Can. J. Phys. 52, (1974b)

Kim, Y. K. and Bagus, P. S. J. Phys. B: At. Mol. Phys. 5,L193 (1972)

King, R. B. and Stockbarger, D. C. Astrophys. F. 91,488 (1940)

Lurio, A. Phys. Rev. 136, A376 (1964)
— and de Zafra, R. L., Goshen, R. J. Phys. Rev. 134, A1198
(1964)

Langmuir, I. and Kingdom, K. H. Science. 57, 58 (1923)

Mathur, M. S., Koh, T. K. and Kelly, F. M. Spect. Lett. 7,3 (1974)

Meggers, W. F., Corliss, C. H. and Scribner, B. F.
U. S. Nat. Bur. Stand. Mono. 32, part I. (1961)

Mitchell, A. C. G. and Zemansky, M. W. Resonance radiation and excited
atoms. (Cambridge University Press, London) (1934)

Moore, C. E. Atomic energy levels. Washington, D. C. Circular 467
Nat. Bur. Stand. (1952)

Omont, A. C. R. Acid. Sci. 262, B, 190 (1966)

Ostrovskii, Yu. I. and Penkin, N. P.
— Sov. Phys. Doklady 3, 558 (1958)
— Opt. Spectrosc. 11, 307 (1961b)
— Opt. Spectrosc. 10, 3 (1961a)

Penkin, N. P. and Shabanova, L. N. Opt. Spectrosc. 12, 1 (1962)
— Opt. Spectrosc. 25, 446 (1968)
— Opt. Spectrosc. 26, 191 (1969)
— and Redko, T. P. Opt. Spectrosc. 22, 106 (1965)

Prokofev, U. K. Z. Physik. 50, 701 (1928)

Rydberg, J. R. Kgl. Svensha Aka. Handl. 23 (1889)

Rayleigh, Proc. Roy. Soc. 102, 190 (1922)

Saha, M. N. Z. Physik. 6, 40 (1921)

Saplakoglu, A. New directions in atomic physics. ed. Condon and Sinanoglu. (Yale University Press, London) (1972)

Series, G. Repts. Prog. Phys. 22, 280 (1959)

Shore, B. W. and Menzel, D. H. Principles of atomic spectra. (John Wiley and Sons. London) (1968)

Smith, W. W. and Gallagher A. Phys. Rev. 145, 26 (1966)

Saloman, E. B. and Happer, W. Phys. Rev. 144, 7 (1966)

Stroke, H. H., Fulop, G., Klepner, S. and Redi, O. Phys. Rev. Lett. 21, 61 (1968)

Wood, R. W. Phil. Mag. 10, 513 (1905)
— and Ellet, A. Proc. Roy. Soc. 103 396 (1923)
— Phys. Rev. 24, 243 (1924)

Weber, E. W., Ackermann, H., Lanlaineu, N. S. and zu Putlitz, G.
— Z. Physik. 259, 371 (1973a)
— Z. Physik. 260, 341 (1973b)

Zeeman, H. P. Phil. Mag. 44, 225 (1897)

Zilitis, V. A. Opt. Spectrosc. 29, 438 (1970)

zu Putlitz, G. Ergebnisse der exakten Naturwissenschaften 37, 105 (Springer-Verlag, Berlin) (1965)

APPENDIX I.

THE EFFECT OF A FINITE INTERACTION VOLUME ON THE HANLE EFFECT

The effect of departure from the ideal geometry described on pages 30 to 33 is for an arbitrary polarization direction. To integrate over asymmetrical angles is similar to taking into account those interaction points apart from the geometrical centre as shown in Figure 18. If narrow slits are used on the monochomater, the detecting system can only received signals from the geometrically central point and forms image A. However, if wider slits are used, signals from the interaction points apart from the geometrical centre also can be reveived by the detecting system as shown in Figure 18 of the image B. Classically, B is equivalent to the situation that the optical axis of the detecting system is not parallel to the y axis, but is making an finite angle, say ϕ, with respect to the y axis.

Recalling the simplest case, when the incident light is along x axis and is polarized with it's electric vector parallel to the y axis, the relation between the observer intensity and the magnetic field H when one is observed along y axis is known to be:

$$I = C\int_0^\infty e^{-\Gamma t}\sin^2\omega t\,dt$$

$$= \frac{C\tau}{2}\left[1 - \frac{1}{1+(2\tau\omega)^2}\right] \qquad A1$$

FIGURE 18.

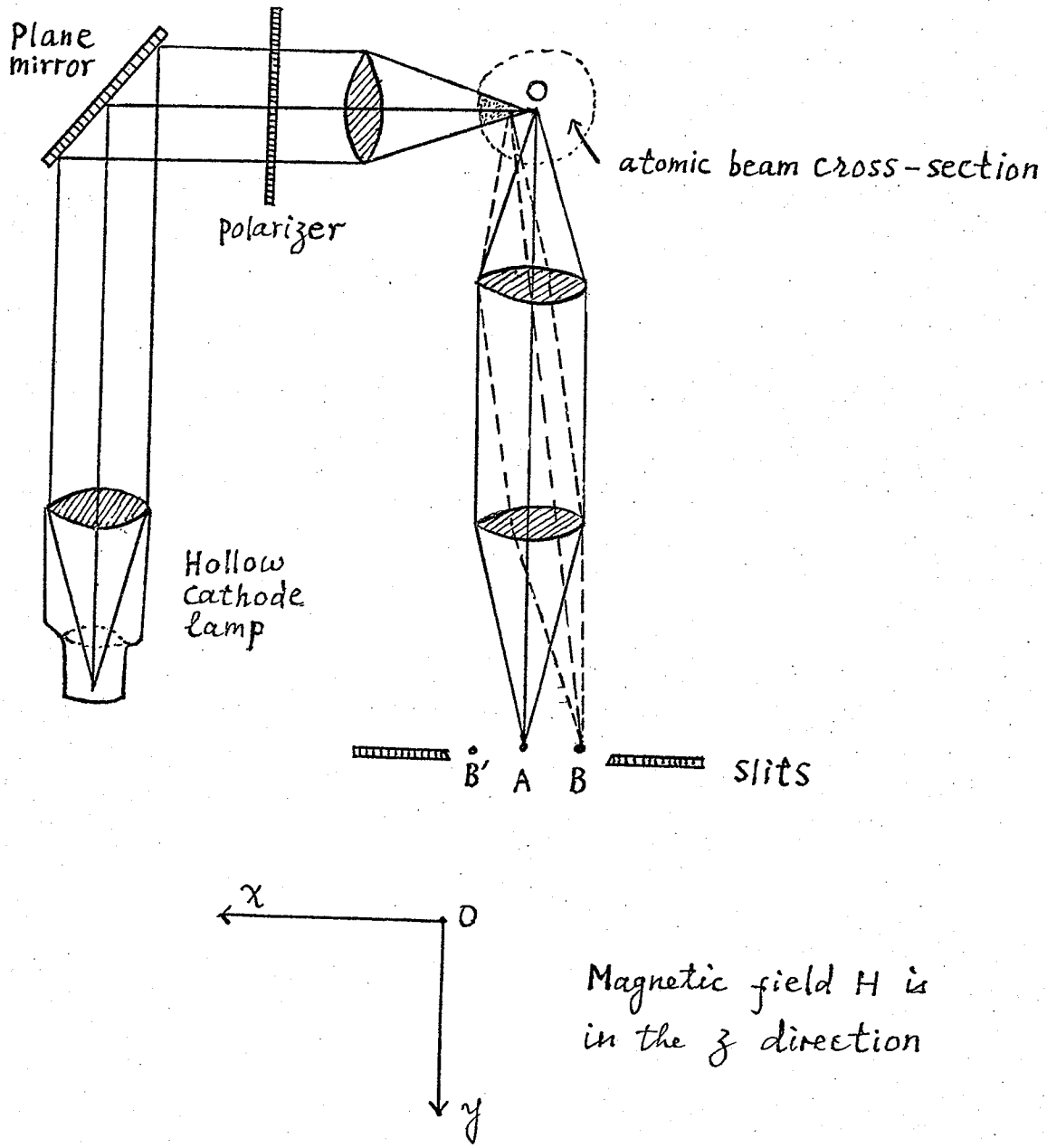
Plane mirror
O
atomic beam cross-section
Polarizer
Hollow cathode lamp
B'
A
B
slits
x
O
y
Magnetic field H is in the z direction

Now, if the direction of observation makes an angle with respect to the y axis, the intensity observed along that direction should be:

$$I' = C\int_0^\infty e^{-\Gamma t}\sin^2(\omega t+\phi)\,dt$$

$$= C\tau\sin^2\phi + \left(\frac{C\tau}{2}\right)\cos 2\phi\left[1-\frac{1}{1+(2\tau\omega)^2}\right] + \left(\frac{C\tau}{2}\right)\sin 2\phi\left[\frac{2\tau\omega}{1+(2\tau\omega)^2}\right] \qquad A2$$

using $(\omega t-\phi)$ obtained the same result.

Several conclusions can be drawn from equation A2.

a) If $\phi=0$ $I'=I$

b) If we have two symmetric interaction points with respect to y axis, the detecting system can 'look' at the image B on one side and B' on the other. Then, since B corresponds to a negative ϕ and B' corresponding to a positive ϕ, when they are equal and substituted into equation A2 at the same time, the effect on last term in equation A2 is cancelled out since $\sin(2\phi)=-\sin(-2\phi)$. This means when the interaction volume which can be observed by the detecting system is spread symmetrically with respect to the y axis, the Hanle signal is still an inverse Lorentzian distribution since the dispersion part are cancelled by considering pairs of points.

c) If we have a pair of unsymmetric interaction points, then the corresponding angles ϕ_1 and ϕ_2 are not equal and the dispersive components can not totally cancel out. Therefore the observed Hanle signal is a mixture of a Lorentzian distribution components with a dispersion distribution component as given by equation A2.

d) Equation A2 can also serve to determine the shape of the Hanle signal observed at different direction with respect to the y axis when the interaction region is considered as a point located at the geometrical centre. For example:

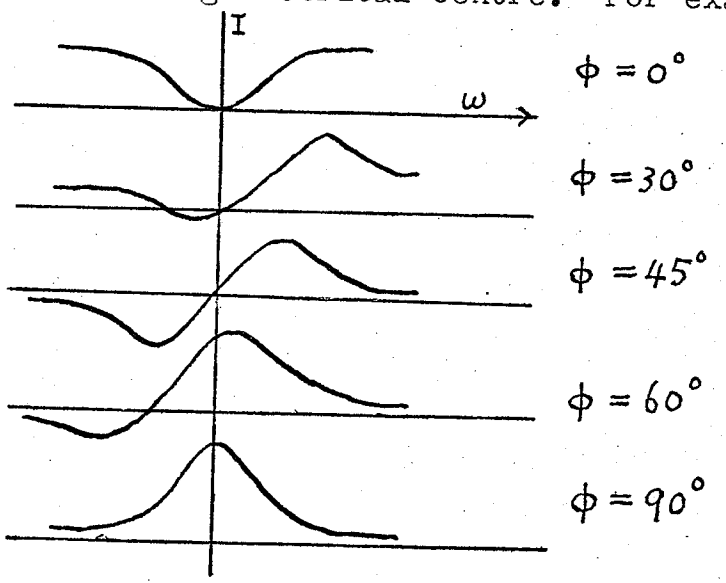

e) I' in equation A2 is considered at a point only. The total intensities received by the detecting system must be the integral over all the possible interaction points contained in the interaction volume. Also, the above discussions are dealing within the xy plane only. For $\theta \neq 90^{o}$, the general cases are given in pages 30 to 33.

APPENDIX II.

SIMPLE DERIVATION OF THE BREIT-FRANKEN FORMULA.

We assume that the incident excitation light is a short pulse and $E_m = 0$.

At time t=0, the system is described by: $|\Psi(0)\rangle = |m\rangle$.

At time t 0, the system is described by:

$$|\Psi(t)\rangle = |m\rangle + \sum_{\mu} f_{\mu m} |\mu\rangle \, e^{-(i\omega_{\mu} t + \frac{1}{2}\Gamma t)}$$

where $f_{\mu m} \equiv \langle \mu | \hat{f} \cdot \vec{r} | m \rangle$, $\omega_{\mu} = E_{\mu}/\hbar$ and Γ is the damping constant of the atoms. After excitation, the rate $R(\hat{f},\hat{g},t)$ is equal to:

$$\begin{aligned} R(\hat{f},\hat{g},t) &= N \sum_{m} \sum_{m'} \langle m' | \hat{g} \cdot \vec{r} \, | \Psi(t) \rangle^2 \\ &= N \sum_{m} \sum_{m'} \langle \Psi(t) | \hat{g}^{*} \cdot \vec{r} | m' \rangle \langle m' | \hat{g} \cdot \vec{r} | \Psi(t) \rangle \\ &= N \sum_{m} \sum_{m'} \sum_{\mu} \sum_{\mu'} f_{\mu m} f_{m\mu'} g_{\mu' m'} g_{m'\mu} \, e^{-(i\omega_{\mu,\mu'} + \Gamma t)} \end{aligned}$$

where N is the number of the atoms, $\omega_{\mu,\mu'} = \omega_{\mu} - \omega_{\mu'}$ and $g_{\mu' m'} \equiv \langle \mu' | \hat{g} \cdot \vec{r} | m' \rangle$ etc.

Integral over the time t, one thus have:

$$\begin{aligned} R(\hat{f},\hat{g}) &= \int_0^{\infty} R(\hat{f},\hat{g},t) \, dt \\ &= K \sum_{m m' \mu \mu'} \frac{f_{\mu m} f_{m\mu'} g_{\mu' m'} g_{m'\mu}}{\Gamma + i\omega_{\mu,\mu'}} \end{aligned}$$

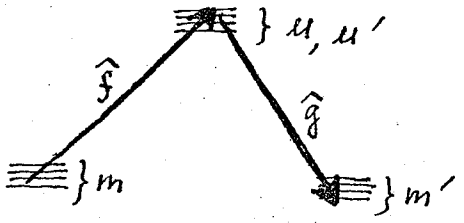

Lifetime of the $5s5p\ ^1P_1$ Level of Strontium

L. O. DICKIE[1], F. M. KELLY, T. K. KOH, M. S. MATHUR, AND F. C. SUK

Department of Physics, University of Manitoba, Winnipeg, Manitoba

Received January 23, 1973

The lifetime of the first excited singlet level, $5s5p\ ^1P_1$, of strontium has been measured using the Hanle resonance of the $5s^2\ ^1S_0 - 5s5p\ ^1P_1$, 4607 Å, resonance line. The lifetime of the $5s5p\ ^1P_1$ level is 5.29 ± 0.10 ns and the oscillator strength of the 4607 Å line is 1.80 ± 0.03. These results are compared with previous measurements.

La durée de vie du premier niveau excité singulet du strontium, $5s5p\ ^1P_1$, a été mesurée, utilisant la résonance Hanle de la raie de résonance $5s^2\ ^1S_0 - 5s5p\ ^1P_1$ à 4607 Å. La vie du niveau $5s5p\ ^1P_1$ est 5.29 ± 0.10 ns, et la force d'oscillateur de la raie 4607 Å est 1.80 ± 0.03. Ces résultats sont comparés avec ceux des mesures antérieures. [Traduit par le journal]

Can. J. Phys., **51**, 1088 (1973)

The Hanle effect, which uses the crossing of Zeeman levels at zero magnetic field, is a convenient method for the measurement of the lifetimes of excited atomic energy levels, particularly those which can be populated by optical excitation from the ground level. Early work on the Hanle effect is discussed in the book by Mitchell and Zemansky (1934). The theory has been given in a useful form for atomic spectroscopy by Lurio, de Zafra, and Goshen (1964) and in a general formulation by House (1970). In the experiments described here we have determined the lifetime of the first excited singlet P level of atomic strontium by observing the Hanle signal in the 4607.3 Å, $5s^2\ ^1S_0 - 5s5p\ ^1P_1$ transition. The apparatus is that described by Dickie and Kelly (1970, 1971*a*,*b*).

The geometry which we used is shown in Fig. 1. The input light is directed along the x axis and is linearly polarized with a type HN38 polaroid, with the electric vector in the x–y plane. The atoms which scatter the radiation are at the origin of coordinates. The magnetic field is along the z axis. The scattered light is observed along the y axis, that is, perpendicular to both the applied magnetic field and the direction of the incident light.

The resonance radiation is produced in a hollow cathode lamp which is cooled with an ice–water bath. The current in the hollow cathode is controlled by a constant current supply. The intensity of the line of interest was found to be constant and it was not necessary to monitor it with a separate system. The resonance radiation scattered from the beam of strontium atoms passes through a further polarizer and is focussed onto the input slit of a small grating monochromator which is used to isolate the desired wavelength.

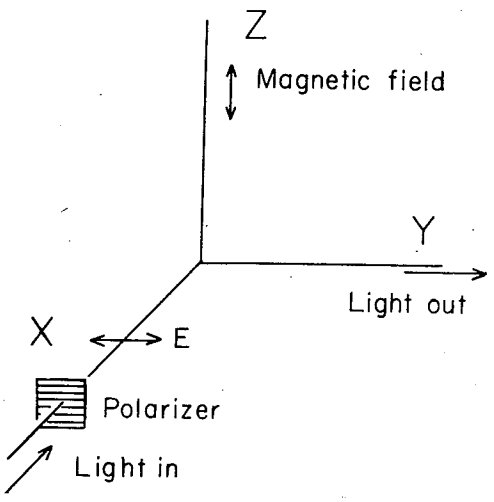

FIG. 1. Geometry of the Hanle experiment.

The atomic beam is produced in a d.c. electrically heated oven with a bifilar winding to reduce stray magnetic fields. Natural strontium, which is 93% isotopes 86 and 88 and 7% isotope 87, was used during the experiment. After passing the scattering region the beam is condensed on a cold trap. With the beam operating the pressure of the residual gas in the scattering chamber is about 10^{-5} mm of Hg.

The static magnetic field in the z direction is supplied by a pair of Helmholtz coils 40 cm in

[1]Present address: John Abbott College, Ste. Anne de Bellevue, Quebec.

diameter. During the experimental runs the current passing through a standard resistor in series with the coils and in a constant temperature oil bath is monitored. The scan through the Hanle resonance was obtained by applying a symmetric sawtooth ramp potential to another concentric set of Helmholtz coils. The fixed and sawtooth fields result in a magnetic field which is swept from about +100 G to −100 G in the scattering region.

Single photon pulses from the EMI6256 photomultiplier are amplified, passed through a single channel amplifier to isolate the single photon peak, then fed to the coincidence input of a multichannel analyzer. The magnetic field controls the address of the analyzer. The voltage across a standard resistance in series with the ramp coil is applied to the direct input of the ADC of the analyzer. A photon pulse arriving at the coincidence input causes the analyzer to sample the voltage in the direct input and to store the count in the appropriate channel. Figure 2 is a schematic diagram of the signal averaging apparatus. Because the count rate of the Hanle peak is different from that in the wings of the resonance, the count rate is kept low enough to ensure that the dead time of the analyzer is not important.

The data is analyzed by a computer program which fits a Lorentzian to the experimental points. As well, the difference between the calculated and experimental counts is plotted to determine if any dispersive component is present. A departure of the scattering angle from 90°, or the use of a solid angle which is too large can produce a dispersive component. These effects have been discussed by Fry and Williams (1969) and none was observed.

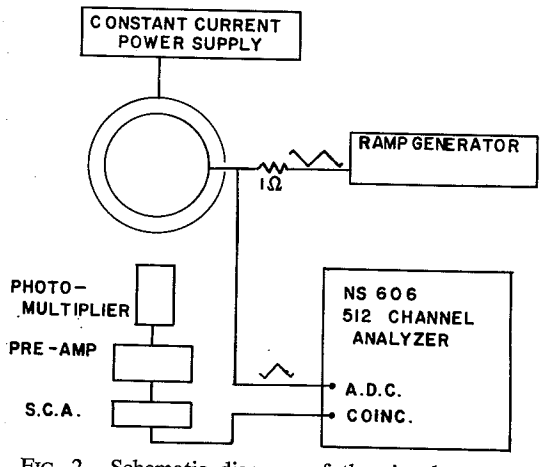

FIG. 2. Schematic diagram of the signal averaging apparatus.

A major advantage of the Hanle method is that the width of the resonance is independent of the density of the atoms, provided that coherence narrowing is not present. The effects of coherence narrowing is easy to observe with the line studied. Its effects were eliminated by operating at very low beam densities where the effect is negligible (Dickie and Kelly 1970).

The full width at half intensity, ΔH, of the Hanle resonance is related to the lifetimes, τ, by

$$\frac{1}{\tau} = \frac{g_J \mu_0}{\hbar} \Delta H$$

The mean life, τ, of the state m is given by

$$\frac{1}{\tau} = \sum_n A_n^m$$

and the Einstein A coefficient, A_n^m, for spontaneous emission from state m to the lower state n is given by

$$A_n^m = \frac{8\pi^2 e^2}{mc} \frac{g_m}{g_n} \frac{f_n}{(\lambda_{mn})^2}$$

where the g's are the statistical weights of the states and f_n is the absorption oscillator strength for the transition of wavelength λ_{nm} (Mitchell and Zemansky 1934; Crossley 1969).

The $5s5p\ ^1P_1$ level of strontium can decay directly to the ground state $5s^2\ ^1S_0$ by emission of a photon of the resonance line 4607 Å and also to the metastable $5s4d\ ^1D_2$. The wavelength of this line, calculated from the tables of Moore (1952), is 64 600 Å. The oscillator strength of this line is not known but is likely to be smaller than that of 4607 Å and due to its much larger wavelength the A coefficient for this transition may be neglected.

The steady field in the main Helmholtz coils were calibrated with a Rawson–Lush rotating coil gaussmeter with an absolute accuracy of 0.01%. The digital voltmeter was accurate to 0.02%. As well, the current in the main coils was calibrated with the channel number of the analyzer so that the width of the resonance in channel numbers can be converted to gauss.

Measurements were made at the lowest possible beam density to avoid coherence narrowing. The results of a typical run are shown

TABLE 1. Lifetimes and oscillator strength for λ 4607 Å

Method	Lifetime (ns)	f(4607)	Reference*
Dispersion	8	1.2	(1)
Theory	—	1.90	(2)
Hook	6.4	1.5 ± 0.2	(3)
Hook	6.2	1.54 ± 0.05	(4)
Hanle	6.1 ± 0.6	1.56 ± 0.16	(5)
Phase	4.56 ± 0.21	2.09 ± 0.10	(6)
Hanle	4.97 ± 0.15	1.92 ± 0.05	(7)
Hanle	5.29 ± 0.10	1.80 ± 0.03	(8)

*References are: (1) Prokofev (1928); (2) Bates and Damgaard (1949); (3) Ostrovskii *et al.* (1958); (4) Ostrovskii and Penkin (1961); (5) De Zafra *et al.* (1962); (6) Hulpke, Paul, and Paul (1964); (7) Lurio, De Zafra, and Goshen (1964); (8) this work.

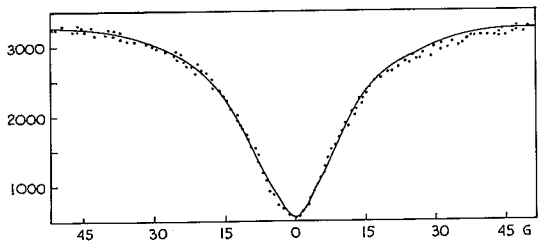

FIG. 3. A plot of the experimental counts, and the fitted Lorentian, against magnetic field.

in Fig. 3. With $g_J = 1.00$ and the average of seven runs at very low density we obtain $\tau = 5.29 \pm 0.02$ ns. We have, however, multiplied the error by 5 to allow for an unknown systematic error. With $g_1 = 1.00$ and $g_2 = 3.00$ and neglecting the transition to the $5s\,4d\,^1D_2$ level, we obtain $f(4607) = 1.80 \pm 0.03$.

Comparisons of measurement are shown in Table 1. Our result for f is lower than that obtained by Hulpke, Paul, and Paul (1964) who measured a phase shift and also that of Lurio *et al.* (1964) who also used the Hanle effect.

Acknowledgments

This work was supported by a grant from the National Research Council of Canada.

BATES, D. R. and DAMGAARD, A. 1949. Phil. Trans. **242**, 101.
CROSSLEY, R. J. S. 1969. Adv. At. Mol. Phys. **5**, 237.
DE ZAFRA, R. R., GOSHEN, R. J., LANDMAN, A., and LURIO, A. 1962. Bull. Am. Phys. Soc. **7**, 433.
DICKIE, L. O. and KELLY, F. M. 1970. Can. J. Phys. **48**, 879.
——— 1971*a*. Can. J. Phys. **49**, 1098.
——— 1971*b*. Can. J. Phys. **49**, 2630.
FRY, E. S. and WILLIAMS, W. L. 1969. Phys. Rev. **183**, 81.
HOUSE, L. L. 1970. J. Quant. Spectrosc. Radiat. Transfer, **10**, 909, 1171.
HULPKE, E., PAUL, E., and PAUL, W. 1964. Z. Phys. **117**, 256.
LURIO, A., DE ZAFRA, R. L., and GOSHEN, R. J. 1964. Phys. Rev. **134**, 1198.
MITCHELL, A. and ZEMANSKY, M. W. 1934. Resonance radiation and excited atoms (Cambridge University Press, London).
MOORE, C. E. 1952. Atomic energy levels, Vol. II, Circ. NBS 467.
OSTROVSKII, YU. I. and PENKIN, W. P. 1961. Opt. Spectrosc. **11**, 307.
OSTROVSKII, YU. I., PENKIN, W. P., and SHABANOVA, L. N. 1958. Sov. Phys. Dokl. **3**, 538.
PROKOFEV, U. K. 1928. Z. Phys. **50**, 701.

Lifetime of the $5s6p\ ^1P_1$ Level of Strontium and Related Oscillator Strengths

F. M. KELLY, T. K. KOH, AND M. S. MATHUR
Department of Physics, University of Manitoba, Winnipeg, Manitoba

Received April 2, 1973

The lifetime of the second excited singlet P level, $5s6p\ ^1P_1$, of strontium has been measured using the Hanle effect of the $5s4d\ ^1D_2 - 5s6p\ ^1P_1$, 7169 Å, transition. The lifetime of the $5s6p\ ^1P_1$ level is 3.64 ± 0.14 ns. Oscillator strengths for the transitions from the $5s6p\ ^1P_1$ level are discussed. There are large discrepancies.

On a mésuré la durée de vie du deuxieme niveau excité singulet du strontium, $5s6p\ ^1P_1$, en utilisant la résonance Hanle de la raie $5s4d\ ^1D_2 - 5s6p\ ^1P_1$ à 7169 Å. Cette durée de vie est 3.64 ± 0.14 ns. On discute les forces d'oscillateur pour les raies du niveau, $5s6p\ ^1P_1$. Ils existent encore des problèmes.

Can. J. Phys., **51**, 1653 (1973)

The Hanle effect, which employs the crossing of Zeeman states at zero magnetic field, has become an important method for the measurement of the lifetimes of excited atomic energy levels, particularly those levels which can be populated by optical excitation from the ground level. In the experiment described in this paper, we have measured the lifetime of the second excited singlet P level of neutral strontium by observing the Hanle signal in the 7169 Å, $5s4d\ ^1D_2 - 5s6p\ ^1P_1$ transition.

The geometry which we used is shown in Fig. 1. The input light is directed along the x axis and is linearly polarized with a type HN38 polaroid, with the electric vector in the x–y plane. The magnetic field is along the z axis and is thus perpendicular to both the input light and the direction of observation which is along the y axis. In principle, with this geometry, there is no scattered light along the direction of observation, when the magnetic field is zero.

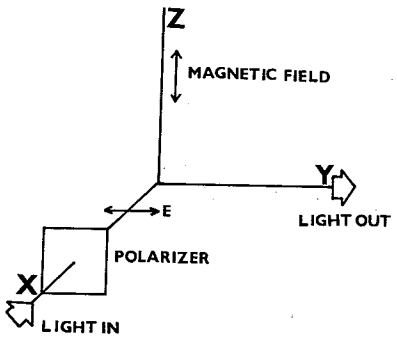

FIG. 1. Geometry of the Hanle experiment.

The apparatus which we used is similar to that described by Dickie and Kelly (1971 *a*, *b*), but the furnace was moved closer to the scattering region, the origin of coordinates in Fig. 1. This was accomplished by making the input and observation direction in the horizontal plane of the laboratory and placing the Helmholtz coils so that the magnetic field is vertical. The modification increased the density of the atoms in the scattering region and made the detection of weaker signals easier. Figure 2 is a schematic diagram of the apparatus. The beam of strontium atoms is produced in a d.c. electrically heated oven with a bifilar winding. Natural strontium, which is 93% isotopes 86 and 88 and 7% isotope 87, was used during the experiment.

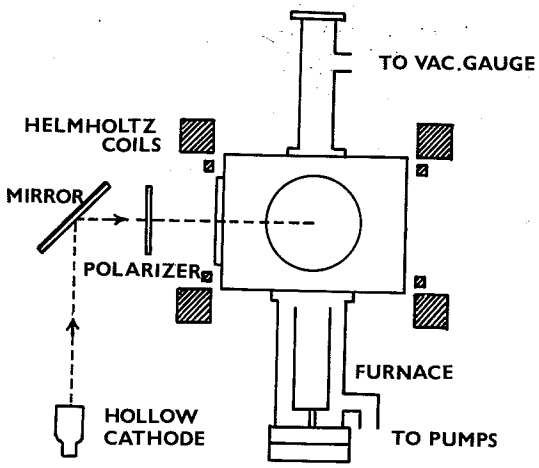

FIG. 2. Schematic diagram of the experimental apparatus; direction of the scattered light is perpendicular to the plane of the diagram.

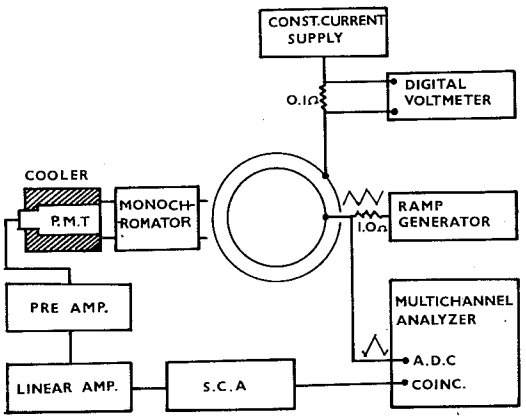

FIG. 3. Schematic diagram of the signal averaging apparatus.

The static magnetic field in the z direction is supplied by a pair of Helmholtz coils 40 cm in diameter. The scan through the Hanle resonance at zero field is obtained by applying a symmetric saw-tooth ramp potential to another concentric set of Helmholtz coils. The fixed and sawtooth fields result in a magnetic field which is swept from about +100 G to −100 G in the scattering region. The field is monitored by passing the current through a standard resistance.

Single photon pulses from an RCA C31034 photomultiplier, sensitive to about 9000 Å and cooled to about −20 °C to reduce the dark noise, are amplified with a low noise amplifier, passed through a single channel analyzer to isolate the photon peak, and then fed to the coincidence of a multichannel analyzer. The voltage across a standard resistance in series with the ramp coil is applied to the direct input of the ADC of the analyzer. A photon pulse arriving at the coincidence input causes the analyzer to sample the voltage in the direct input and to store the counts in the appropriate channel. The count rate in the wings is low enough to ensure that the dead time of the analyzer is not important. Figure 3 is a block diagram of signal averaging apparatus.

The data which consist of counts versus channel number are analyzed by a computer program which fits a Lorentzian to the points. The difference between the calculated and experimental counts is plotted to determine if any dispersive component is present. Such a dispersive component can arise from a scattering angle deviating from 90° or the use of too large a solid angle. These effects have been discussed by Fry and Williams (1969) and none was observed.

A major advantage of the Hanle method is that the width of the resonance is independent of the density of the atoms in the scattering region provided coherence narrowing is not present. With several values of the heating current for the furnace and thus several beam densities we did not discover a significant trend in the values of the widths of the Hanle resonances. The full width at half intensity, ΔH, of the Hanle resonance is related to the lifetime, τ, by

$$\frac{1}{\tau} = \frac{g_J \mu_0}{\hbar} \Delta H$$

From the mean value of ΔH for 10 independent runs, we find that the lifetime of the $5s6p\ ^1P_1$ is $(3.64 \pm 0.14) \times 10^{-9}$ s. The magnetic fields of the coils are calibrated as a function of current with a Rawson–Lush rotating coil gaussmeter with an absolute accuracy of 0.01%. The calibration of the number of channels versus magnetic field in gauss is obtained by changing the steady magnetic field to a number of different values so that the peak of the Lorentzian appears at a different channel.

The mean life, τ, of the state m is given by

$$\frac{1}{\tau} = \sum_n A_n^m$$

and the Einstein A coefficients, A_n^m, for spontaneous emission from upper state m to the lower state n is given by

$$A_n^m = \frac{8\pi^2 e^2}{mc} \frac{g_n}{g_m} \frac{f_{mn}}{(\lambda_{nm})^2}$$

where the g's are the statistical weights of the states and f_{mn} is the absorption oscillator strength for the transition of wavelength λ_{nm} (Mitchell and Zemansky 1934; Crossley 1969).

The $5s6p\ ^1P_1$ level of strontium can decay directly to the ground level $5s^2\ ^1S_0$ by the emission of a photon of 2932 Å, and to the metastable $5s4d\ ^1D_2$ level with a photon of wavelength 7169 Å. This latter transition is the one observed in this experiment. Also, there is a transition to the $5s6s\ ^1S_0$ level with a wavelength of 28 517 Å. The wavelengths given here are vacuum wavelengths calculated from the energy level tables of Moore (1952). With numerical values substituted into the equation for $1/\tau$, we obtain

TABLE 1. Oscillator strengths in strontium

Method	Reference*	$f(2932)$	$f(7169)$
Theory	1	0.02	—
Theory	2	0.356	—
Theory	3	4.4×10^{-3}	—
Emission	4	0.95	0.13
Intensity 4607/2932	5	1.5×10^{-3}	1.27
Intensity 2932/7169	5	0.26	0.96
$f(4607)/f(2932)$	6	$(6.29 \pm 0.22) \times 10^{-3}$	1.26 ± 0.05

*1, Bates and Damgaard (1949), our calculations; 2, Helliwell (1964); 3, Zilitis (1970); 4, Eberhagen (1955); 5, Meggers, Corliss, and Scribner (1961); 6, Penkin and Shabanova (1962).

$$\frac{1}{\tau} = \frac{10^7}{1.499}\,[38.76 f(2932) + 32.43 f(7169) + 0.41 f(28\,517)]$$

From this equation it is evident that neglecting the long wavelength line produces an error which is small compared with the others in the experiment.

The oscillator strength of 4607 Å measured by Penkin and Shabanova (1962) using the hook method is 1.54 ± 0.08. This does not agree with the recent Hanle measurements. The weighted mean of the last three entries of Table 1 of Dickie *et al.* (1973) for the oscillator strength of this line is 1.85 ± 0.06. However, the relative oscillator strengths from the hook method are reliable. Penkin and Shabanova (1962) estimate the error of the absolute oscillator strengths at 5%, while the relative oscillator strengths are measured with much greater accuracy.

Penkin and Shabanova (1962) give the ratio $f(4607)/f(2932) = 1000/3.40$, which makes the absolute oscillator strength of 2932 Å equal to $(6.29 \pm 0.22) \times 10^{-3}$. The error is estimated from an assumed 0.3% error in the ratio and a 3.2% error in $f(4607)$. With the above value of the absolute oscillator strength of 2932 Å, we calculate the oscillator strength of 7169 Å to be 1.26 ± 0.05 where the error arises almost entirely from the error in the measured lifetime.

Another approach to the f values is through the experimentally observed intensities from arc spectra in emission. The intensity ratio of 4607 Å to 2932 Å is 650:2.0 (Meggers, Corliss, and Scribner 1961). This leads to $f(4607)/f(2932) = 1260$ so that $f(2932)$ is 1.5×10^{-3}. The measurement of an intensity ratio of this size is likely to contain a large systematic error. However, the result is of the same order of magnitude as that obtained with the f ratio of Penkin and Shabanova (1962) and supports a small value for the oscillator strength of 2932 Å.

Meggers, Corliss, and Scribner (1961) give the ratio of the intensities of 2932 Å to 7169 Å as 2.0:2.5. From this we obtain $f(2932)/f(7169) = 0.274$, and using our value of the lifetime of the $5s6p$ singlet level we calculate $f(7169) = 0.96$ and $f(2932) = 0.26$. The experimental error is about 20% but there likely is a larger systematic error from the measurement of the intensity ratio. The disagreement between this result and the f values using the ratio found by Penkin and Shabanova (1962) is large.

The results are collected in Table 1. Our lifetime of the $5s6p\ ^1P_1$ level, 3.64 ± 0.14 ns, and $f(4607) = 1.85 \pm 0.06$ from Dickie *et al.* (1973) are used in our calculations.

We have already used the method of Bates and Damgaard to calculate the oscillator strength of 4706 Å (Dickie *et al.* 1973) and obtained the value 1.90 in good agreement with the weighted mean of the experimental values, 1.85 ± 0.06. The method of Bates and Damgaard gives $f(2932) = 0.02$, a small value, but three times the most reliable experimental value. Helliwell (1964) with another method of calculations obtains $f(4607) = 2.12$ in reasonable agreement with the experimental result, but calculates $f(2932) = 0.356$, considerably larger than any experimental result, with the exception of our calculation of $f(2932)$ from Eberhagen's (1955) emission measurement of $f(7169)$. Zilitis (1970) with a semi-empirical method gives data from which we calculate $f(4607) = 2.45$, about 25% too large, and $f(2932) = 4.4 \times 10^{-3}$, which considering the other theoretical values is reasonably close to the best experimental one.

The table shows considerable disagreement for the observed and calculated f values. We consider that the most reliable values are those in the last

line of the table which uses the Hanle lifetime measurement of the $5s6p$ level together with the hook measurement of the ratio of $f(4607)/f(2932)$. The lack of consistency with the values calculated from the intensity ratios is likely due to the experimental difficulty in determining these ratios.

Acknowledgment

This work was supported by a grant from the National Research Council of Canada.

BATES, D. R. and DAMGAARD, A. 1949. Phil. Trans. **242**, 101.
CROSSLEY, R. J. S. 1969. Adv. At. Mol. Phys. **5**, 237.
DICKIE, L. O. and KELLY, F. M. 1971*a*. Can. J. Phys. **49**, 1098.
——— 1971*b*. Can. J. Phys. **49**, 2630.
DICKIE, L. O., KELLY, F. M., KOH, T. K., MATHUR, M. S., and SUK, F. C. 1973. Can. J. Phys. **51**, 1088.
EBERHAGEN, A. 1955. Z. Phys. **143**, 392.
FRY, E. S. and WILLIAMS, W. L. 1969. Phys. Rev. **183**, 81.
HELLIWELL, T. M. 1964. Phys. Rev. A, **135**, 325.
MEGGERS, W. F., CORLISS, C. H., and SCRIBNER, B. F. 1961. U.S. Nat. Bur. Stand. Mono. 32, Part I.
MITCHELL, A. and ZEMANSKY, M. W. 1934. Resonance radiation and excited atoms (Cambridge University Press, London).
MOORE, C. E. 1952. Atomic energy levels, Vol. II, U.S. Nat. Bur. Stand. Circ. 467.
PENKIN, W. P. and SHABANOVA, L. N. 1962. Opt. Spectrosc. **12**, 1.
ZILITIS, U. A. 1970. Opt. Spectrosc. **29**, 438.

Lifetimes of the $5s7p$ and $5s8p\ ^1P_1$ Levels of Strontium and Related Oscillator Strengths

F. M. KELLY, T. K. KOH, AND M. S. MATHUR
Department of Physics, University of Manitoba, Winnipeg, Manitoba

Received July 9, 1973

The lifetimes of the $5s7p$ and $5s8p$ excited singlet P level of strontium have been measured using the Hanle effect of the 5331 and 4755 Å transitions to the $5s4d\ ^1D_2$ level. The lifetimes of the $5s7p$ and $5s8p\ ^1P_1$ levels are 4.93 ± 0.35 and 5.46 ± 0.17 ns. The related f values are discussed.

On a mésuré la durée de vie des niveaux excité singulet du strontium, $5s7p$ et $5s8p\ ^1P_1$, en utilisant la résonance Hanle des raies à 5331 et 4755 Å au niveau $5s4d\ ^1D_2$. Ces durées de vie sont 4.93 ± 0.35 et 5.46 ± 0.17 ns. On discute les forces d'oscillateur pour les raies de ces niveaux.

Can. J. Phys., **51**, 2295 (1973)

Introduction

In previous papers (Dickie *et al.* 1973; Kelly *et al.* 1973), we have reported measurements of the lifetimes of the $5s5p$ and $5s6p$ singlet P levels of strontium. In this paper, we report the extension of the measurements to the $5s7p$ and $5s8p$ singlet P levels, again using the Hanle effect, which employs the crossing of the Zeeman levels at zero magnetic field and the consequent spatial redistribution of the intensity of the resonance fluorescence. The theory of Hanle effect has been given in a useful form for atomic spectroscopy by Lurio *et al.* (1964). Under the geometry of our experiment, the spontaneous emission from the excited state to the metastable $5s4d\ ^1D_2$ state is shown in Fig. 1. The π components ($\Delta m_J = 0$) are field independent and are not relevant in our case, whereas the σ components ($\Delta m_J = \pm 1$) are field dependent and are shown in the figure. Out of the σ components a, b, c, and d, only a and b take part in the Hanle signal because the reradiation matrix elements for c and d are zero. The Hanle resonance obtained in this case will be similar to the case where the lower level is $^1S_0$.

The full width at half intensity, ΔH, of the Hanle resonance is related to the lifetime, τ, by

$$1/\tau = (g_J \mu_0/\hbar)\Delta H \qquad [1]$$

The mean life, τ, of the upper state m is given by

$$\frac{1}{\tau} = \sum_n A_n{}^m \qquad [2]$$

and the Einstein A coefficients, $A_n{}^m$, for spontaneous emission from state m to the lower state n are given by

$$A_n{}^m = \frac{8\pi^2 e^2}{m_e c}\,\frac{g_n}{g_m}\,\frac{f_n}{(\lambda_{mn})^2} \qquad [3]$$

where the g's are the statistical weights of the states and f_n is the absorption oscillator strength for the transition of wavelength λ_{mn} (Mitchell and Zemansky 1934; Crossley 1969).

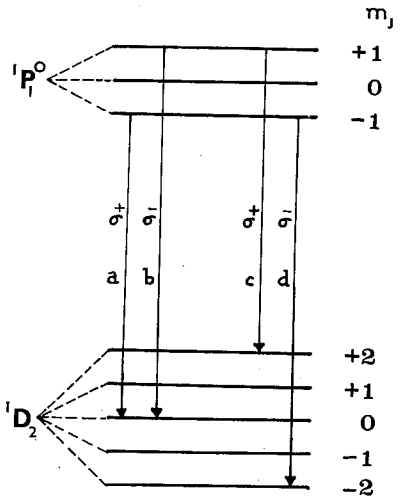

FIG. 1. Zeeman structure of upper and lower levels.

Experimental

For the measurements reported in this paper, we have used the apparatus, geometry, and signal averaging technique described earlier (Kelly *et al.* 1973). In each case, the appropriate

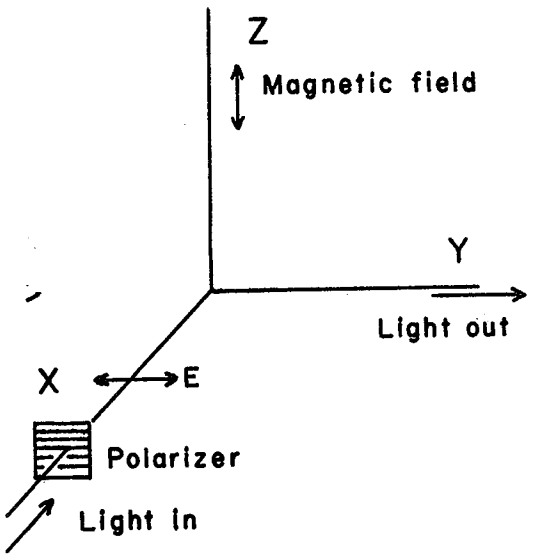

FIG. 2. Geometry of the Hanle experiment.

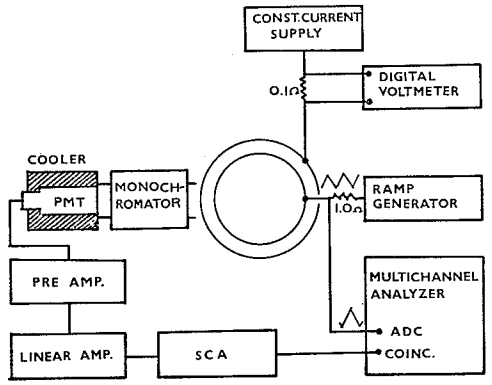

FIG. 3. Schematic diagram of the signal averaging apparatus.

wavelength of the output light was selected with a grating monochromator. The geometry employed is shown in Fig. 2, while Fig. 3 is a block diagram of the signal averaging apparatus.

The input light was produced in an ice-water-cooled hollow cathode lined with metallic strontium and with neon to carry the discharge. The time of an individual run was limited to 2 to 3 h by instability in the hollow cathode due to changes in the neon gas pressure. A polarizer is used in the input arm so that the input light is plane polarized with the electric vector in the x–y plane. The light is scattered from a beam of strontium atoms with natural isotopic abundance. The single-photon pulses from the photomultiplier are amplified, passed through a single-channel analyzer to isolate the photon peak, and then fed to the coincidence input of a multichannel analyzer. The voltage across a standard resistance in series with the ramp coil is applied to the direct input of the analog to digital converter circuit of the analyzer. The single-photon pulse arriving at the coincidence input causes the analyzer to sample the voltage in the direct input and store the counts in the appropriate channel as the magnetic field is swept from $+10^{-2}$ T to -10^{-2} T. The period of the sweep is 2.5 s. To obtain the calibration of channel number versus magnetic field, we change the steady magnetic field to a number of values and observe the channel at which the zero of the Lorentzian appears.

In an attempt to increase the counting rate, the widest possible slits on the monochromator are used, consistent with the elimination of the scattered light from the triplet system of levels of the strontium atom. The $5s7p$ and $5s8p\ ^1P_1$ levels are excited with 2570 and 2428 Å radiation from the hollow cathode. The Hanle resonance is observed in the decays to the $5s4d\ ^1D_2$ metastable level using the lines with wavelengths 5331 and 4755 Å (see Fig. 6).

Results

$5s7p\ ^1P_1$ Level

The lifetime of the $5s7p\ ^1P_1$ level is measured by studying the Hanle resonance in the 5331 Å transition to the $5s4d\ ^1D_2$ level. From 10 individual runs, each about 2 h counting time, the average width at half height is 96.2 channels with a standard deviation of 2.7 channels. This leads to $\Delta H = 23.0 \times 10^{-4}$ T and a lifetime, $\tau = 4.93 \pm 0.14$ ns. The error in this value is from the standard deviation of our measurements alone.

In the experiments with 5331 Å, the signal to noise ratio was about 3:1. To improve the statistics, a computer program is used to add the number of counts of the individual runs, channel by channel. For 5331 Å, we shifted the zero of the Lorentzian to obtain the calibration of T per channel mentioned in the paragraph above. For this reason, the computer had to shift the counts to appropriate channels, and the composite curve has a half-width of 89.3 channels,

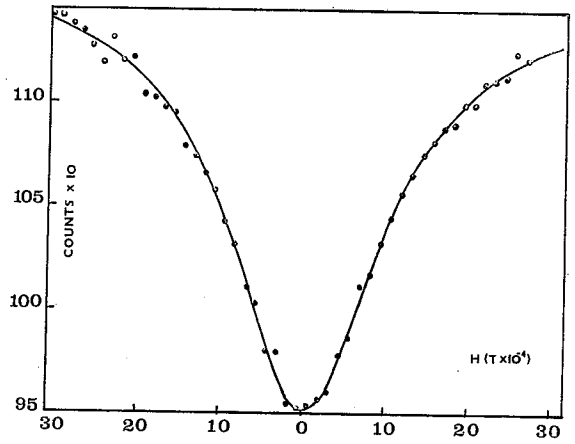

FIG. 4. Composite Hanle curve for 5331 Å.

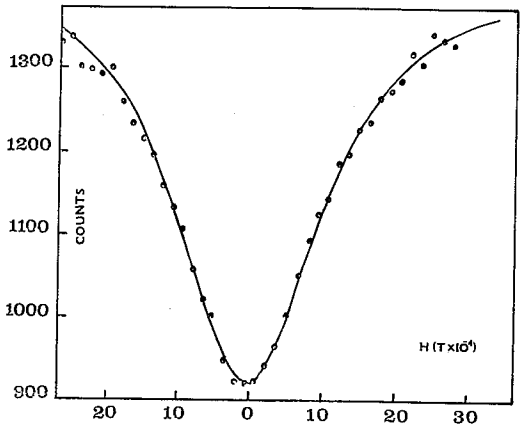

FIG. 5. Composite Hanle curve for 4755 Å.

about 7% less than the average of the individual runs. This approach improves the statistics, but the process of shifting the counts to appropriate channels introduces an extra error, and we consider 96.2 channels, the average value from the individual runs, to be better. However, we increase the error in the measured lifetime to 7% and take 4.93 ± 0.35 ns as the best value for the lifetime of the $5s7p\ ^1P_1$ level.

We checked the effect of the sweep field by obtaining a Hanle curve using a step by step increase in the steady magnetic field with the ramp field off, and good agreement was found. Figure 4 is the composite Hanle curve for $\lambda = 5331$ Å.

$5s8p\ ^1P_1$ Level

The lifetime of the $5s8p$ level is measured from the Hanle resonance in the 4755 Å line. The calibration of the analyzer in T per channel was known, and the runs are taken under identical conditions. For 5 individual runs, the average value of the width at half height is 86.6 ± 2.6 channels. The composite data of the 5 individual runs give a value of 87.0 channels. In this case, the zeros of the Lorentzian curves were all at the same channel number, and no shifting of counts to other channels is required. In contrast to the 5331 Å experiments, the agreement is excellent, and we use the composite value where the statistics are much improved. However, to allow for an unknown systematic error, we are using the larger error from the average of the individual runs. This leads to $\Delta H = 20.8 \pm 0.6 \times 10^{-4}$ T and $\tau = 5.46 \pm 0.17$ ns for the $5s8p\ ^1P_1$ level. Figure 5 is the composite Hanle curve for $\lambda = 4755$ Å.

Discussion

A major advantage of the Hanle method is that the width of the resonance is independent of the density of the atoms in the scattering region, provided neither coherence narrowing nor collision broadening are present. The effect of coherence narrowing depends upon the population of the metastable $5s4d\ ^1D_2$ level, which in our case can be populated by transitions from $5s7p$ and $5s8p$ levels. This population tends to be small compared with the ground state population; thus the chances of trapping the 5331 and 4755 Å radiation are negligible, and hence the coherence narrowing will be insignificant.

To increase the counting rate, the experiments reported here employ a high beam density; but the use of a strontium beam suggests that very few collisions producing Holtsmark broadening are to be expected.

Hsieh and Baird (1972) have studied the shape of Hanle resonance when coherence narrowing and collision broadening are present. We have applied their equation (4) to the work done in this paper and with reasonable values of the parameters find that due to the low f values for the transitions to the ground state, both coherence narrowing and collision broadening introduce contributions which are much smaller than the experimental errors in our measured lifetimes.

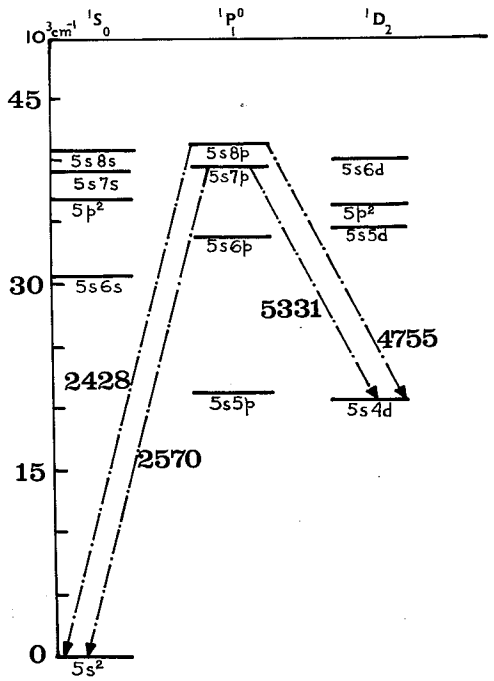

FIG. 6. Energy level diagram for the singlet levels of strontium.

The energy level diagram, Fig. 6, based on the energy level tables of Moore (1952) shows that there are seven transitions from the $5s7p$ level and nine from the $5s8p$ level. However, when numerical values are substituted in the sum of the A's, only two terms in each of the series are important due to the fact that the A's are inversely proportional to the square of the wavelengths of the transitions. Penkin and Shabanova (1962) have used the hook method to determine the relative f values of principal series lines of strontium. From their data and from the weighted average of the last three entries of Table 1 of Dickie *et al.* (1973), we obtain $f(2570) = (1.32 \pm 0.04) \times 10^{-2}$ and $f(2428) = (3.87 \pm 0.13) \times 10^{-2}$. With these values of the f's, our measurements of the lifetimes of the excited levels, and the sum of the A coefficients, we can determine the f's of the transitions to the $5s4d\,^1D_2$ level. When we neglect all but the transitions to the ground level and the transitions to the $5s4d$ level in the sum of the A's, we obtain $f(5331) = 0.507$ and $f(4755) = 0.344$. These are upper limits for the f's since there is an unknown contribution from the other transitions.

There is no experimental information which enables us to estimate the f values of the other transitions from these levels. However, the relatively large values of the wavelengths of these other transitions make their coefficients in the sum of the f's much smaller than the coefficients for the lines already considered, and unless some of these f's have unusually large values, their contribution to the lifetime of the level is small. For the $5s7p$ singlet level we have neglected five transitions. If we assume that the f's of each is 0.1, the calculated value of $f(5331)$ becomes equal to 0.497, instead of 0.507. Thus, we make $f(5331) = 0.50 \pm 0.04$. The error comes almost entirely from the error in the measured lifetime.

For the $5s8p$ singlet level, seven transitions, all with small coefficients, have been neglected in the calculation. If we assume that each of the neglected transitions has an f value equal to 0.08, $f(4755)$ becomes 0.329, in place of the upper limit, 0.344. Thus, we make the value of $f(4755) = 0.33 \pm 0.02$. We have doubled the 3% error in the lifetime measurement to allow for extra uncertainties.

Eberhagen (1955) has used an emission method and gives $f(5331) = 0.12$ and $f(4755) = 0.075$, each with a 20% error. The agreement with our results is not good. The accuracy of the data obtained by the emission method can be questioned on the grounds that:

(*i*) The intensity cannot be measured accurately due to the reabsorption of the spectral lines;

(*ii*) the temperature of the arc cannot be measured accurately.

This suggests that the accuracy of our f values is better than those reported by Eberhagen.

The various f values for the transitions from the $5s7p$ and $5s8p$ levels are collected in Table 1.

Acknowledgment

This work was supported by a grant from the National Research Council of Canada.

ALTICK, P. L. and GLASSGOLD, A. E. 1964. Phys. Rev. **133**, A632.

BATES, D. R. and DAMGAARD, A. 1949. Phil. Trans. **242**, 101.

CROSSLEY, R. J. S. 1969. Adv. At. Mol. Phys. **5**, 237.

DICKIE, L. O., KELLY, F. M., KOH, T. K., MATHUR, M.S., and SUK, F. C. 1973. Can. J. Phys. **51**, 1088.

EBERHAGEN, A. 1955. Z. Phys. **143**, 392.

TABLE 1. Oscillator strength of transitions from the $5s7p$ and $5s8p$ $^1P_1$ levels

	$5s7p$		$5s8p$		
Method	f(2570)	f(5331)	f(2428)	f(4755)	Reference*
Theory	0.0012	—	0.033	—	(1)
Theory	0.011	—	0.030	—	(2)
Theory	0.057	—	—	—	(3)
Emission	—	0.12	—	0.075	(4)
Hook	0.0110	—	0.032	—	(5)
Hanle	0.0132	0.50	0.0387	0.33	(6)

*References are: (1) Bates and Damgaard (1949), our calculations; (2) Zilitis (1970) Coulomb approximation, our calculations; (3) Altick and Glassgold (1964) random phase approximation; (4) Eberhagen (1955); (5) Penkin and Shabanova (1962); (6) present work.

The difference between the hook result of Penkin and Shabanova (1962) and our Hanle result arises only from a different f value for the resonance line, 4607 Å (Dickie *et al.* 1973).

HSIEH, J. C. and BAIRD, J. C. 1972. Phys. Rev. **6**, 141.

KELLY, F. M., KOH, T. K., and MATHUR, M. S. 1973. Can. J. Phys. **51**, 1653.

LURIO, A., DE ZAFRA, R. L., and GOSHEN, R. J. 1964. Phys. Rev. **134**, A1198.

MITCHELL, A. and ZEMANSKY, M. W. 1934. Resonance radiation and excited atoms (Cambridge University Press, London).

MOORE, C. E. 1952. NBS Circ. 467, Vol. II.

PENKIN, N. P. and SHABANOVA, L. N. 1962. Opt. Spectrosc. **12**, 1.

ZILITIS, V. A. 1970. Opt. Spectrosc. **29**, 438.

SPECTROSCOPY LETTERS, 7(3), 153-159 (1974)

HANLE SIGNAL CORRECTION FOR ASYMMETRIC SCATTERING REGION

Key Words: Hanle signal correction

M. S. Mathur, T. K. Koh and F. M. Kelly

Department of Physics, Univ. of Manitoba, Winnipeg, Canada

ABSTRACT: Hanle technique is used for the lifetime measurement of the atomic excited states. Field dependent Hanle signal is Lorentzian under ideal conditions. Any departure from ideal situation reflects in the shape of the Hanle signal resulting in erroneous lifetime. One such factor and the elimination of its effect has been discussed here.

Level crossings involving resonance fluorescence are observed experimentally by noting the change in the intensity of the scattered resonance radiation as a function of an applied magnetic field. Zero-field crossings were first observed by Hanle[1]. The commonly used geometry of the Hanle experiment is given in figure 1. θ, ψ and θ', ψ' are the azimuthal and polar angles for the incident and observed light directions.

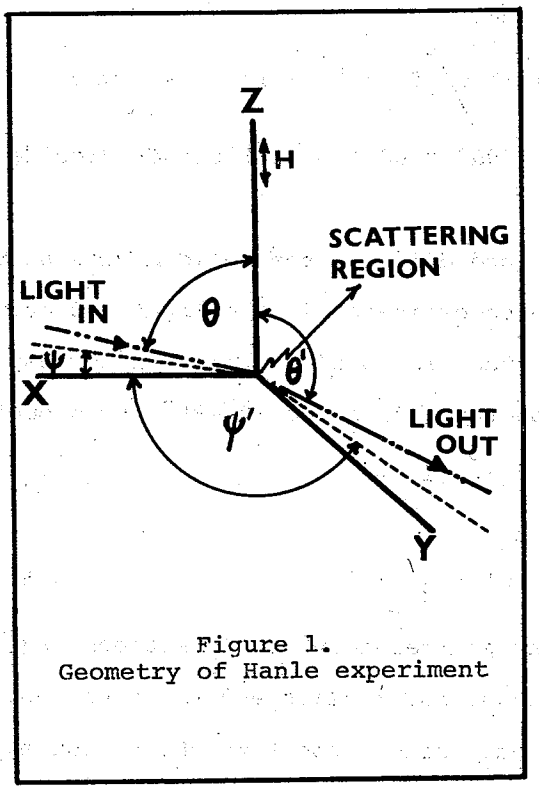

Figure 1.
Geometry of Hanle experiment

Several authors[2-6] have shown that for a Hanle effect level crossing, the scattering rate I in $J = 0 \rightarrow J = 1 \rightarrow J = 0$ is

$$I \propto (2-\sin^2\theta') + \frac{\sin^2\theta'\cos 2(\psi'-\psi)}{1+x^2} + \frac{x\sin^2\theta\sin 2(\psi'-\psi)}{1+x^2} \quad \ldots 1$$

$$I \propto I_1 + I_2 + I_3$$

where $x = (2g_J\mu_0 H\tau/\hbar) \propto H$; τ and g_J are the mean lifetime and g value of the excited state; μ_0 is the Bohr magneton and H is the magnetic field strength.

According to Fry and Williams[7], the experimental geometry requires that equation 1 be averaged over the symmetric solid angle centered about a 90^o-90^o-90^o geometry, so that

$$\bar{I} = \int I d\Omega \Big/ \int d\Omega = \bar{I}_1 + \bar{I}_2 + \bar{I}_3 \quad \text{where} \qquad \ldots 2$$

$$d\Omega = d\Omega' \times d\Omega'' = \sin\theta'\sin\theta d\theta' d\theta d\psi' d\psi$$

$d\Omega'$ and $d\Omega''$ are the solid angles subtended at the origin of the co-ordinates in the input and output branches respectively, and the limits of integration correspond to the symmetric departures from the 90^o-90^o-90^o geometry that is,

$$\theta' = \frac{\pi}{2} \pm \delta \qquad \theta = \frac{\pi}{2} \pm \gamma$$

$$\psi' = \frac{\pi}{2} \pm \beta \qquad \psi = \pm \alpha$$

Weak scattered outputs sometimes require the use of wider monochromator slits and these may not be symmetrically located with respect to the output axis of the 90^o-90^o-90^o geometry. Under this situation

θ' lies between $\frac{\pi}{2} - \delta_1$ and $\frac{\pi}{2} + \delta_2$; $\delta_1 \neq \delta_2$

ψ' lies between $\frac{\pi}{2} - \psi_1'$ and $\frac{\pi}{2} + \psi_2'$; $\psi_1' \neq \psi_2'$

$\theta = \frac{\pi}{2} \pm \gamma$

$\psi = \pm \alpha$

and under these new limits of integration,

$$\int d\Omega = \int_{\frac{\pi}{2}-\delta_1}^{\frac{\pi}{2}+\delta_2} \sin\theta' d\theta' \int_{\frac{\pi}{2}-\gamma}^{\frac{\pi}{2}+\gamma} \sin\theta d\theta \int_{\frac{\pi}{2}-\psi_1'}^{\frac{\pi}{2}+\psi_2'} d\psi' \int_{-\alpha}^{+\alpha} d\psi$$

$$= (\sin\delta_1 + \sin\delta_2)(2\sin\gamma)(\psi_1' + \psi_2')(2\alpha)$$

$$= 4\alpha\sin\gamma(\psi_1' + \psi_2')(\sin\delta_1 + \sin\delta_2) \qquad \ldots.3$$

Substituting I_1, I_2, I_3 from equation 1 and $\int d\Omega$ from equation 3 and integrating we have;

$$\bar{I}_1 = \int I_1 d\Omega \Big/ \int d\Omega = [1 + \tfrac{1}{3}(\sin^2\delta_1 - \sin\delta_1\sin\delta_2 + \sin^2\delta_2)] \qquad \ldots.4$$

$$\bar{I}_2 = \frac{\int I_2 d\Omega}{\int d\Omega}$$

$$= \frac{-1}{1+x^2} \cdot \frac{(\sin 2\alpha)(\sin 2\psi_1 + \sin 2\psi_2)[1 - \frac{1}{3}(\sin^2\delta_1 - \sin\delta_1\sin\delta_2 + \sin^2\delta_2)}{4\alpha(\psi_1' + \psi_2')} \qquad \ldots.5$$

$$\bar{I}_3 = \frac{\int I_3 d\Omega}{\int d\Omega}$$

$$= \frac{x}{1+x^2} \cdot \frac{(\sin 2\alpha)(\cos 2\psi_2' - \cos 2\psi_1')\left[1-\frac{1}{3}(\sin^2\delta_1 - \sin\delta_1 \sin\delta_2 + \sin^2\delta_2)\right]}{4\alpha(\psi_1' + \psi_2')} \quad \ldots.6$$

Addition of equation 4, 5 and 6 results in an expression for $\bar{I}$,

$$\bar{I} \propto \frac{\sin 2\alpha\left[1-\frac{1}{3}(\sin^2\delta_1 - \sin\delta_1\sin\delta_2 + \sin^2\delta_2)\right]}{4\alpha(\psi_1' + \psi_2')} \times$$

$$\left\{ \frac{4\alpha(\psi_1' + \psi_2')\left[1+\frac{1}{3}(\sin^2\delta_1 - \sin\delta_1\sin\delta_2 + \sin^2\delta_2)\right]}{\sin 2\alpha\left[1-\frac{1}{3}(\sin^2\delta_1 - \sin\delta_1\sin\delta_2 + \sin^2\delta_2)\right]} - \right.$$

$$\left. \frac{1}{1+x^2}(\sin 2\psi_1' + \sin 2\psi_2') + \frac{x}{1+x^2}(\cos 2\psi_2' - \cos 2\psi_1') \right\} \quad \ldots.7$$

$$\bar{I} \propto C_1 - \frac{C_2 + C_3 x}{1+x^2} \quad \ldots.8$$

where

$$C_1 = \frac{4\alpha(\psi_1' + \psi_2')\left[1+\frac{1}{3}(\sin^2\delta_1 - \sin\delta_1\sin\delta_2 + \sin^2\delta_2)\right]}{\sin 2\alpha \cdot \left[1-\frac{1}{3}(\sin^2\delta_1 - \sin\delta_1\sin\delta_2 + \sin^2\delta_2)\right]}$$

$$C_2 = \sin 2\psi_1' + \sin 2\psi_2'$$

$$C_3 = -(\cos 2\psi_2' - \cos 2\psi_1')$$

equation 8 is still of the form;

$$\bar{I} \propto \left[1 - \frac{A+Bx}{1+x^2}\right] \text{ where } A = \frac{C_2}{C_1} \text{ and } B = \frac{C_3}{C_1} \quad \ldots.9$$

$$\propto \left[\frac{1}{A} - \frac{1}{1+x^2} - \frac{(B/A)x}{1+x^2}\right]$$

The term $\left[\frac{1}{A} - \frac{1}{1+x^2}\right]$ represents a inverted Lorentzian

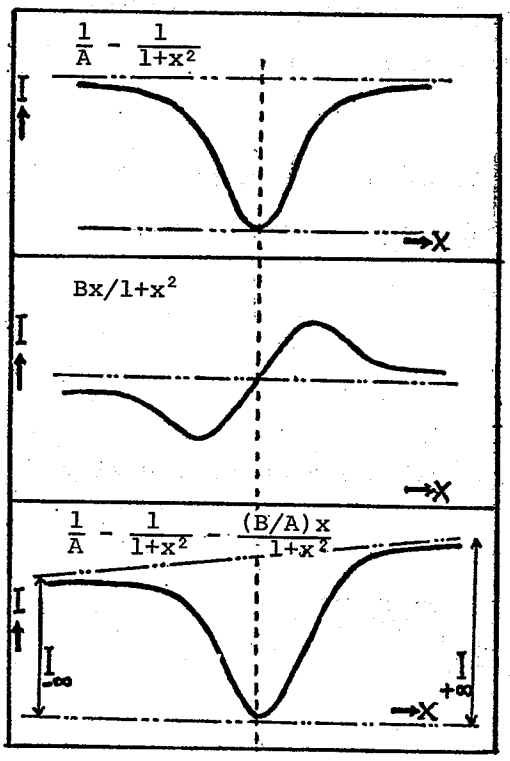

Fig. 2. Effect of dispersion component (not to scale)

However $\overline{I} = 0$ when $x = H = 0$ is not necessarily true, and a field independent background has been added to the inverted Lorentzian. The term $(B/A)x(1+x^2)^{-1}$ is a dispersion component which causes a skewness in the resultant Lorentzian as shown in figure 2, and $I_{-\infty} < I_{+\infty}$. If this type of asymmetry is observed experimentally and can be traced to a lack of symmetry of the scattering region with respect to the optic axis, a correction needs to be applied so that the full width at half maximum (FWHM) of the Hanle Lorentzian can be determined. To eliminate the dispersive component and to obtain the true Lorentzian line shape, the equation 9 can be rewritten as:

$$\overline{I} = K_1 - \frac{K_1 A}{1+x^2} - \frac{Bx \cdot K_1}{1+x^2}$$

where K_1 is the constant of proportionality and if $K_1 A = A_1$ and $K_1 B = B_1$;

$$\overline{I} = K_1 - \frac{A_1}{1+x^2} - \frac{B_1 x}{1+x^2} \qquad \ldots\ldots 10$$

In a typical Hanle experiment I and x are known, and a computer program can be used to solve equation 10 by fitting a polynominal to find A_1, B_1 and K_1.

Now if the $(B_1x/1+x^2)$ term, (the dispersive component) is dropped the true FWHM can be obtained from the standard Lorentzian,

$$\bar{I} = K_1 - \frac{A_1}{1+x^2} \qquad \ldots.11$$

At $x = \pm \infty$, $\bar{I} = K_1$ and therefore at half the maximum intensity.

$$\frac{K_1}{2} = K_1 - \frac{A}{1+x^2_{\frac{1}{2}}} \quad \text{or} \quad x_{\frac{1}{2}} = \sqrt{\frac{2A_1}{K_1} - 1}$$

$$\therefore \quad \text{FWHM} = 2x_{\frac{1}{2}} = 2\sqrt{\frac{2A_1}{K_1} - 1} \qquad \ldots.12$$

The difference between the experimentally observed Hanle curve and corrected Hanle curve as well as their FWHM is evident in figure 3.

The method described above can be used to correct the Hanle line shape for the dispersive component when wider exit slits are in use which may be asymmetrically located,or the scattering region may be asymmetrically located with respect to the observation axis of the 90^{o}-90^{o}-90^{o} experimental geometry.

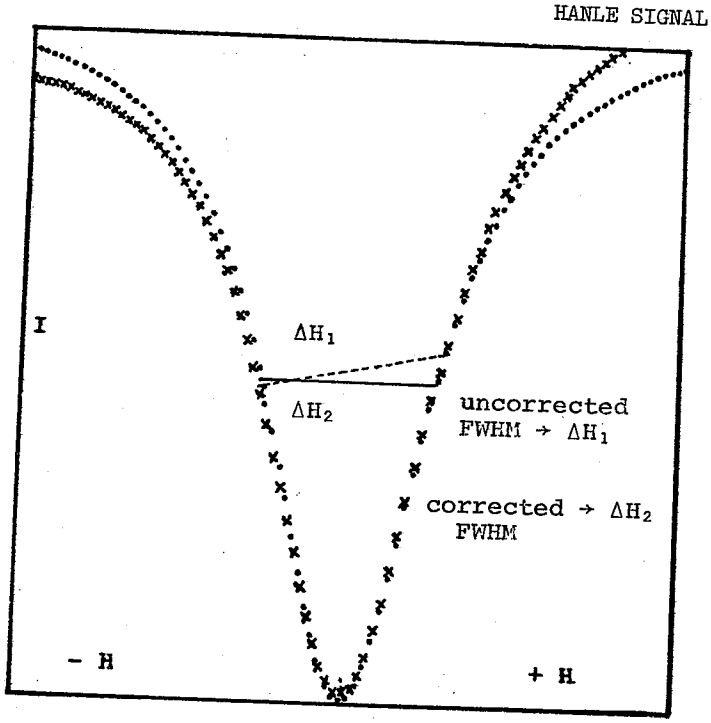

Fig. 3. Experimental plot of fluorescent light intensity I, from a scatterer, recorded as a function of magnetic field H. (×)→ Hanle Lorentzian + dispersion component; (•) → Hanle Lorentzian - Dispersion Component.

ACKNOWLEDGMENTS

This work was supported by a grant from National Research ıcil of Canada.

REFERENCES

W. Hanle, Z. Physik 30, 93 (1924).
A. Lurio, R. L. de Zafara, and R. J. Goshen, Phys. Rev. 134, A1198 (1964).
W. L. Williams and E. S. Fry, Phys. Rev. Letters 20, 1335 (1968).
G. Breit, Rev. Mod. Phys. 5, 91 (1933).
P. A. Franken, Phys. Rev. 121, 508 (1961).
D. A. Anderson, Phys. Rev. 137, A21 (1965).
E. S. Fry and W. L. Williams, Phys. Rev. 138, 81 (1969).

Received February 20, 1974
Accepted March 1, 1974

Lifetimes and Oscillator Strengths in Singlet Levels of Strontium

F. M. KELLY, T. K. KOH, AND M. S. MATHUR
Department of Physics, University of Manitoba, Winnipeg, Manitoba
Received September 19, 1973

Coherence narrowing and collision broadening of the $5s5p\ ^1P_1$ level of strontium have been studied. The natural lifetime of this level has been determined to be 4.68 ± 0.10 ns. The oscillator strength of the 4607 Å transition is 1.94 ± 0.06, and the f values of the transitions from the $5s6p$, $5s7p$, and $5s8p\ ^1P_1$ levels to the ground level and the $5s4d\ ^1D_2$ metastable level have been reevaluated. The cross section for Sr–Sr collisions is found to be $5.2 \times 10^{-7}/\bar{v}$ cm².

On à fait des études du rétrécissement par cohérence et de l'élargissement par chocs du niveau $5s5p\ ^1P_1$ du strontium. La durée de vie de ce niveau est de 4.68 ± 0.10 ns. La force d'oscillateur de la transition à 4607 Å est de 1.94 ± 0.06. On a réévalué les valeurs de f des transitions des niveaux $5s6p$, $5s7p$ et $5s8p\ ^1P_1$ au niveau fondamental et au niveau métastable $5s4d\ ^1D_2$. On trouve que la section efficace pour les chocs Sr–Sr est de $5.2 \times 10^{-7}/\bar{v}$ cm².

Can. J. Phys., **52**, 795 (1974)

1. Introduction

The Hanle effect, which uses the crossing of the Zeeman states of an atomic energy level as the magnetic field is swept through zero, is a convenient method for the measurement of lifetimes of atomic energy levels, particularly those which can be populated by optical excitation. Early work on the Hanle effect is discussed in the book by Mitchell and Zemansky (1934). The theory has been put in useful form for atomic spectroscopy by Lurio *et al.* (1964) and in a general formulation by House (1970).

Quantum mechanically, the Hanle effect can be described by the Breit–Franken formula (Franken 1961)

$$[1] \qquad R \sim \sum_{\substack{\mu,\mu' \\ m,m'}} \frac{f_{\mu m} f_{m\mu'} g_{\mu' m'} g_{m'\mu}}{1 + i\tau\omega(\mu, \mu')}$$

In this equation, R is the rate at which photons of polarization f are absorbed and photons of polarization g are reemitted in the resonance fluorescence; the atoms, which are initially in some magnetic state m of the ground level, can be excited to magnetic states μ and μ' of an excited level, and subsequently decay to a lower level with magnetic quantum number m'; m and m' may belong to the same ground level or m' may be a magnetic state of some other level; the magnetic states μ and μ' of the excited level can become degenerate due to level crossing. $\omega(\mu,\mu') = 2\pi(E_\mu - E_{\mu'})/h$ and τ is the mean lifetime of the excited level. The f's are matrix elements for the absorption process and the g's for the reradiation.

Lurio *et al.* (1964) consider the external static magnetic field to be along the z axis, and define a set of unit complex vectors $\hat{e}$ and $\hat{e}'$ which specify the direction and the polarization of the incoming and the scattered photons, and, give this equation a more useful form;

$$[2] \qquad R \sim \sum_{\mu\mu'} \frac{F_{\mu\mu'} G_{\mu'\mu}}{1 + i\tau\omega(\mu, \mu')}$$

where

$$F_{\mu\mu'} = \sum_m f_{\mu m} f_{m\mu'} \quad \text{and} \quad G_{\mu'\mu} = \sum_{m'} g_{\mu' m'} g_{m'\mu}$$

are the excitation and reradiation matrices respectively. Figure 1 shows the directions of the incoming and outgoing photons and their polarizations.

Lurio *et al.* (1964) have calculated $F_{\mu\mu'}$ for resonance scattering with $J = 0 \to J = 1 \to J = 0$ and find

$$[3] \qquad F_{\mu\mu'} = \begin{vmatrix} \frac{1}{2}(e_+ e_-) & -e_- e_z/\sqrt{2} & -\frac{1}{2}e_-^2 \\ -e_+ e_z/\sqrt{2} & e_z^2 & e_z e_-/\sqrt{2} \\ -\frac{1}{2}e_+^2 & e_z e_+/\sqrt{2} & \frac{1}{2}e_+ e_- \end{vmatrix} \times C$$

For this case, the reradiation matrix $G_{\mu'\mu}$ is identical to this except that all quantities are primed. This leads to

$$R = R(\Delta\mu = 0) + R(\Delta\mu = 1) + R(\Delta\mu = 2)$$

where,

[4] $$R(\Delta\mu = 0) \sim (\tfrac{1}{2}e_+e_-e_+'e_-' + e_z^2e_z'^2)$$

[5] $$R(\Delta\mu = 1) \sim \frac{e_ze_z'}{2}\left\{\frac{(e_-e_+' + e_+e_-') + i\tau\omega(1,0)(e_+e_-' - e_-e_+')}{1 + \tau^2\omega^2(1,0)} + \frac{(e_+e_-' + e_-e_+') + i\tau\omega(0,-1)(e_+e_-' - e_-e_+')}{1 + \tau^2\omega^2(0,-1)}\right\}$$

[6] $$R(\Delta\mu = 2) \sim \frac{1}{4}\frac{(e_-^2e_+'^2 + e_+^2e_-'^2) + i\tau\omega(1,-1)(e_+^2e_-'^2 - e_-^2e_+'^2)}{1 + \tau^2\omega^2(1,-1)}$$

These equations differ slightly from 10, 11, and 12 in Lurio *et al.* (1964) due to the correction of the sign in the denominator (Stroke *et al.* 1968).

For resonance scattering with $J = 2 \to J = 1 \to J = 2$

[7] $$F_{\mu\mu'} = \begin{vmatrix} \frac{7}{2}e_+e_- + 3e_z^2 & \left(\sqrt{2} - \frac{\sqrt{18}}{2}\right)e_ze_- & -\frac{1}{2}e_-^2 \\ \left(\sqrt{2} - \frac{\sqrt{18}}{2}\right)e_ze_+ & 4e_z^2 + 3e_+e_- & \left(\frac{\sqrt{18}}{2} - \sqrt{2}\right)e_ze_- \\ -\frac{1}{2}e_+^2 & \left(\frac{\sqrt{18}}{2} - \sqrt{2}\right)e_ze_+ & \frac{7}{2}e_+e_- + 3e_z^2 \end{vmatrix} \times C$$

$G_{\mu'\mu}$ is the same as $F_{\mu\mu'}$ except that all quantities are primed. A direct calculation shows that $R(\Delta\mu = 1)$ and $R(\Delta\mu = 2)$ are identical, except for a constant, to those for $J = 0 \to J = 1 \to J = 0$, but, $R(\Delta\mu = 0)$ is different and

[8] $$R(\Delta\mu = 0) \sim 33(e_+e_-e_+'e_-' + e_+e_-e_z'^2 + e_+'e_-'e_z^2 + e_z^2e_z'^2) + (\tfrac{1}{2}e_+e_-e_+'e_-' + e_z^2e_z'^2)$$

For scattering with $J = 0 \to J = 1 \to J = 2$, the expression for $F_{\mu\mu'}$ is the same as [3] and $G_{\mu'\mu}$ is the same as [7], except that all quantities are primed. Again, a direct calculation shows that $R(\Delta\mu = 1)$ and $R(\Delta\mu = 2)$ are the same as [5] and [6] except for a constant and

[9] $$R(\Delta\mu = 0) \sim 3(e_+e_-e_+'e_-' + e_+e_-e_z'^2 + e_+'e_-'e_z^2 + e_z^2e_z'^2) + \tfrac{1}{2}(e_+e_-e_+'e_-' + e_z^2e_z'^2)$$

With our experimental geometry, which is shown in Fig. 2, each of the three situations, $J = 0 \to J = 1 \to J = 0, J = 2 \to J = 1 \to J = 2$, and $J = 0 \to J = 1 \to J = 2$ leads to a simple Lorentzian expression

[10] $$R \sim \left[A + \left(1 - \frac{1}{1 + 4\tau^2\omega^2}\right)\right]$$

In this equation, R is the intensity of the scattered

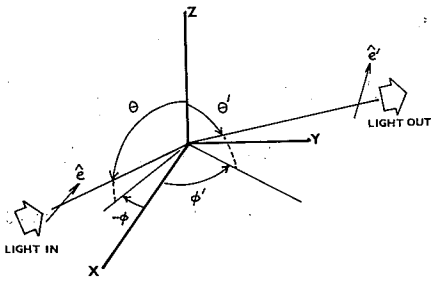

FIG. 1. Coordinate and polarization system used in the calculation of the Hanle effect.

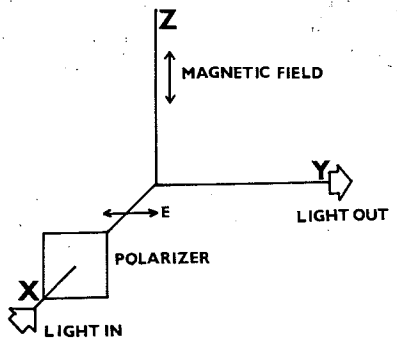

FIG. 2. Geometry of the Hanle experiment.

light, A is a constant which has a different value for the three cases considered, τ is the mean radiative lifetime of the upper level, and $\omega = g_J\mu_0 H/\hbar$, the Larmor angular frequency of precession of the atom in the applied magnetic field H.

If the angle between the incident and observation direction is not exactly 90°, the shape of the Hanle resonance is a combination of a Lorentzian and a dispersion curve (Fry and Williams 1969). This introduces a skewness in the shape of the Hanle resonance which can be represented by

$$[11] \quad R \sim A + B\left(\frac{D^2H^2}{1 + D^2H^2}\right) + C\left(\frac{DH}{1 + D^2H^2}\right)$$

where A, B, C, and D are constant, H is the magnetic field, and the last term represents the dispersive component.

The full width of the Hanle resonance at half maximum intensity, ΔH, is related to the lifetime, τ, of the level by

$$[12] \quad 1/\tau = \Gamma = (g_J\mu_0/\hbar)\,\Delta H$$

where g_J is the Landé g factor of the upper level of the transition and μ_0 is the Bohr magneton. The mean lifetime, τ, of the upper level is also given by

$$[13] \quad 1/\tau = \Gamma = \sum A_n^m$$

The Einstein coefficients, A_n^m, for spontaneous emission from the upper level m to the lower level n are given by

$$[14] \quad A_n^m = \frac{8\pi^2e^2}{m_e c}\,\frac{g_n}{g_m}\,\frac{f_{mn}}{(\lambda_{mn})^2}$$

where the g's are the statistical weights of the levels and f_{mn} is the absorption oscillator strength for the transition of wavelength λ_{mn} (Mitchell and Zemansky 1934; Crossley 1969).

In a Hanle experiment, an incoming resonance photon excites a sample atom which subsequently decays with the emission of another photon. This photon may escape from the scattering region or it may be absorbed by a second atom. This multiple scattering of resonance radiation leads to an apparent increase in the lifetime of the excited state which appears experimentally as a narrowing of the Hanle resonance. The extent to which multiple scattering occurs depends upon the density of the scattering atoms. At very low densities, there is no radiation trapping and the Zeeman states decay with the natural lifetime of the level. As the density of the atom is increased, the coherence narrowing of the Hanle resonance due to radiation trapping occurs until a saturation level is reached. At higher densities, collisions between atoms broaden the Hanle curve and become the dominant factor.

For the general case, which includes different initial and final levels, Happer and Saloman (1967) and Hsieh and Baird (1972) give

$$[15] \quad \Gamma = \Gamma_0 - \Gamma_0 \sum_i \alpha_i\beta_i x_i + \sum_j n_j\sigma_j\bar{v}$$

where Γ is the reciprocal of the observed lifetime and Γ_0 is the reciprocal of the radiative lifetime of the excited state, α_i is an angular factor which depends on the angular momentum of the excited and final states and is tabulated by Saloman and Happer (1966), β_i is the branching ratio for a decay from the excited level, and x_i is the reabsorption probability which depends on a characteristic dimension of the scattering region and the mean free path of the photon, and contains an integral tabulated by Mitchell and Zemansky (1934). In the third term, n_j is the density of the atoms in the ground state or the final state, σ_j is the resonance broadening cross section for like atom collisions, and $\bar{v}$ is the relative velocity of the two atoms. For our experiment, each sum has two terms corrresponding to the ground and the metastable levels of the strontium atoms.

2. Experiment

The Hanle resonance technique was used by us (Dickie *et al.* 1973) to determine the lifetime of the first singlet P level of strontium, and a value of 5.29 ns was reported. However, the photomultiplier tube which we used in the experiments had a high background which prevented observations at very low densities of strontium atoms in the atomic beam. After modifications were made in the experimental apparatus, and the lifetimes and related oscillator strengths for the $5s6p\ ^1P_1$, $5s7p\ ^1P_1$, and $5s8p\ ^1P_1$ levels were determined (Kelly *et al.* 1973*a*,*b*), the $5s5p\ ^1P_1$ level has been reexamined. The geometry, the experimental setup, and the signal averaging system shown in Figs. 2, 3, and 4 and described earlier (Kelly *et al.* 1973*a*), have been used to measure the variation of the lifetime of the $5s5p\ ^1P_1$ level of strontium with the density of the strontium atoms.

At low atomic densities, (low furnace currents), the Hanle signal is weak. To improve the signal to

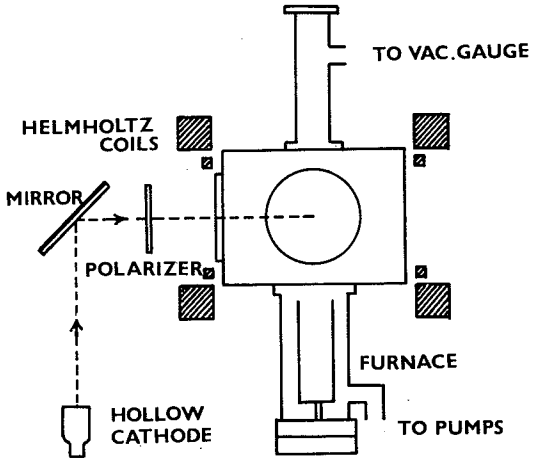

FIG. 3. Schematic diagram of the experimental apparatus; the direction of observation is perpendicular to the plane of the diagram.

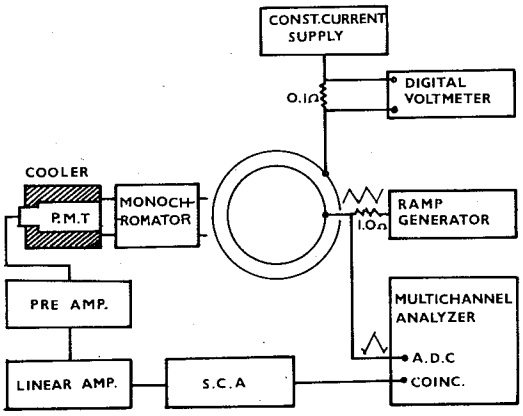

FIG. 4. Schematic diagram of the signal averaging apparatus.

noise ratio, wide slits are used on the monochromator, which is in the output arm of the apparatus. When the wider slits are used, a slight skewness in the Hanle signal is observed. The skewness indicates the presence of a dispersive component, which in turn is traced to the fact that the region of irradiation of the atomic beam is not completely symmetrical about the optical axis of the system. The image of the hollow cathode source formed with resonance radiation, 4607 Å, scattered from the beam, and focussed on the plane of the monochromator is pear shaped with a sharpened end. When a narrow slit is used, only a small section of this image is admitted to the monochromator. However, with a wide slit, the illumination is no longer angularly symmetric about the optical axis, and the skewness results. A computer program, based on [11], is used to eliminate the effect of the dispersive component on the width of the Hanle resonance. Narrow slits are used on the monochromator for observations at medium and high densities and this problem does not arise.

The density of the atoms in the beam is varied by changing the heating current in the furnace, while the current in the hollow cathode lamp, and the steady and the sweep magnetic field are kept the same. A density parameter ρ, in arbitrary units, is defined as

$$\rho = \frac{\text{maximum counts in wings} - \text{background}}{(\text{accumulation time}) \times (\text{lamp current})^2}$$

With the low atomic densities, wider slits are used, and a geometric factor is used to convert the value of ρ to a constant slit width.

3. Results and Discussion

The width of the Hanle resonance is determined over a wide range of densities of the atoms in the atomic beam. The width, in channel numbers, can be converted to ΔH in tesla from the known calibration (Kelly *et al.* 1973*b*). Figure 5 shows a plot of the width in channels of the Hanle signal against the density parameter ρ in arbitrary units. The solid curve is obtained when the full spectrum of strontium, including the ultraviolet lines, irradiates the strontium beam. The curve shows coherence narrowing in the region of very low densities and a collision broadening region at high atomic densities separated by a saturation region at intermediate atomic densities.

For our experiment, each of the sums in [15] has two terms and the equation can be written as

$$[16] \quad \Gamma = \Gamma_0(1 - \alpha_1 x_1 \beta_1 - \alpha_2 x_2 \beta_2) + N_1 \sigma_1 \bar{v} + N_2 \sigma_2 \bar{v}$$

In this equation, the subscript 1 refers to the ground $^1S_0$ level while the subscript 2 refers to the metastable $^1D_2$ level. In the low density region, N_1 and N_2 are relatively small, and the second and third terms corresponding to multiple scattering of the resonance radiation are the important ones. α_1 and α_2 are constants tabulated by Saloman and Happer (1966) and β_2 (the branching ratio for $\lambda = 64\,600$ Å) is much smaller than β_1. Thus, at low beam densities (d'Yakonov and Perel' 1965), we can approximate [15] by $\Gamma = \Gamma_0(1 - Ax)$ where A is a constant and x,

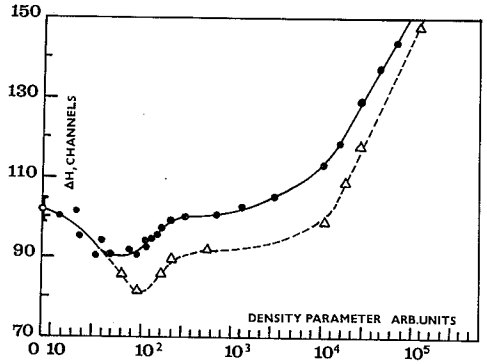

FIG. 5. The variation of the Hanle width of 4607 Å with density.

the probability of scattering of $\lambda = 4607$ Å, depends on the density in a complicated manner. However, at these low densities, x is small and changes slowly with density so that we can assume that the Hanle width varies linearly with density in the low density region. A least squares fit and an extrapolation to zero density gives a value of $\Delta H = (24.29 \pm 0.54) \times 10^{-4}$ T which, with [12], gives a value of $\tau_0 = 4.68 \pm 0.10$ ns for the radiative lifetime of the $5s5p\ ^1P_1$ level.

Saloman and Happer (1966) have shown that the ratio Γ/Γ_{min}, is equal to 10/3, where Γ_{min} corresponds to the minimum width of the Hanle resonance, provided the absorption of the transition $\lambda = 64\,600$ Å from the $^1D_2$ level can be neglected. From the solid line in Fig. 5, the observed ratio is 1.1, considerably smaller than the theoretical value. This indicates that the $^1D_2$ level must be taken into account for a discussion of the intermediate density region of Fig. 5.

The $5s4d\ ^1D_2$ metastable level can be populated by: (1) transitions from optically excited levels which lie above $5s5p\ ^1P_1$, (2) direct decay from $5s5p\ ^1P_1$ with the emission of a photon of 64 600 Å, and (3) excitation of the level by low energy electrons in the vicinity of the furnace mouth. The first of these processes can be blocked by the inclusion of a glass plate in the input arm of the apparatus, because the optical excitation of levels above $5s5p$ is entirely by ultraviolet lines. The result of the elimination of the ultraviolet excitation is pronounced and is shown in Fig. 5 by the dotted curve. The ratio Γ_0/Γ_{min} has been increased to 1.3, but, this is still well below the theoretical value. The energy levels and transitions are shown in a partial energy level diagram in Fig. 6.

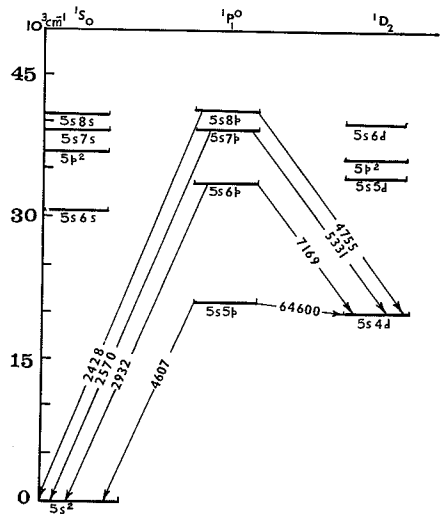

FIG. 6. Partial energy level diagram for neutral strontium.

When the density of the atoms in the beam is in the high range, the last two terms of [16] are dominant. During our experiments at high densities, the intensity of the input light is kept constant. Under these conditions N_2, the number of atoms per cm^3 in the $^1D_2$ level reaches a maximum value, because the excitation of this level is mostly by decays from upper excited levels, but, N_1, the number of atoms per cm^3 in the ground $^1S_0$ level, continues to increase. Thus, at the highest densities, the fourth term of [16] is the most important, and, the width of the Hanle resonance under collision broadening conditions becomes proportional to the density of the atoms. This result allows us to make a numerical evaluation of the ratio between our arbitrary density parameter ρ, and N, the number of atoms per cm^3 in the beam.

Byron *et al.* (1964) have pointed out that if the oscillator strength is unity or larger, broadening due to collisions between like atoms is velocity independent. Moreover, for a $J = 1 \rightarrow J = 0$ transition, as is the case in our experiment, d'Yakonov and Perel' (1965) have shown $\Gamma_2 = \Gamma_0 \times 0.028\, N\lambda^3$, where Γ_2 is the contribution to the Hanle width for like atom collision broadening. Thus, when the density of atoms is large, and the observed width of the Hanle resonance is mostly dependent on collision broadening, we may write $\Gamma = \text{constant} + \Gamma_0 \times 0.028\ N_1\lambda_1{}^3$. A least squares fit to the slope of the straight line part of our curve with $\rho > 10^4$ gives us $N_1 =$

TABLE 1. Lifetimes and oscillator strengths in strontium

	$5s5p$		$5s6p$		$5s7p$		$5s8p$		Method	Reference
Lifetime in ns	8								Dispersion	1
	6.4								Hook	2
	6.2								Hook	3
	6.1 ±0.6								Hanle	4
	4.97±0.15								Hanle	5
	4.56±0.21								Phase	6
	5.29±0.10								Hanle	7
	4.68±0.10		3.64±0.14		4.93±0.32		5.46±0.17		Hanle	8
Decay to	$5s^2$	$5s4d$	$5s^2$	$5s4d$	$5s^2$	$5s4d$	$5s^2$	$5s4d$		
Wavelength Å	4607	64,600	2932	7169	2570	5329	2428	4755		1
Oscillator strength	1.2									2
(experimental)	1.5 ±0.2									3
	1.54±0.05		0.0052		0.0110		0.032			4
	1.56±0.16									5
	1.92±0.05									6
	2.09±0.10									8
	1.94±0.06	$3.8^{+0.2}_{-3.0}$	0.0066	1.22	0.0138	0.49	0.041	0.34		9
	2.20±0.7			0.13		0.12		0.075	Emission	10
Oscillator strength	1.90		0.02		0.0012		0.033		B and D	11
(theoretical)	3.18		0.228		0.057				RPA	12
	2.12		0.356						NBC	13
	2.45		0.0044		0.011		0.030		SE	14
	2.39								CPC	15
	1.95								MCHF	

[1]Prokofev (1928).
[2]Ostrovskii *et al.* (1958).
[3]Ostrovskii and Penkin (1961).
[4]De Zafra *et al.* (1962).
[5]Lurio *et al.* (1964).
[6]Hulpke *et al.* (1964).
[7]Dickie *et al.* (1973).
[8]This work and Kelly *et al.* (1973 *a*, *b*); error estimates are given in *a* and *b*.
[9]Eberhagen (1955).
[10]Bates and Damgaard (1949).
[11]Altick and Glassgold (1964).
[12]Helliwell (1964).
[13]Zilitis (1970).
[14]Hameed (1972).
[15]Kim and Bagus (1972).
RPA = Random phase approximation, NBC = Nodal boundary condition, SE = Semi-empirical method, CPC = Core polarization correction, MCHF = Multi configuration Hartree–Fock.

$1.64 \times 10^9 \times \rho$, and we are able to convert our density parameter ρ to number of atoms per cm^3.

D'Yakonov and Perel' point out that when the density of the atoms is large enough that the condition, $N\lambda^3 \ll 1$, is no longer valid, collision broadening of the Hanle resonance is important. If we assume $N_1\lambda_1{}^3 = 1$, with $\lambda_1 = 4607$ Å, collision broadening becomes dominant at $N_1 = 10^{13}$, corresponding to our density parameter $\rho = 6 \times 10^3$. This agrees with the observations in Fig. 5. The wavelength of the transition to the metastable $^1D_2$ level is 64 600 Å which is 14 times the wavelength of the resonance line. Consequently, when N_2, the number of atoms in the $^1D_2$ level, reaches about 4×10^9 per cm^3, collisions between the excited level and the metastable level will contribute to the broadening of the Hanle width. There is no reliable way to estimate the relative number of atoms in the metastable $^1D_2$ level, but, provided the population of the metastables is greater than $1/(14)^3 = 3.7 \times 10^{-4}$ times the beam density, collision broadening due to the metastable level becomes important, and may be effective before broadening due to collisions with ground state atoms. The dip in our curve near $\rho = 100$ may be due to this effect.

The slope of the broadening curve at high densities will also yield the broadening cross section (Happer and Saloman 1967). From the slope of our experimental curve, we obtain $\sigma(\bar{v}) = 5.2 \times 10^{-7}/\bar{v}$ cm^2 for our experimental value.

There are a number of theoretical formulae for the calculation of this cross section. D'Yakonov and Perel' (1965) modify a formula given by Byron and Foley (1964), and we obtain

$$\sigma(\bar{v}) = 0.028 \times \lambda^3 \times \Gamma_0/\bar{v} = 5.6 \times 10^{-7}/\bar{v} \text{ cm}^2$$

This result agrees very well with our experimental value. A formula given by Omont (1966) yields $\sigma(\bar{v}) = 4.4 \times 10^{-7}/\bar{v}$ cm^2. The agreement is not as good but is still within experimental error.

Penkin and Shabanova (1969) have used the hook method to determine collision cross section, and their result, corrected with our larger f value, is $\sigma(\bar{v}) = 4.7 \times 10^{-7}/\bar{v}$ cm^2. The agreement is within experimental errors.

This paper corrects our earlier measurement (Dickie *et al.* 1973) of the lifetime of the $5s5p\ ^1P_1$ level. There is no experimental data for a reliable value of the branching ratio for the two transitions from this level. We assume a branching ratio which gives 5% to the $^1D_2$ level. This value is consistent with the curves in Fig. 5 but cannot be completely justified. The lifetime τ_0 is 4.68 ± 0.10 ns. With [13] and [14] and the 5% branching, we determine $f(4607) = 1.94 \pm 0.06$. The error has been increased by 50% to allow for uncertainties in the branching ratio. If the decay to the metastable level is neglected, the f value is 2.04. Kim and Bagus (1972) in a theoretical paper assume a branching ratio of 4%.

The assumption of the 5% branching also means that $f(64\,600) = 3.8$. The error in this is large, as the change in f is large for small changes in the branching ratio. A 1% branching ratio reduces the f value to 0.8.

We have previously reported lifetimes and related oscillator strengths for the $5s6p$, $5s7p$, and $5s8p$ singlet levels (Kelly *et al.* 1973*a*,*b*). The calculations of the oscillator strengths involve $f(4607)$, and the previously reported oscillator strengths require modification. In Table 1, we have collected lifetime measurements from the literature and give corrected f values for the higher excited singlet P levels. Our previous value, (Dickie *et al.* 1973, ref. 7 in Table 1), contained a systematic error due to coherence narrowing. The agreement of the recent lifetime measurement (Table 1, refs. 5, 6, and 8) is very good.

Acknowledgments

The work reported in this paper was supported by a grant from the National Research Council of Canada.

Altick, P. L. and Glassgold, A. E. 1964. Phys. Rev. **133**, 632.
Bates, D. R. and Damgaard, A. 1949. Phil. Trans. **242**, 101.
Byron, F. W. and Foley, H. M. 1964. Phys. Rev. **134**, 625.
Byron, F. W., McDermott, Jr., M. N., and Novick, R. 1964. Phys. Rev. **134**, A615.
Crossley, R. J. S. 1969. Adv. At. Mol. Phys. **5**, 237.
De Zafra, R. R., Goshen, R. J., Landman, A., and Lurio, A. 1962. Bull. Am. Phys. Soc. **7**, 433.
Dickie, L. O., Kelly, F. M., Koh, T. K., Mathur, M. S., and Suk, F. C. 1973. Can. J. Phys. **51**, 1088.
D'Yakanov, M. I. and Perel', V. I. 1965. Sov. Phys.-JETP, **21**, 227.
Eberhagen, A. 1955. Z. Phys. **143**, 392.
Franken, P. A. 1961. Phys. Rev. **121**, 508.
Fry, E. S. and Williams, W. L. 1969. Phys. Rev. **183**, 81.
Hameed, S. 1972. Atom. Molec. Phys. **5**, 746.
Happer, W. and Saloman, E. B. 1967. Phys. Rev. **160**, 23.
Helliwell, T. M. 1964. Phys. Rev. **135**, A325.

HOUSE, L. L. 1970. J. Quant. Spectrosc. Radiat. Transfer, **10**, 909, 1171.
HSIEH, J. C. and BAIRD, J. C. 1972. Phys. Rev. **6**, 141.
HULPKE, E., PAUL, E., and PAUL, W. 1964. Z. Phys. **117**, 256.
KELLY, F. M., KOH, T. K., and MATHUR, M. S. 1973*a*, *b*. Can. J. Phys. **51**, 1653, 2295.
KIM, Y-K. and BAGUS, P. S. 1972. Atom. Molec. Phys. **5**, L193.
LURIO, A., DE ZAFRA, R. L., and GOSHEN, R. J. 1964. Phys. Rev. **134**, 1198.
MITCHELL, A. and ZEMANSKY, M. W. 1934. Resonance radiation and excited atoms (Cambridge University Press, London).
OMONT, A. 1966. CR, B, **262**, 190.
OSTROVSKII, YU. I. and PENKIN, W. P. 1961. Opt. Spectrosc. **11**, 307.
OSTROVSKII, YU. I., PENKIN, W. P., and SHABANOVA, L. N. 1958. Sov. Phys.-Dokl. **3**, 538.
PENKIN, N. P. and SHABANOVA, L. N. 1969. Opt. Spectrosc. **26**, 191.
PROKOFEV, U. K. 1928. Z. Phys. **50**, 701.
SALOMAN, E. B. and HAPPER, W. 1966. Phys. Rev. **144**, 7.
STROKE, H. H., FULOP, G., KLEPNER, S., and REDI, O. 1968. Phys. Rev. Lett. **21**, 61.
ZILITIS, V. A. 1970. Opt. Spectrosc. **29**, 438.